Simulation-Based Study and Analysis of the Wind Power Integration Using Heat Pump and Thermal Energy Storage

Vorgelegt von

M.Sc.

Hamidreza Heidar Esfehani

ORCID: 0000-0003-2819-5623

an der Fakultät III – Prozesswissenschaften

der Technischen Universität Berlin

zur Erlangung des akademischen Grades

Doktor der Ingenieurwissenschaften
-Dr.-Ing.-

genehmigte Dissertation

Promotionsausschuss:

Vorsitzender:	Prof. Dr.-Ing. Frank Behrendt
Gutachter:	Prof. Dr.-Ing. Martin Kriegel
Gutachter:	Prof. Dr. Hatef Madani

Tag der wissenschaftlichen Aussprache: 4. November 2019

Berlin, 2020

ACKNOWLEDGMENTS

The completion of this thesis would not have been possible without the valuable support of others. First and foremost, I must express my deepest gratitude and admiration to my thesis supervisor Prof.Dr.-Ing. Martin Kriegel for accepting me as a PhD student and having faith and trust on my educational background. His invaluable input, precious guidance, and supervision lead me to accomplish various tasks of my PhD work. His critical observations and remarks on the submitted reports during the course of my PhD thesis helped me to shape, scrutinize, and improve the adopted approach. Many thanks to Prof.Dr. Hatef Madani for his interest and time to countercheck my PhD progress and to review my PhD thesis as one of the members of the thesis evaluation committee. I would like to thank the Climate-KIC organization for granting me the scholarship and providing administrative support during my PhD. More profoundly, I want to thank my lovely parents and sisters for their prayers, continuous encouragement, dedication, and endless patience. Lastly, I offer my regards and blessings to all my friends who supported me in any respect during the completion of the thesis.

KURZFASSUNG

Aufgrund des zunehmenden Anteils von erneuerbaren Energien und da Windkraftanlagen und Photovoltaikanlagen fluktuierende Energiequellen sind, kommt es infolge der Einspeisung durch Windkraft und Photovoltaik zunehmend zu einer Diskrepanz zwischen Angebot und Nachfrage im Stromnetz. Darüber hinaus stellen nur beschränkt regelbare fossile Kraftwerke und die begrenzte Netzkapazität die Stromnetzbetreiber vor eine große Herausforderung. Deswegen droht, wenn kein Ausgleich zwischen aktuellem Angebot und Nachfrage erzielt wird, eine Überlastung des Netzes und anschließend ein Stromausfall. Der Stromeinsatz zu Heizzwecken (Power-to-Heat), mittels Wärmepumpen oder Kraft-Wärme-Kopplungsanlagen (KWK-Anlagen), ist eine effiziente Lösung für die Gebäudebeheizung. Er wird als wichtige Alternative zu konventionellen Heizsystemen wie Heizkesseln angesehen, um den Anteil fossiler Brennstoffe im Heizungssektor erheblich reduzieren zu können. Um die Integration von volatilen erneuerbaren Energien durch Wärmepumpen zu verbessern, ist eine geeignete Methode zur Dimensionierung von Wärmepumpe und Wärmespeicher im Zusammenhang mit der Windeinspeisung notwendig. Das Ziel dieser Doktorarbeit ist zu bewerten inwiefern eine Stromgeführte Dimensionierung von Wärmepumpen und Wärmespeichern zusammen mit einer Überschuss-Regelstrategie zur Netzintegration der Windeinspeisung wirksam sein kann. In dieser Arbeit wird zunächst eine Dimensionierungsstrategie von Wärmepumpen mit Wärmespeichern auf Basis der Verfügbarkeit der Windeinspeisung sowie der Standardlastprofile von Wohngebäuden entwickelt. Anschließend wird mittels Simulationen der Einfluss der Überdimensionierung der Wärmepumpen-Anlagen auf die Integration des Windüberschussstroms sowie Jahresarbeitszahl von verschiedenen Wärmepumpen mit Wärmespeichern untersucht. Es ist zu erwarten, dass durch die Realisierung dieses Dimensionierungskonzepts statt Konventionelle Methode, großen Anteil von Grundlast aus fossilen Kraftwerken durch Windstrom ersetzt wird, welche zur Netzstabilisierung führt. Drei Arten von Wärmepumpen wurden in dieser Arbeit untersucht: 1. Festdrehzahl/Fixed-speed (Einstufig) Sole-Wasser-Wärmepumpe 2. Festdrehzahl/Fixed-speed Luft-Wasser Wärmepumpe und 3. Leistungsgeregelte (mehrstufige) Luft-Wasser-Wärmepumpe. Die Wärmepumpen werden monovalent betrieben und stellen zusammen mit den Wärmespeichern den Wärmebedarf verschiedener Mehrfamilienhäuser zur Verfügung. Um die Wirkung dieses Lastmanagements sowie das Wind-Integrationspotential der Wärmepumpen-Anlage zu bewerten, wurden zwei Regelszenarien für die Wärmepumpen verwendet: 1. Grundlast/Base-Load-Szenario, wo die Wärmepumpe von Grundstrom versorgt und aufgrund von Sperrzeiten (Peak-Zeiten) maximal 3x2 Stunden pro Tag ausgeschaltet wurde. 2. Überschuss/Surplus-Szenario, wo die Wärmepumpe betrieben wird, wenn Windeinspeisung zur Verfügung steht, und eine Wärmeversorgung benötigt wird. Für die dynamischen Simulationen wurde die Software TRNSYS (Transient System Simulation Tool) genutzt. Drei Modelle wurden in TRNSYS eingesetzt und es wurden jeweils Simulationen für verschiedene Verbrauchs-Lastprofile für die Zeiträume Januar bis März sowie Oktober bis Dezember durchgeführt.

ABSTRACT

Despite the fast-growing rate of the implementation of renewable energy technologies, high fluctuations of wind feed-in supply are currently seen as the main challenge facing further feeding of wind power to electricity grids and consequently increasing the renewable share of the energy market. Considering the fact that the utility network has no capability of storing excess power production, the unexpected increase of wind power supply mostly during off-peak hours, where the demand is lowest, might cause high rates of electricity surplus in the power network that if not controlled, would interrupt the grid stability leading to power outages and blackouts. Utilizing electricity for heating purposes through Power-to-Heat technologies is one of the most reliable solutions used to optimize management of renewable energies. Heat pumps or combined heat and power (CHP) systems compose the majority of the power to heat technologies that are used as alternatives for conventional heating systems such as boilers and can reduce the fossil fuel share in the heating sector significantly. Heat pumps operating under smart load control scenarios have demonstrated to be well suited for maintaining active load management to resolve the mismatch between supply and demand sides in the energy market. The aim of this PhD thesis is to evaluate the potential of load management with over dimensioning scenario for heat pump coupled with a thermal storage mechanism for integrating wind feed-in by taking the advantage of surplus electricity during off-peak hours. Based on the availability of wind power generation as well as standard electrical load profiles and heating load profiles of the buildings, a surplus load control scenario will be developed for the heat pump system that incorporates the flexible operating hours of the heat pump and charging/ discharging of the heat storage. The heat pumps operate in monovalent mode and supply domestic hot water and space heating demands of the multi-family residential building. The entire system is modeled and simulated in the simulation software Transient Simulation System (TRNSYS) where dynamic simulations are carried out for the heating season with different boundary conditions. Finally using simulation results, the adaptation rate of the wind feed-in will be characterized in correlation with dimensions of the components as well as heating demand of the building. Three types of heat pumps are investigated in this work: 1. Single-speed ground source (water-water) heat pump 2. Single-speed air source (air-water) heat pump and 3. Variable speed air-water heat pump. The synthetic heating load profiles of the buildings are calculated and implemented in the simulation model based on the test reference year of the city of Berlin and the VDI 4655 standard. In order to evaluate the load shifting and wind integration potential of the heat pump system two control scenarios are applied for the system and the results will be compared; 1. Base Load Scenario: where the electricity demand of the heat pump system is supplied by baseload (conventional) electricity and will be shut down maximum 3x2 hours on a daily basis, and 2. Surplus Scenario: where the heat pump system is operated based on the availability of wind electricity and the necessity of the heat supply. It is anticipated that over-dimensioning heat pump and thermal storage within the designed surplus control strategy will result in a considerable increase of the wind share of the power consumption whilst supplying the entire heating demand of the building.

Table of Contents

ACKNOWLEDGMENTS I
KURZFASSUNG II
ABSTRACT III
List of Figures VI
Abbreviations IX
Units IX
Other abbreviations IX
Nomenclature X
Indices X
Parameters X
Variables X
1. Introduction 1
1.1. Wind Energy: Opportunities and Challenges 1
1.2. Energy Utility in Berlin 4
1.3. Research Motivation 5
2. Research Background 7
2.1. Heat Pumps and Their Role in the Heating Sector 7
2.1.1. Basic Principals of the Heat Pump Performance 7
2.1.2. Ground Source Heat Pumps 8
2.1.3. Large Scale Heat Pumps and Their Applications 12
2.1.4. Role of the Heat Pump in German Heating Market 13
2.2. Load Management 15
2.2.1. Demand Side Management through Heat Pump and Heat Storage 16
2.2.2. Control methods for operating heat pumps 16
2.2.3. Integrating renewable electricity through the heat pump and heat storage 17
3. Methodology and Modelling of the Heating System 19
3.1. Heat Pump Heating System Model 19
3.1.1. Heat Pump Model 20
3.1.2. Thermal Storage Tank Model 24
3.1.3. Temperature Control 25
3.2. Building Model 26

3.2.1. Load Profile of the Multi-Family Residential 26
3.3. Load Management Strategy 32
3.3.1. Load Control Unit 35
3.4. Dimensioning of The Heat Pump Heating System 36
3.4.1. Bivalent Operation Mode 37
3.4.2. Monoenergetic and Monovalent Operation Mode 37
3.5. Dimensioning Methods 39
3.6. Simulation Cases 41
3.7. Surplus Sizing Strategy of the System 42
4. Results and Discussions 44
4.1. Model I: Ground Source Heat Pump Heating System 44
4.2. Model II: Air Source Heat Pump Heating System 54
4.3. Comparison between Models I and II 64
4.4. Model III: Variable Speed Heat Pump Heating System 65
4.5. Comparison of all simulation cases 74
5. Summarizing Discussions and Outlook 77
5.1. Summarizing Discussions 77
5.2. Conclusions 80
5.3. Outlook and Future Research Potentials 80
Bibliography 82
Appendixes 86
A: Datasheets of the heat pump systems of the Viessmann company [48] 86
B: Normalized diagrams of heating capacity and power input of the considered GSHP and ASHP 89
C: Dimensions of the thermal storage tank [50] 90
D: Simulation Layouts in TRNSYS environment 91
E: Surplus Control Scenario for Heat Pump Models in TRNSYS 92
F: Wind Integration Factor Vs. Demand Factor of the Ground-source heat pump Model 95
G: The Impact of Enlarging Thermal Storage Volume on SPF of the Heat Pump Unit 96
H: Office Building: A Case Study for Single Speed Heat Pumps 97

List of Figures

Figure 1-1: Leading countries worldwide by wind power installed capacity 2015 1
Figure 1-2: Wind power installation and its growth-rate in Germany 2
Figure 1-3: Growth rate of Installed power generation and corresponding surplus power prediction in Germany [4] 3
Figure 1-4: The distribution of the heat power plants in Berlin 5
Figure 1-5: The wind installation capacity of top 5 states of Germany in GW 6
Figure 2-1: Work principle of a heat pump 7
Figure 2-2: Three main methods of using groundwater heat [34] 9
Figure 2-3: Seasonal Progression of Groundwater Temperature [36] 10
Figure 2-4: Heat pump field test of BINE [37] 11
Figure 2-5: The source temperatures of all ground source heat pumps tested in the monitoring project [37] 12
Figure 2-6: HP using the waste heat of the flue gas of industrial plant, in combination with CHP and Cold/Hot Storage [11] 13
Figure 2-7: Heating structure of the housing stock in Germany in 2015 14
Figure 2-8: Sales Figures of ground and air source HP systems in Germany during the last 5 years 14
Figure 2-9: Different Types of Demand Side Management [49] 15
Figure 2-10: Using heat pump in residential buildings for integrating more wind energy for heat supply [28] 18
Figure 3-1: Schematic of the heating system describing different blocks of the system 20
Figure 3-2: Schematic of the heat pump with a variable-speed compressor 22
Figure 3-3: Flowchart of the variable speed heat pump mode [26] 22
Figure 3-4: The Variable Speed Heat Pump model in TRNSYS 23
Figure 3-5: Stratified Storage tank with temperature nodes 24
Figure 3-6: Energy consumptions of the investigated multi-family buildings 26
Figure 3-7: 15 climate regions in Germany according to DWD [43] 28
Figure 3-8: Weather data of Berlin-Dahlem for the year 2014 30
Figure 3-9: Heating load profiles of the Reference multi-family residential during heating season (a) January-March, (b) First week of October 31
Figure 3-10: Seasonal heating load duration curve (LDC) of the considered demand levels 32
Figure 3-11: SLP for multi-family residential in the first week of January [7] 33
Figure 3-12: Wind power profile of Eastern Germany in 2015 [7] 34
Figure 3-13: Daily Average Wind Feed-in 2015 34
Figure 3-14: Surplus Signal for controlling the heat pump for the first week of January 35
Figure 3-15: The Flowchart of the load management control unit 36
Figure 3-16: Dimensioning curve of the heat pump in monoenergetic operation [48] 38
Figure 3-17: Simulation Cases: Load Management Strategy applied for different HP Types 41
Figure 3-18: The variation of the blocking hours during the heating season of the year 2014 42
Figure 3-19: Heating curves for considered specific heating demand levels 43
Figure 4-1: GSHP operation under Base-Case and Surplus scenarios in the first week of February 45

Figure 4-2: GSHP monthly baseload electric energy consumption in Base-Case and Surplus Operation Scenarios 45
Figure 4-3: The growth of the adaptation rate of wind feed-in for different dimensions of the GSHP and TES for the reference case 47
Figure 4-4: Logarithmic regression of the results for the reference simulation case..... 48
Figure 4-5: Wind adaptation curves for different system dimensions and heating demand levels..... 49
Figure 4-6: Distribution of the Wind Integration Factor of the GSHP system for the considered demand levels 50
Figure 4-7: Correlation between a_0 and a_1 coefficients and heating demand of the building ($Q_{heating}$)..... 51
Figure 4-8: the impact of changing storage volume for each GSHP on SPF for the reference building 52
Figure 4-9: Variation of the SPF of the GSHP by oversizing the system for the reference building..... 53
Figure 4-10: Distribution of the operation hours of GSHP for the reference building 54
Figure 4-11: ASHP operation under Base-Case and Surplus scenarios during the first week of February . 55
Figure 4-12: ASHP monthly base-load electricity consumption in Base-Case and Surplus Operation Scenarios 56
Figure 4-13: The growth of adaptation rate of wind feed-in for different dimensions of the ASHP and TES for the reference case..... 57
Figure 4-14: Logarithmic regression of the results for the reference simulation case..... 58
Figure 4-15: Wind adaptation curves for different system dimensions and heating demand levels..... 59
Figure 4-16: Distribution of the Wind Integration Factor of the ASHP system for the considered demand levels 60
Figure 4-17: Correlation between a_0 and a_1 coefficients and heating demand of the building ($Q_{heating}$).... 61
Figure 4-18: the impact of changing storage volume for each ASHP on SPF for the reference building ... 62
Figure 4-19: Variation of the Seasonal Performance Factor (SPF) of the ASHP by oversizing the system for the reference building..... 63
Figure 4-20: Distribution of the operation hours of ASHP for the reference building 64
Figure 4-21: WIF comparison between GSHP and ASHP for the reference building..... 64
Figure 4-22: SPF comparison between GSHP and ASHP for the reference building..... 65
Figure 4-23: Heating capacities of variable speed heat pump at different compressor frequencies 66
Figure 4-24: Impact of increasing the storage volume on the compressor frequencies and integrated wind power for the specific annual heating demand of 50 kWh/m². a 67
Figure 4-25: Impact of increasing the storage volume on the compressor frequencies and integrated wind power for the specific annual heating demand of 100 kWh/m². a 68
Figure 4-26: Impact of increasing the storage volume on the compressor frequencies and integrated wind power for the specific annual heating demand of 140 kWh/m². a 69
Figure 4-27: Impact of increasing the storage volume on the compressor frequencies and integrated wind power for the specific annual heating demand of 180 kWh/m². a 70
Figure 4-28: the impact of increasing demand level for the identical system dimensions on the operation hours and WIF of the VSHP 71
Figure 4-29: the impact of increasing storage volume and heating load on the WIF..... 71
Figure 4-30: Variation of the compressor frequencies and integrated wind power for the same storage volume and different demand levels..... 73

Figure 4-31: The impact of increasing the thermal storage volume on SPF 74
Figure 5-1: Oversizing Procedure for single-speed heat pumps supplying multi-family building 78

List of Tables

Table 3-1: Monthly Brine Temperature in Berlin during the winter season 21
Table 3-2: Inputs and Outputs of each operation case of the variable speed heat pump model 23
Table 3-3: Inputs and outputs of the temperature controllers 25
Table 3-4: Demand factors for all day-type categories for TRY4 28
Table 3-5: Annual demands of the reference building 29
Table 3-6: Daily Energy Demands for each day-type for the Ref. Building 29
Table 3-7: Distribution of the day-type categories for the year 2014 30
Table 3-8: Oversizing steps of the heat pump based on daily blocking hours 43
Table 4-1: Variation of adaptation rate of the GSHP by changing the system dimensions for the reference building 47
Table 4-2: Constant of the reference Equation 4-5 for the considered demand levels 50
Table 4-3: Constant of the reference Equation 4-5 for the considered demand levels 60
Table 4-4: Baseline scenario- performance comparison for heat pumps in the reference simulation case 74
Table 4-5: Extreme sizing scenario -performance comparison for the heat pumps in the reference simulation case 75

Abbreviations

Units

J ..... Joul
kJ ..... Kilo joul
kW ..... Kilo watt
kWh ..... Kilo watt hour
MW ..... Mega watt
TWh ..... Tera watt hour

Other abbreviations

ASHP ..... Air Source Heat Pump
CHP ..... Combined Heat and Power
COP ..... Coefficient of Performance
Cap ..... Heat Pump Capactiy
DF ..... Dimension Factor
DHW ..... Domestic Hot Water
DSM ..... Demand Side Management
DWD ..... Deutsche Wetterdienst (German Weather Service)
EU ..... Europian Union
GCHP ..... Ground-Coupled Heat Pump
GHG ..... Green House Gases
GHI ..... Global Horizontal Irradiance
GSHP ..... Ground Source Heat Pump
GWHP ..... Ground Water Heat Pump
HP ..... Heat Pump
KWK ..... Kraft-Wärme-Kopplung
IEA ..... International Energy Agency
LDC ..... Load Duration Curve
MDU ..... Multi-Dewling Unit
SH ..... Space Heating
SLP ..... Standard Load Profile
SPF ..... Seasonal Performance Factor
SWHP ..... Surface Water Heat Pump
TES ..... Thermal Energy Storage
TESS ..... Thermal Energy System Specialist
TRNSYS ..... Transient System Simulation
TRY ..... Test Reference Year
WIF ..... Wind Integration Factor

Nomenclature

Indices

a ..... Annum
ave ..... Average
bui ..... Building
c, C ..... Cold, Cold Reserviour, Heat Sink
comp ..... Compressor
cond ..... Condenser
evap ..... Evaporator
el ..... Elektrisch(Electrical)
h,H ..... Time period (hour), Hot, Heat Researviour, Heat Source
Heiz ..... Heizung (Heating)
max ..... Maximum
min ..... Minimum
TES ..... Thermal Energy Storage
TT ..... Type-Tag (Day-Type)
TWW ..... Trink-Warm-Wasser(Domestic Hot Water)
req ..... Required
w ..... Water

Parameters

C_p ..... Specific heating capacity of the heating medium [kJ/kg.K]
T_{amb} ..... Ambient (Outdoor) Temperature [°C]
ρ ..... Density [kg/m^3]

Variables

W ..... Requierd compressor work for the heat transfer from heat source to the heat sink [kJ], [kWh]
Q_c ..... Heat transfer from the heat source to the heating medium [kJ], [kWh]
Q_H ..... Heat transfer from the heating medium to the heat sink [kJ], [kWh]
T_H ..... Temperature of the heat sink [°C]
T_C ..... Temperature of the heat source [°C]
$\dot{E}_{comp}$ ..... Power input of the compressor [kJ/hr],[kW]
$\dot{Q}_{cond}$ ..... Heat transfer rate of the condencer [kJ/hr],[kW]
$\dot{Q}_{evap}$ ..... Heat transfer rate of the evaporator [kJ/hr],[kW]
$\dot{E}_{comp,wind}$ ..... Wind share of the power input of the compressor [kJ], [kWh]
$\dot{E}_{comp,baseload}$ ..... Base-load share of the power input of the compressor [kJ], [kWh]
$Q_{Heating}$ ..... Annual specific heating demand of the building [kWh/m^2.a]
DF ..... Dimension factor of the heat pump heating system [m^3/kW]
C_p ..... Specific heating capacity of the heating medium [kJ/kg.K], [Wh/kg.k]
V_{TES} ..... Thermal Storage Volume [m^3]
$\dot{Q}$ ..... Heating Power [kJ/hr],[kW]

1. Introduction

1.1.Wind Energy: Opportunities and Challenges

In many developed countries wind power is considered as a key renewable energy technology in achieving the goals of reducing greenhouse gas emissions and relieving the dependency on fossil fuels. During the last decade, a considerable drop in the cost of renewable energy systems including wind energy created an economically viable situation for the installation of renewables and accelerated the generation of wind power. If the trend continues and renewables replace conventional power plants, this will lead to a considerable reduction of grid feed-in tariffs. According to the International Energy Agency (IEA), by the end of 2015, the entire installed capacity of wind energy worldwide reached over 432 000 MW. The top five countries with the highest installed capacity of wind energy are illustrated in Figure 1-1:

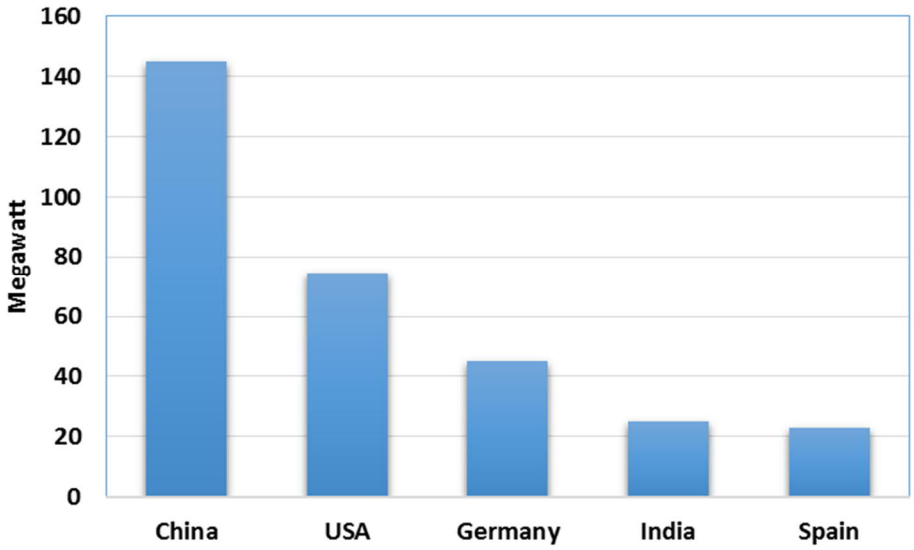

Figure 1-1: Leading countries worldwide by wind power installed capacity 2015

European countries combined reached a total installed capacity of 153.7 GW in 2016, which indicates that wind energy now overtakes coal as the second largest form of power generation in Europe [1]. Considering 12.5 MW of wind power capacity was installed in 2016, wind energy generation reached over 300 TWh and covered almost 10.4% of the EU's electricity demand. The quantity of wind turbine installations in Germany represents 44% of the entire EU wind turbine fleet. With 25980 wind turbines installed by the end of 2015, Germany reached a total installed capacity of 41,651 MW. Figure 1-2 shows the growth rate of wind power installations during 2000-2015 in Germany.

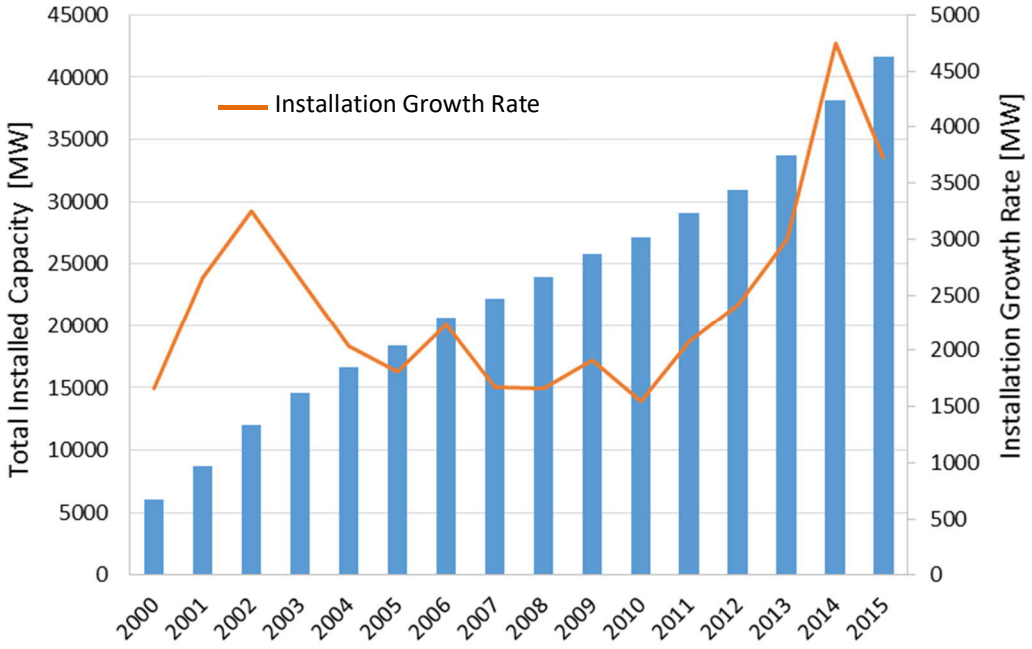

Figure 1-2: Wind power installation and its growth-rate in Germany

Currently wind power has more than 13% of the 30% share of renewable energies in gross electricity production in Germany. However, because of the fluctuating and only partly predictable nature of wind, effectively integrating large-scale wind power is challenging. If the intermittent wind power generation were applied as baseload power in the grid, this would lead to a destructive instability in the power network and a consequent mismatch between the supply and demand sides. A study carried out by the German Federal Association of Wind Energy (BWE[1]) shows that until now wind turbines have been affected mostly locally, in some cases considerably, by feed-in management. At least 1.6 GW of installed wind power was affected by feed-in management in 2009; depending on the network operator, it varies between 3% and 42% of the installed wind power. The reason is most probably overloading in the high-voltage or medium-voltage networks. Since more than one-third of Germany's wind turbines are installed in the eastern side of the country; this concentration of generating capacity regularly overloads the region's electricity grid. According to the 50Hertz Transmission GmbH, the major power network operator in north and east of Germany, wind power surplus threatens electricity transmission with power outages and accordingly blackouts; in extreme cases the produced power by conventional power plants and windmills is three to four times the total amount of actual consumption (See Figure 1-3). At the moment in order to prevent these fluctuations and imbalance between supply and demand that might cause blackouts, the renewable energies and respectively wind energy feed-in have to be restricted by the grid operators during times of impending overload on the grid. The amount of reduced renewable energy in 2013 was 554.8 GWh in Germany to curb grid overload which was an increase of 44% in comparison with 2012

[1] Bundesverband WindEnergie e.V. (BWE)

[2]; considering the average annual demand of 4000 kWh/residential unit, over 140,000 households could be supplied by this reduced renewable energy. Although this energy is not fed in the power grid, the plant operators paid for the management of mitigating grid overload and therefore there is an overall cost associated with the regulating process. This cost was approximately 44 Million Euro in 2013[3]; this feed-in management represents at best a short-term transitional solution. On the other hand, an accelerated network expansion seems to be a very costly and time taking solution. Since this problem is likely to increase significantly in the future, the optimal long-term solution such as transformation and conversion systems should be applied to ensure the largest possible integration of the wind energy in energy networks.

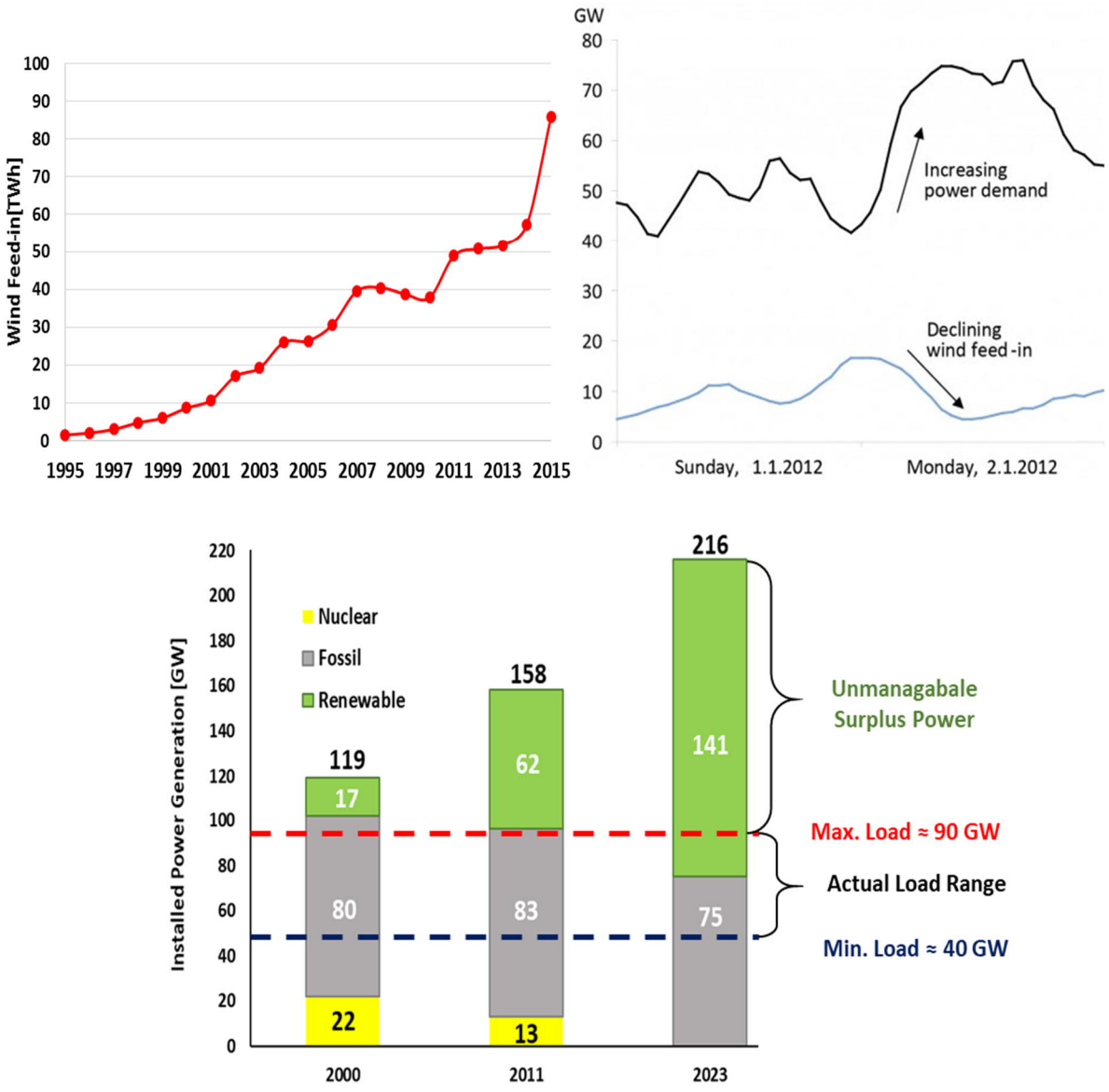

Figure 1-3: Growth rate of Installed power generation and corresponding surplus power prediction in Germany [4]

According to the German government's energy and climate roadmap (Energiewende), by 2025 renewable energies are expected to meet 40-45% of gross electricity consumption and at least 80% by 2050. For wind energy, the target is to reach an annual installation growth rate of 9400 MW in 2020 and 17900 MW by 2030 [4]. This represents the importance of a resistant and reliable solution for the upcoming challenges in the German energy network.

1.2. Energy Utility in Berlin

The electricity network operator in Berlin is Stromnetz Berlin GmbH, which is a subsidiary of the Vattenfall Europe Sales Group. At the moment, 11 power plants in Berlin including GuD Mitte, Charlottenburg, Lichterfelde, Klingenberg, Reuter West, and the Moabit are responsible for supplying electricity to the power grid. [6]

Except for the Reuter West power station, which feeds into the high-voltage grid of 50Hertz Transmission with 380 kV, the power is fed in the low-voltage grid of Berlin with 110 kV, the feed-in of the renewable energies is also carried out within the distribution network with a maximum of 110 kV. According to the annual report of Stromnetz Berlin GmbH, in 2015 the annual electricity consumption in Berlin amounted to 13.8 TWh, but only about 2.5 % of this amount was supplied by renewable sources, which were mostly from Biomass and solar energy. Over 38% of the power demand comes from households. Since the generation capacity of the power plants in Berlin is not able to cover the consumption load, electricity is imported through a high voltage transmission network operated by 50Hertz Transmission GmbH, which is supplied by neighboring federal states such as Brandenburg and Hamburg. For instance, in 2014 the entire feed-in from local power plants was 4.21TWh, while the overall gross electricity demand reached 14.51TWh; therefore, almost 9.9TWh was imported by the 50 Hz transmission network [7]. Since the amount of the power feed-in from the local distribution network in Berlin has been never sufficient to cover the demand level, the state of Berlin is considered as "energy sink", which is constantly dependent on the neighboring networks for its power supply. This indicates the critical situation of energy supply in Berlin.

On the other hand, for heating, the entire demand in Berlin is covered mainly through three variants: District heating networks, local heating networks, and individual heating systems. In the case of district/ local heating networks heat is supplied by heating power plants that mainly consist of natural/bio gas power plants, coal power plants and oil power plants. The overall heating power of local heating power plants in Berlin is 8000 MW, of which the heat is supplied by these power plants as shown in Figure 1-4.

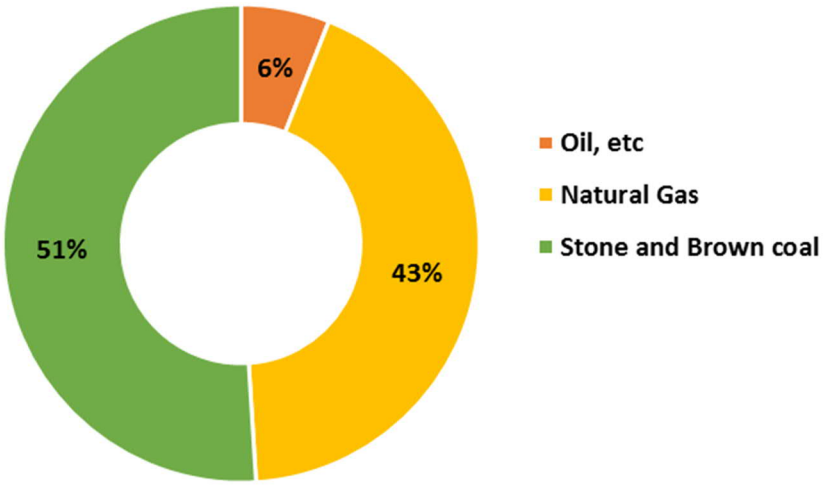

Figure 1-4: The distribution of the heat power plants in Berlin

Since a majority of the existing power plants and individual heating systems in Berlin are old, having low efficiency and high rates of emissions, it seems advantageous to substitute them with new technologies such as heat pumps and combined heat and power systems. A combination of heat pumps and local heating networks has been already tested and proven in Denmark and Sweden and represents a strong alternative for the future supply of urban heating [8].

1.3. Research Motivation

Considering the destructive impact of the power generated by the high concentration of wind power installations in the northern and eastern parts of Germany, to stabilize the grid, a reliable and practical load management solution is fairly necessary to overcome this problem. Since the amounts of wind are particularly high during the winter season (heating season) in Germany, a significant potential of wind energy is available during this period. On the other hand, heating demand reaches its maximum during winter, which creates peak time and places considerable pressure on the power utility to supply this demand.

One of the promising tools that accelerates the integration of a significant part of wind generation is to electrify a heating section to benefit the large potential of wind power during winter to supply the peak heating demand. A heat pump heating system, in cooperation with thermal energy storage, is a suitable combination and strong alternative for electrification of the heating sector. Individual heat pumps, in connection with thermal storage tanks, the building structure, and the central heating system can provide a distributed flexible electricity demand profile. Compared to conventional heating systems, such as boilers, which are restricted to satisfying the demand for heat, heat pump operation can be shifted in time, representing electricity demand that can be shifted. The aim of this PhD is to evaluate to which extent heat pumps complemented by heat storage can support the shifting and integration of wind power.

Moreover, the focus is to investigate the impact of dimensioning of the heat pump and thermal storage on the energy-saving and load shifting potential. The system is operated under a specific control scenario considering the time profiles of electricity supply and heat demand for different cases.

Having the highest population (over 3,480,000 consumers and 1,680 two and multifamily dwellings [5]) and highest rate of heat demand (478 m² low voltage supplied area) on the one hand, and the highest share of conventional power plants and lowest penetration rate of wind power in the grid network, on the other hand, Berlin is a critical energy sink for the power supply network in northern Germany. Although Berlin only has 5 MW of wind power installation, it would significantly benefit from the neighboring states such as Brandenburg and Niedersachsen with, which have the highest wind power installation capacities (see Figure 1-5). According to the Office for Statistics of Berlin Brandenburg, the living area in Berlin is about 137 km². This area consists of 1,883,161 apartments in 316,047 residential buildings as well as 28,566 apartments in non-residential buildings, which are mostly not used for residential purposes. From the entire residential buildings, there are 161,729 single-family houses (51.2%), 16,976 two-family houses (5.3%), 136,762 multi-families residential (43.3%) and 580 dormitories; therefore, excluding non-residential apartments about 88.4% of the entire apartments belongs to multi-family residential [39]; it points out the significance of the multi-dwelling units in heating demand of Berlin. This reason is the main motivation for choosing Berlin as a case study for this PhD work. By flexibly operating heat pumps and heat storage for residential and commercial sections in Berlin, the integration rate of wind power in the energy network of Berlin will be massively increased, and at the same time, the share of conventional power plants in the energy supply and the corresponding CO_2 and GHG emissions will be reduced as a consequence.

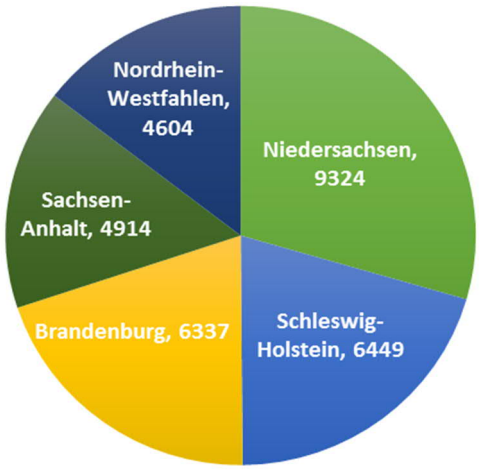

Figure 1-5: The wind installation capacity of top 5 states of Germany in GW

2. Research Background

2.1. Heat Pumps and Their Role in the Heating Sector

2.1.1. Basic Principals of the Heat Pump Performance

A heat pump is a device that transfers energy from a low-temperature source to a higher temperature sink. It differs from a pure refrigeration cycle in that the end result of the application could be either to heat or cool depending upon the direction that the refrigerant is currently flowing through the system [10]; so, heat pumps offer an energy-efficient alternative to cover moderate heating and cooling needs. Basically, the heat pump cycle is the same as the refrigeration cycle but works in the opposite direction means that by adding work W heat is extracted from a low-temperature heat source (Q_c) and rejected to a higher temperature heat sink(Q_H) as it is seen in Figure 2-1. In simple word during cooling season heat pumps are able to cool down space by transferring heat from the place to the warm outdoors whilst during the heating season by transferring heat from the cool outdoors to place, warm-up the indoor space.

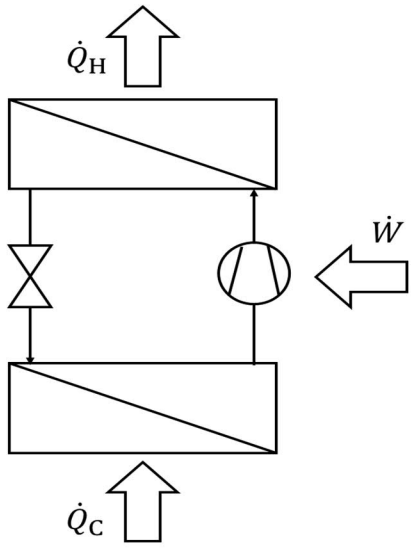

Figure 2-1: Work principle of a heat pump

The thermal balance of the heat pump for an adiabatic system can be defined as:

$$\dot{Q}_H = \dot{Q}_C + \dot{W} \qquad \textit{Equation 2-1}$$

The efficiency of the heat pump is determined by the Coefficient of Performance (COP), which is the ratio between the useful heat rejected to the energy sink to the power required, see Equation 2-2:

$$COP = \frac{\dot{Q}_H}{\dot{W}}$$ *Equation 2-2*

As theoretically the heat pump is assumed to operate between the condensation temperature (T_H) and evaporation temperature(T_C), in reversible isotropic condensation and expansion, the upper limit of the COP can be expressed by Carnot Coefficient of Performance COP_C as follows:

$$COP_C = \frac{T_H}{T_H - T_c}$$ *Equation 2-3*

But in reality, due to the heat losses from the compressors and working liquid (refrigerant) in heat exchangers, there are irreversibilities and because of the temperature differences in the heat exchangers $(\Delta T_H, \Delta T_C)$ the real temperature levels that the heat pumps operate between are: $T_C - \Delta T_C \; and \; T_H + \Delta T_H$. Thus, in order to improve the thermal performance of the heat pump, these temperature differences must be reduced as much as possible.

Depending on the type of heat source of the heat pump systems, two types of heat pumps are determined: air source and ground source. In Air source heat pumps the ambient energy in outside/exhaust air is used for heating, cooling, and hot water preparation, the heat in ground source heat pumps is extracted from the energy stored in the ground, surface or seawater through borehole heat exchangers drilled in the ground as well as vertical or horizontal collectors. For common residential applications heat is distributed and rejected to the indoor air through hydronic distribution systems as radiator and floor heating systems or for air-air heat pumps by air using fan coils or ventilation systems. As this research focuses on the potential of the heat pump system to integrate wind power in the heating network and intra-day power balancing of the low/medium voltages grid. The heat pump has been focused as the heart of the heating system and has the main role in supplying heat demand and integrating wind power for this purpose. Considering the Equation 2-2 the electricity consumption of the compressor $(\dot{E}_{comp})$ in the heat pump and the heat capacity of the heat pump represented by condenser heat power $(\dot{Q}_{cond})$ are formulated as follows in Equation 2-4:

$$\dot{E}_{comp} = COP * \dot{Q}_{cond}$$ *Equation 2-4*

2.1.2. Ground Source Heat Pumps

The ground-source heat pump (GSHP) is a general term for a variety of systems that use the ground, groundwater, or surface water as a heat source and sink. Basically, a ground source heat pump system consists of two circuits: 1. Primary circuit and 2. Secondary circuit or heating circuit.

In the heating process, the heat is removed from the primary loop by the heat pumps and is delivered through secondary loop to the building; the primary circuit is between the heat source (ground) and heat pump where heat is extracted from the ground and transferred through an evaporator to the working fluid of the heat pump. The secondary circuit is located between condenser of the heat pump and heat sink or consumption point, in this case thermal storage tank, where heat is transferred through the condenser to the secondary working medium which will be stored in the storage/buffer tank and used to supply hot water and space heating demands. Three main technologies applied to transfer the heat from the ground source to the heat pump through ground collectors the heat from the top layer of the earth's crust as a source of heat is harvested and transferred to the working medium of the heat pump whilst in ground-coupled heat pumps (GCHPs) also called geothermal heat pumps the heat is captured from lower layers of underground through closed-loop piping systems including a heat exchanger installed inside a borehole; In the other type called ground-water heat pump (GWHP) there is an open-loop piping system with water well used to capture or reject the heat from/to the ground; In surface-water heat pumps (SWHPs) closed-loop piping coils or open-loop systems connected to lakes, streams or other reservoirs are responsible for this.

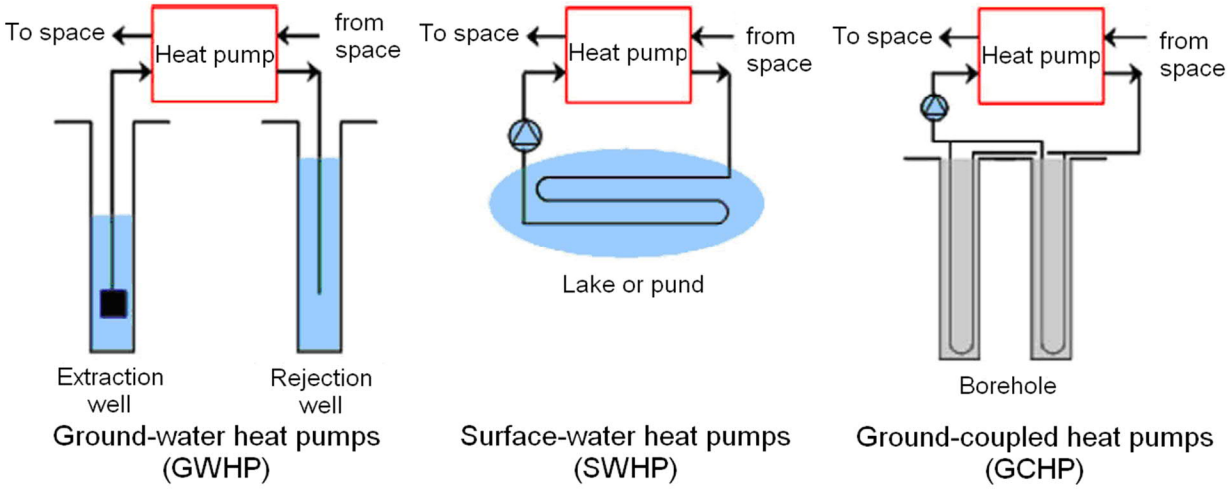

Figure 2-2: Three main methods of using groundwater heat [34]

In cold climates such as northern Europe due to the fact that ground source heat pumps are more efficient in cold temperatures where the ground temperature is relatively constant all over the year, they are mostly used for residential heating and sanitary water. Whilst in Mediterranean climate air source heat pumps are applied as they perform best in mild temperature where the differential between seasonal temperatures is not very important. Comparing main two technologies of heat pumps, as stable temperature is necessary for efficient operation of the heat pump, taking the advantage of consistent temperature of the ground, ground source heat pumps offer more efficient heating operation in wintertime than air source heat pump; However large

required space for ground source heat pumps as well as high installation costs are main limitations that make it infeasible for small unites, indoor use and single-family houses.

2.1.2.1. Geothermal Potential in Berlin

The solar irradiation warms the near-surface ground, and this accordingly warms the atmosphere and the underground. The Global Horizontal Irradiance (GHI) in Berlin amounts to an average of 750 W/m². Different surface types and elevations, as well as both seasonal and daily changes to the amount of sun exposure, lead to local and time deviations from the median value. As it is shown in the Figure 2-3, in Berlin, the groundwater temperature from a depth of 25 meters is constant about 12.5°C; This depth is called neutral zone, where no temperature change can be measured during different seasons of the year. Depending on the thermal conductivity of the substrate as well as its thermal current density, the temperature increases continuously with increasing depth. For Berlin from the neutral zone values of 2.5 to 3°C per 100m depth can be assumed [35].

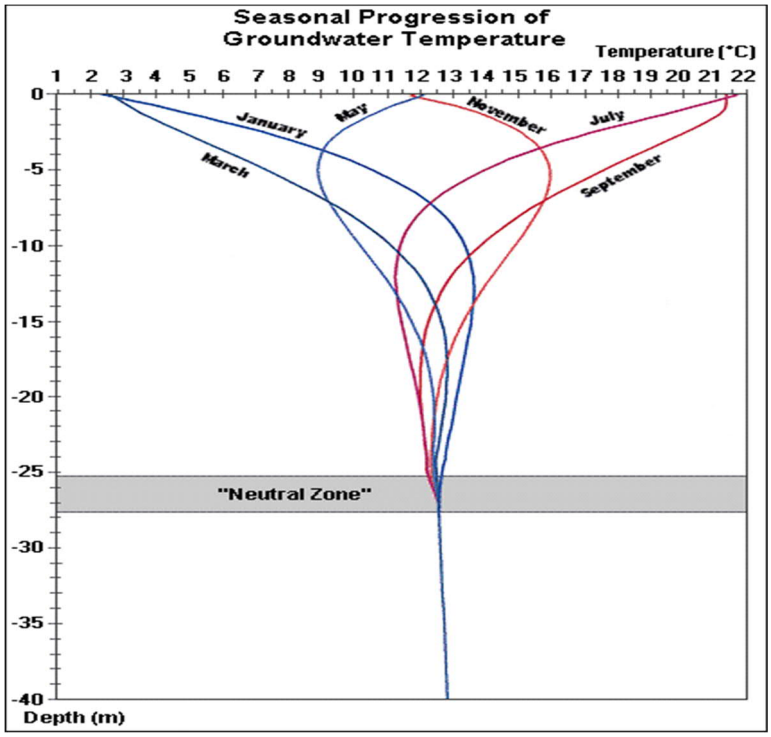

Figure 2-3: Seasonal Progression of Groundwater Temperature [36]

During a two-year field test called "Heat Pump Efficiency" conducted by BINE, 68 ground source heat pumps, installed for new buildings, were tested. In which 50 systems were operated with borehole heat exchanger and 18 with ground collectors. This investigation showed that the source water temperature of these heat pumps fluctuates between 4 °C and 13 °C in the course of the year [37]. Figure 2-4 shows the source water temperatures and the supply temperatures of the

secondary cycle, as well as the annual performance factor of the heat pumps which are measured for all considered plants.

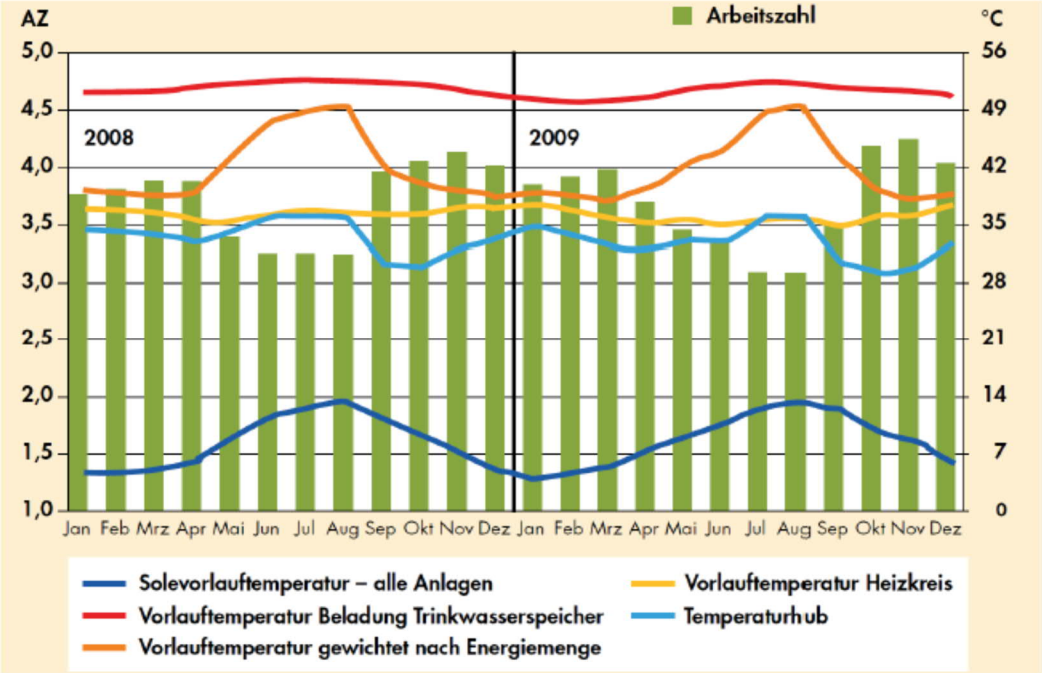

Figure 2-4: Heat pump field test of BINE [37]

In another experiment, 70 ground source heat pump systems installed for partly renovated and not-renovated buildings, as a replacement for oil boilers, were tested. The study indicated that while the average annual performance operation of 3.9 was achieved by heat pumps in the new buildings, this for the heat pumps in the existing buildings was 3.3. On the other hand, it is also understood that the seasonal operation of the systems with borehole heat exchangers is more stable than the ones with ground collectors. Furthermore, since in winter the source water temperature for borehole heat exchangers is higher, 6°C compare to 3°C for ground collectors (See Figure 2-5), their efficiency is improved; For these reasons applying heat pumps with borehole heat exchangers for supplying heating demand during wintertime is advantageous.

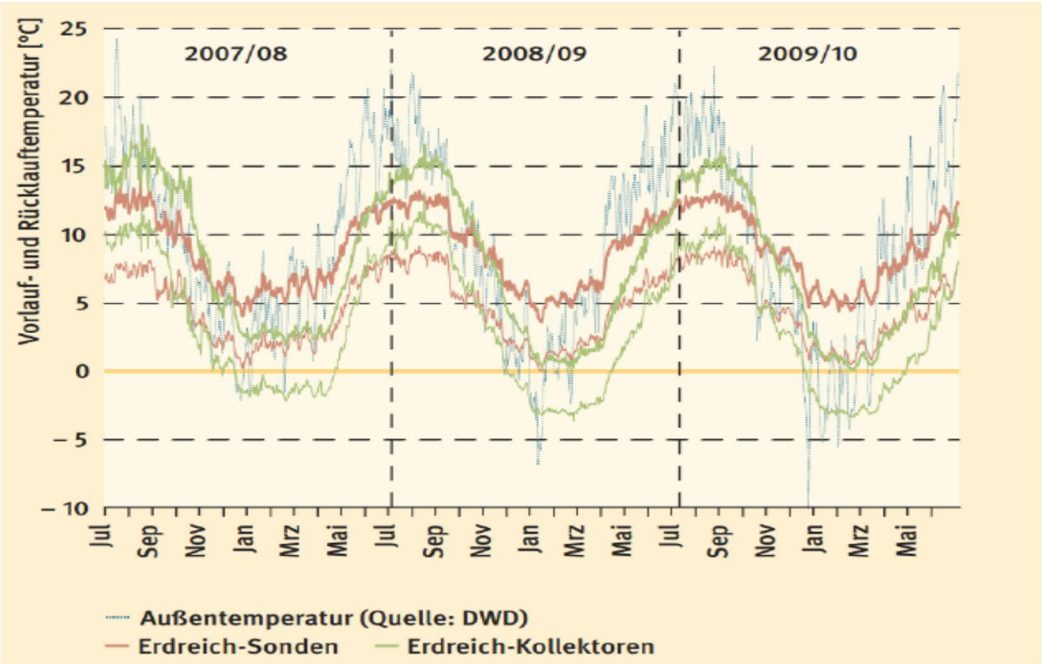

Figure 2-5: The source temperatures of all ground source heat pumps tested in the monitoring project [37]

2.1.3. Large Scale Heat Pumps and Their Applications

Previously some concepts of large-scale heat pump system have been introduced by Scandinavian HP manufacturers laying on heat recovery from an external source such as ground source (geothermal), wastewater, or other external low-temperature heat sources. The most possible application of the large HP systems is in district heating where HP can be installed with an existing CHP plant. Furthermore, large HP's can be applied in several industrial processes using both waste heat flows such as wastewater, hot humid air, condenser heat from refrigeration systems and heat consumers such as process water, central heating systems, blanchers, dryers, etc., within the industrial plants. These types of heat pumps can be possibly used in combination with CHP and possibly a cold storage (Figure 2-6).

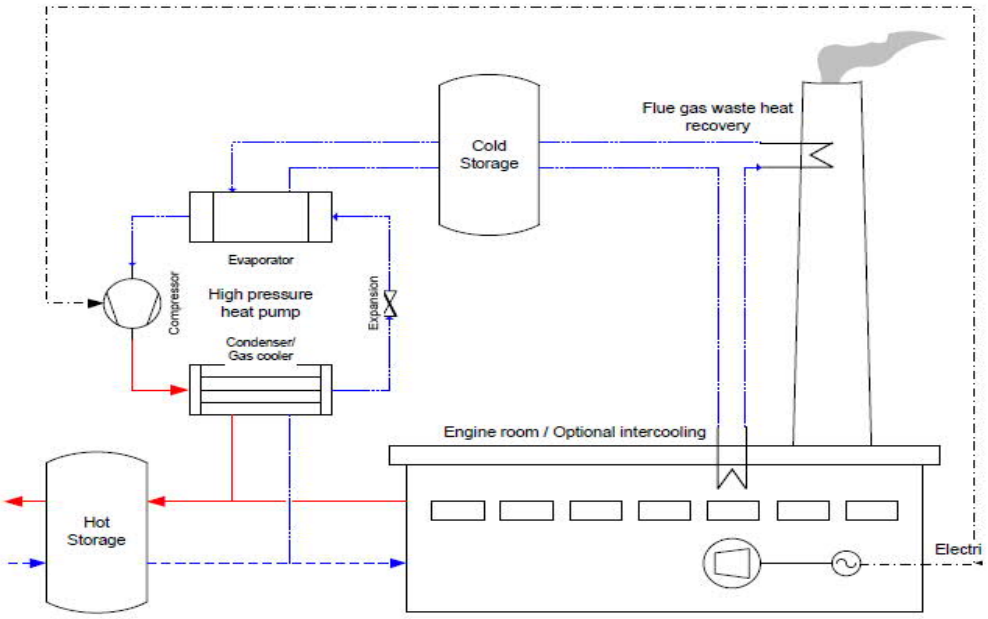

Figure 2-6: HP using the waste heat of the flue gas of industrial plant, in combination with CHP and Cold/Hot Storage [11]

Basically, waste heat flows with a temperature level lower than the heat consumers do not offer a possibility for direct heat exchange. It may then be an interesting option to increase the temperature level using heat pumps. The efficiency of the system will depend on the temperature levels, power and hours of operation, thereby heat pump may be established anywhere on the district heating network using the grid's return flow as a low-temperature heat source. This alternative solution will cause a reduction of heat losses in the district heating network.

2.1.4. Role of the Heat Pump in German Heating Market

In the 27 EU member states, building sector consumes 68% of the total final energy consumption where space heating is responsible for 70% of this share [12]. This represents the substantial flexibility potential of load management in the residential sector. Given the fact that the heat pump technology has been developed constantly and the efficiencies of heat pumps have increased by 50-100% during last 30 years [13], heat pump systems turned to be the strong and competitive alternatives for conventional heating systems to supply the heating demands more efficiently. Over the last years use of the heat pump for efficient heat generation in the residential sector, especially for all new building in the EU, is expected to rise to have nearly zero-energy by the end of 2020 [14]. In Germany about 35% of the end-energy is consumed for heating purposes in the residential section, Figure 2-7 shows the shares of the heating sources for supplying German housing stock.

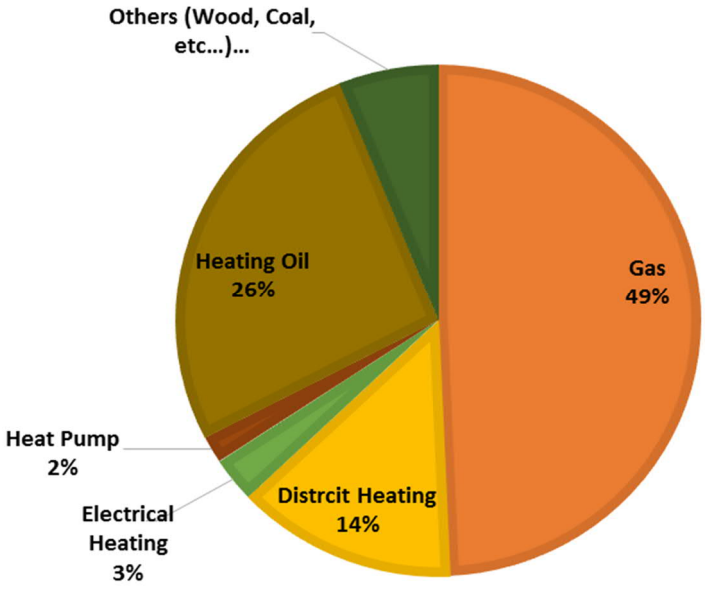

Figure 2-7: Heating structure of the housing stock in Germany in 2015

Since one of the main focus of the energy roadmap in Germany is to increase the energy efficiency and energy saving potential in this section, the role of the electrifying heating systems and increasing the efficiency by heat pumps is quite crucial. The heat pump market in Germany is continuously growing until 2015 about 61,500 heat pump heating units with a power demand of 2.4 GW were installed which is still increasing [15]; Figure 2-8 shows the market growth during last 5 years:

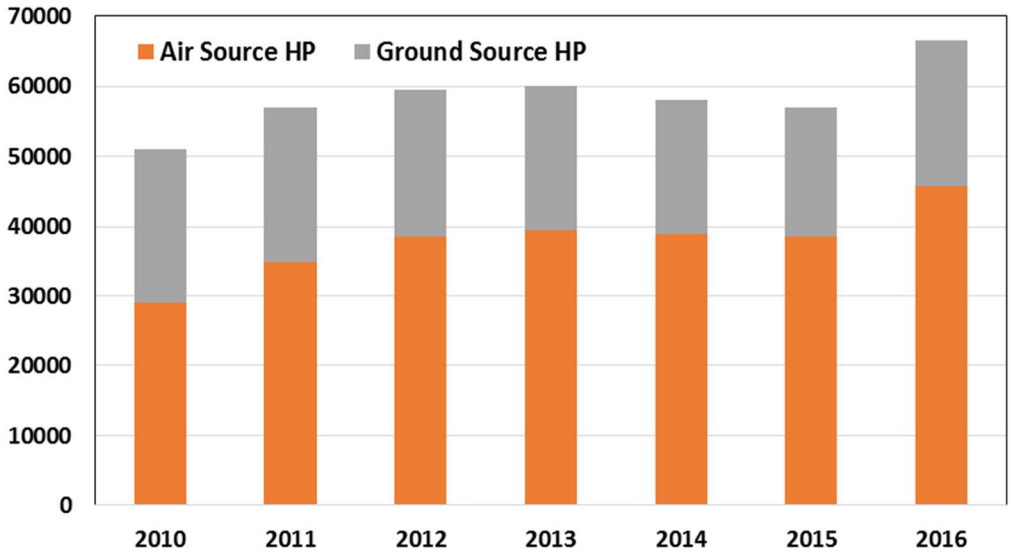

Figure 2-8: Sales Figures of ground and air source HP systems in Germany during the last 5 years

By 21.8% increase in 2016 compared with the previous year, about 20,700 GSHP's are currently installed in Germany, while this rate for air source heat pump (ASHP) is 14.5% which means 45,800 installed ASHP's by the end of this year; Almost 21 % of 281,000 new residential units in Germany are supplied by heat pumps, whilst less than 2% of the entire residential section is supplied by heat

pumps. These numbers represent the significant role of HP systems in German heating market that along with an effective load management strategy would create a considerable potential for highly efficient heating and renewable electricity adaptation.

2.2. Load Management

Currently, electric utilities adjust the amount of power feed-in by means of controlling conventional (baseload) power plants at certain generation levels on the basis of the electricity demand prognosis; however, adapting supply to the demand would be fairly restricted, and to some extent, impossible if the base load is supplied by the fluctuating energy sources. The process of matching energy supply to the demand is called load control or Demand Side Management (DSM). The key objective of this method is to balance the generation load profile, increasing supply/demand flexibility and avoiding mismatch between supply and demand sides through efficient use of the excess generated power, also called surplus power, in the electricity network, which would consequently end up accelerating the integration of the fluctuating renewable power sources. Some methods of DSM are illustrated in Figure 2-9.

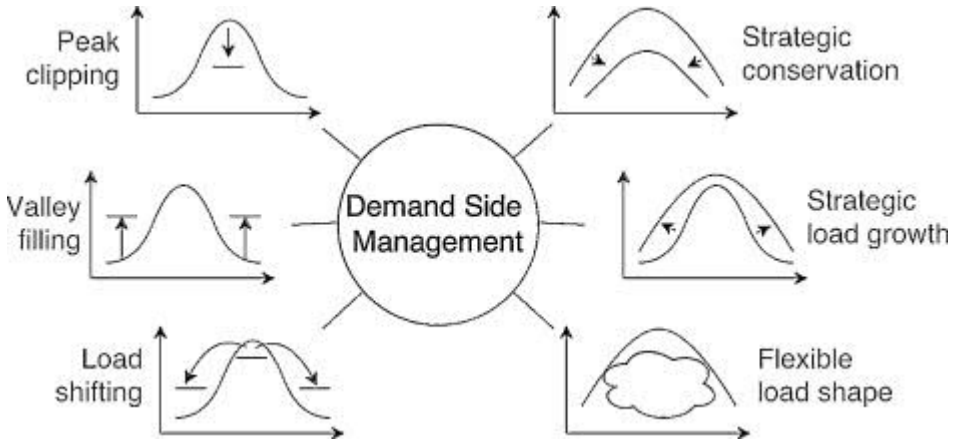

Figure 2-9: Different Types of Demand Side Management [49]

One of the primary solutions for demand-side management aiming to generate flexible load profiles is to modify consumer behavior through various methods such as financial incentives and flexible feed-in tariffs, as well as consumer education; however, during past few years, it has been proven that due to the negative impacts of this method on consumer lifestyle and comfort level, its effectiveness was limited and did not have significant effects on load shifting and behavioral change of consumers; Recently, an advanced and promising technical method towards tackling the main goal of DSM has been introduced. It is based on smart controlling electrical appliance and consumers during peak and off-peak hours and actively applying consumers to balance load

profiles. For instance, during an overproduction period, the consumers, such as heat pumps, are switched on to harvest the surplus electricity, while during peak consumption, they are switched off or reduce certain consumers. Therefore, developing an intelligent energy load management is necessary to achieve a reliable energy supply through intermittent renewable energy sources. However, due to the constant day-night electricity feed-in tariffs in Germany at the moment, it is not possible to actively carry out the DSM for private households and adapt the electricity supply and demand [9]. Nevertheless, there is significant potential to shift loads and save energy in the heating sector through various energy storage technologies without negative impacts on the comfort level of consumers. In this case, electrifying the heating sector besides reducing fossil fuel consumption and mitigating CO_2 emissions could offer considerable potential to relieve the electricity surplus and adapt more renewable electricity.

2.2.1. Demand Side Management through Heat Pump and Heat Storage

A combination of heat pump and thermal energy storage could be considered as one of the stronger alternatives for conventional heating systems in this strategy. A heat pump when combined with a thermal storage tank (TES), offers the possibility of decoupling heat generation from heat consumption. One of the main purposes of using combined HP and TES system is to enable the flexible time control of the HP and provide the advantage of consuming a low electricity tariff during off-peak hours as well as integrating renewable electricity. The following relevant topics have been mainly focused on in previous research.

Shifting loads from peak time to off-peak time by charging the DHW storage tank during the night is one of the solutions given in previous research works. Since SH demand depends on the $T_{indoor\ air}$, shifting SH load varies, depending on the outdoor temperature (T_{amb}) and decreases by increasing the $T_{amb.}$ In this area, a number of previous studies have focused on demand-side management (DSM) for a single building through various optimal and flexible control strategies for individual HP and TES [16,17,18]. For instance [18] focused on load shifting by the heat pump and thermal storage where the reference temperature-controlled HP is compared with the operator-based control strategy. This is based on day-ahead storage and price-based control scenario where the heat pump with a TES system is operated by considering the day-ahead electricity price in the low voltage grid. By introducing the minimal operation time of the compressor and thereby, the daily flexible (shiftable) hours of the HP it indicated that the average load shift in price control strategy is more than the operator control strategy, especially during cold weather (below –10° C).

2.2.2. Control methods for operating heat pumps

Some other studies investigate specifically the different control methods for single and variable speed compressors of the heat pump [19,20,21]. Capacity control in a heat pump system has been

analyzed by several authors [22,23,24]. The energy-saving potential of capacity control heat pump heating systems has been initially introduced by [25], where through a dynamic model of hydronic heating systems validated by experimental results, the seasonal performance factor (SPF) of the system has been compared between continuously capacity-controlled HP and intermittently controlled HP and what is achieved with steady-state models. Considering different factors such as thermal inertia, temperature levels and control dead bands, it indicates that the COP of the HP is reduced in dynamic model compared to the static model and despite very little changes caused by changing thermal inertia and control dead-band, changing the temperature levels from 55/45 °C to 35/28°C increased the SPF of the system by 30-35 %.

Later, variable speed heat pumps and the corresponding control strategies, have been investigated by [26] where variable-speed heat pumps have been introduced like a system that can perform in different capacities according to the desired demands. They are considered a serious alternative to conventional on/off controlled heat pumps. [27] studied the seasonal performance of a system equipped with a variable speed compressor heat pump in comparison with a mono-compressor and multi-compressor heat pump. Considering the partial load effects, they suggested different approaches for optimal sizing of the heat pump in different systems.

2.2.3. Integrating renewable electricity through the heat pump and heat storage

The focus of the remainder of the recent research is on developing and applying various scenarios, such as operation and sizing scenarios, that aim to integrate renewable electricity, mostly photovoltaic, through an HP system; In this regard, different system configurations have been evaluated and effective factors have been investigated [28,29]. As an example [30] has developed an optimal sizing procedure with respect to the air-source HP system operation considering space heating/ DHW load profiles, annual renewable electricity generation and variable electricity prices aiming to increase the photovoltaic self-consumption of the HP coupled with TES. Different building models with the various number of inhabitants were implemented in the model to evaluate the self-consumption potential of the system. [31] also investigated the same approach through demand-side management by means of so-called real price control of the HP and the level of the local electricity generation from photovoltaics. It has been ensured that through the proposed control strategies the relevant money savings reaches up to 30% whilst the energy self-consumption is increased up to 12% for exported electricity and 22% for imported electricity. [28] and some other articles focused on integrating wind power through the heat pump and thermal storage for heating purposes. (Figure 2-10)

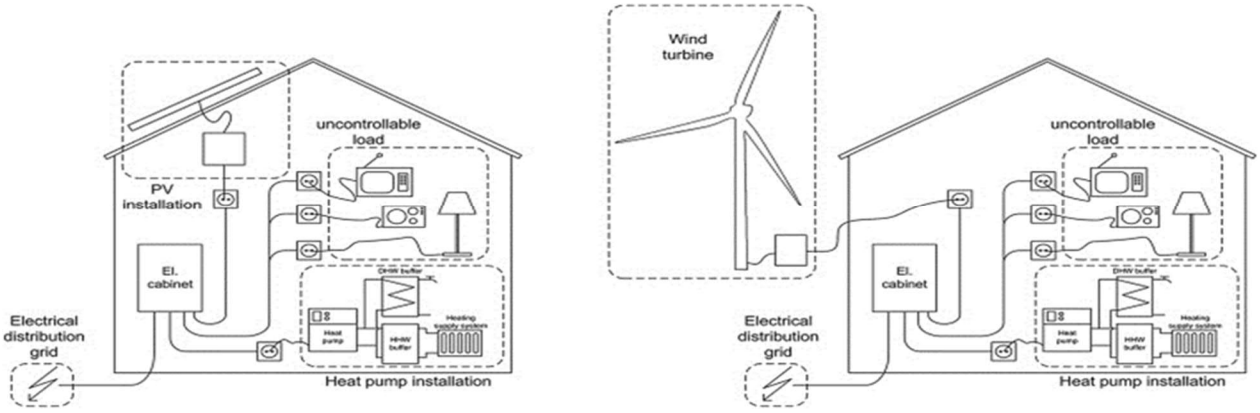

Figure 2-10: Using heat pump in residential buildings for integrating more wind energy for heat supply [28]

The aim of this work is to develop a load management strategy for heat pump system coupled with thermal storage to integrate fluctuating wind electricity for residential heating purposes and hot water preparation as well as investigating the impact of dimensioning of the system on the potential of wind power adaptation. Essentially, the priority of the proposed control strategy is to perform a heat pump heating system when surplus wind power is available, thus, minimizing the power drawn by the heat pump during peak hours. In this case, the heat pump, along with the storage tank, shift the wind overproduction during the off-peak period where there is less demand in order to supply the heat demand during peak period. The next chapter will explain the methodology applied in this research in details.

3. Methodology and Modelling of the Heating System

Basically, the investigated model in this research consists of three parts: 1. Heat supply system: where a heat pump system and accompanied by a stratified thermal storage tank are modeled 2. Building heat load model: where a heat load profiles of different buildings are calculated and 3. Load control system: where the proposed load management scenario alongside the boundary conditions are developed to control the operation of the heat supply system. Each of these sub-models is developed separately and are finally merged together to create the model applied to investigate the different simulation cases for wind energy integration through heat pump system to supply the heat demand of the building. Following sections will highlight respectively the modeling procedure of these three parts as well as the considered sizing strategies and the simulation cases.

3.1. Heat Pump Heating System Model

The heat pump heating system model is implemented in Transient System Simulation Tool (TRNSYS) version 17 [32] and the dynamic simulation is carried out over the heating season (January-March and October-December). The simulation is carried out for the Berlin climate, at a time step of 15 minutes, so that it is feasible to analyze the system behavior accurately during the considered period. The weather data for Berlin is obtained from the climate data center of the German Meteorological Service (DWD[2]) database [33]. Basically, the heating system model in this research consists of a heat pump equipped with a storage tank used to supply the space and sanitary hot water heating of buildings. The simple layout of the system is shown in Figure3-1. The following sections explain the main components of the system simulation in detail.

[1] Deutsche Wetter Dienst (http://www.dwd.de/EN/Home/home node.html)

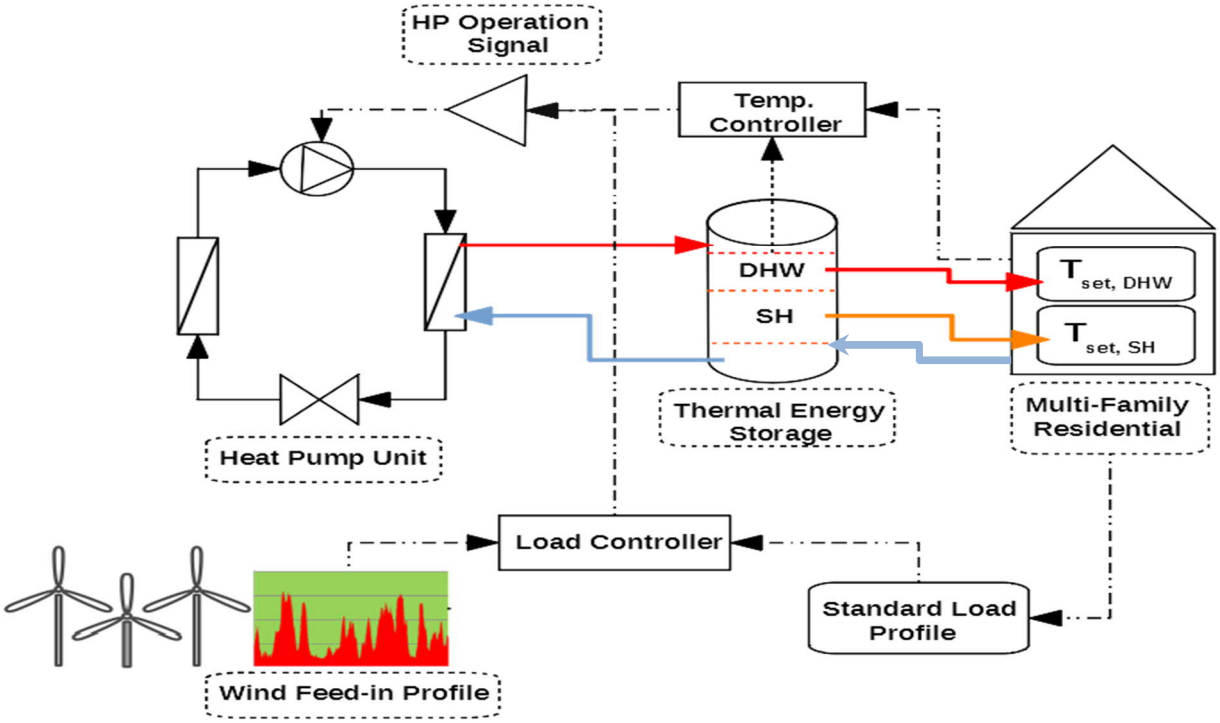

Figure 3-1: Schematic of the heating system describing different blocks of the system

3.1.1. Heat Pump Model

Three types of heat pumps are applied in the heating system model including variable speed ground source heat pump, single-speed ground source heat pump and single speed air source heat pump to study and compare the potential of each type within the considered load control scenario.

Single-speed ground source and air source heat pumps are modeled in TRNSYS using component types 927 and 941 for single stage water/water and air/water heat pumps respectively; This heat pump model is based on a performance map meaning that its results are based on information contained in a user-supplied data files including a file containing cooling performance data, and a file containing heating performance data. Both data files provide normalized capacity and power draw of the heat pump (whether in heating or cooling mode) as functions of entering source fluid temperature $\left(\mathrm{T}_{source,in}\right)$ and entering load fluid temperature$\left(\mathrm{T}_{load,in}\right)$. in this case, normalization means that each value in the data file is a multiplier on either device capacity or device power draw at a rated condition. The rated conditions are entered by the user as parameters to the model. These types operate in temperature level control much like an actual heat pump would; when the user-defined control signal indicates that the unit should be ON in either heating or cooling mode, it operates at its capacity level until the control signal values changes; Following equations show the calculation process of outlet temperature of two primary

and secondary liquid streams of the heat pump model for the heating mode based on rated heating capacity ($Cap_{heating}[\frac{\text{kJ}}{\text{hr}}]$) and rated heating power($\dot{P}_{heating}[\frac{\text{kJ}}{\text{hr}}]$) as well as rated flow rates and specific heating capacities of the fluid streams ($\dot{m}_{source/Load}[\frac{\text{kg}}{\text{hr}}], Cp_{source/Load}[\frac{kJ}{kg.K}]$) as user-provided parameters:

$$COP = \frac{Cap_{heating}}{\dot{P}_{heating}} \qquad \textit{Equation 3-1}$$

$$\dot{Q}_{absorbed} = Cap_{heating} - \dot{P}_{heating} \qquad \textit{Equation 3-2}$$

$$T_{source,out} = T_{source,in} - \frac{\dot{Q}_{absorbed}}{\dot{m}_{source}.Cp_{source}} \qquad \textit{Equation 3-3}$$

$$T_{load,out} = T_{load,in} - \frac{Cap_{heating}}{\dot{m}_{load}.Cp_{load}} \qquad \textit{Equation 3-4}$$

Where $\dot{Q}_{absorbed}$ $[\frac{\text{kJ}}{\text{hr}}]$ is the amount of energy absorbed from source flow stream and $T_{source,out}$ and $T_{load,out}$ are the outlet temperatures of source and load flow streams respectively.

Based on the measurements presented in section 2.1.2.1 the $\text{T}_{\text{source,in}}$ as the input of the heat pump model is assumed to be equal to the average monthly brine temperatures in Berlin; $\text{T}_{\text{source,in}}$'s for the entire heating season are illustrated in the below Table:

Table 3-1: Monthly Brine Temperature in Berlin during the winter season

Annual hours [h]	T_{source} [K]
0	5.33
744	5.82
1416	6.42
2160	9.92
2904	7.67

Variable Speed Heat Pump

Variable-speed heat pumps can perform in different capacities according to the desired demands as a serious alternative to on/off controlled heat pumps. In this system a variable speed compressor is utilized, which operates in different frequencies, varying from 30 to 120 Hz; depending on the demand level. Thereby the heat pump is able to operate in different capacity stages which causes less power consumption of the compressor and consequently higher COP

compared to the single-speed systems [38]. Figure 3-2 is a schematic of the heat pump with a variable speed compressor.

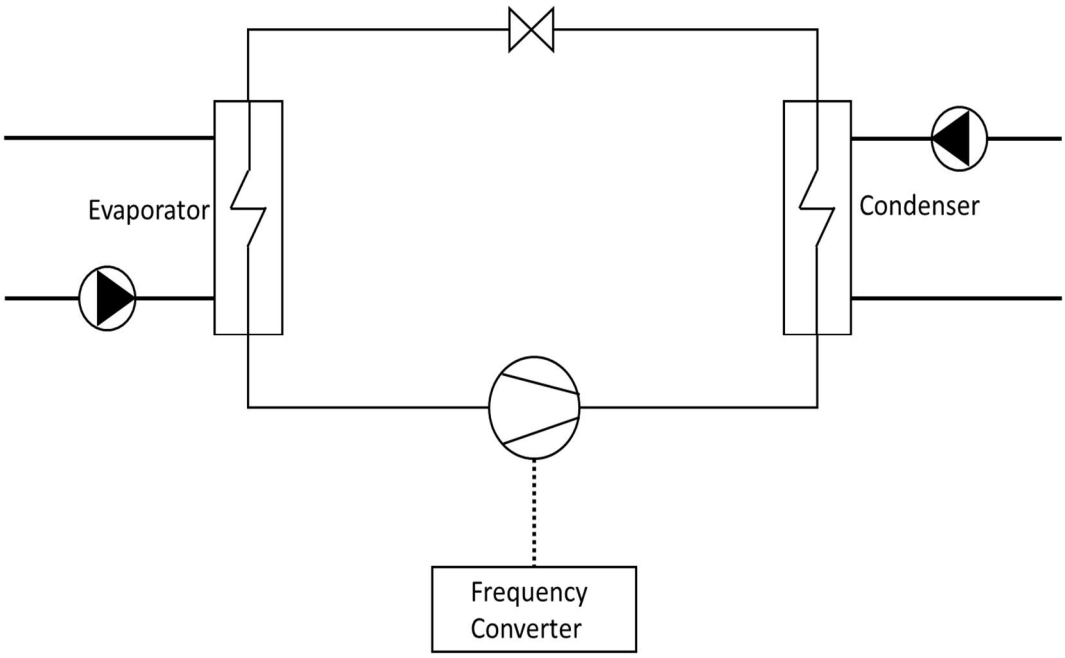

Figure 3-2: Schematic of the heat pump with a variable-speed compressor

Since there is no type for variable speed ground source heat pump in TRNSYS, this type is developed based on a black-box model of variable speed water to water heat pump unit by using the performance map of the unit. The performance map, in this case, means a multi-dimensional table that requires at least three independent inputs to find the model outputs. The content of the table is derived from the experimental studies on the variable capacity heat pumps [26] (Figure 3-3).

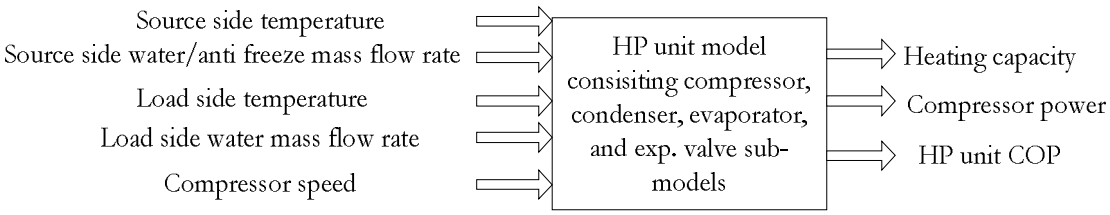

Figure 3-3: Flowchart of the variable speed heat pump mode [26]

Based on this concept, a model for variable speed heat pump is developed in TRNSYS. Since the power demand of the heat pump is provided either from wind-feed-in (surplus power) or baseload electricity, depending on the off-peak hours and availability of the surplus power, the model is designed to have two operation modes: 1. Base-Case where the heat pump is provided by baseload power, given the power utility condition for heat pumps and 2. Surplus-Case where the power demand of the heat pump is drawn from wind-feed in during off-peak hours. Each

operation case consists of a performance map based on the real operation data set of an air to water variable speed heat pump. For each map a 3-Dimensional interpolation is carried out by utilizing Type 581 (multi-dimensional interpolation component) in TRNSYS (see Figure 3-4).

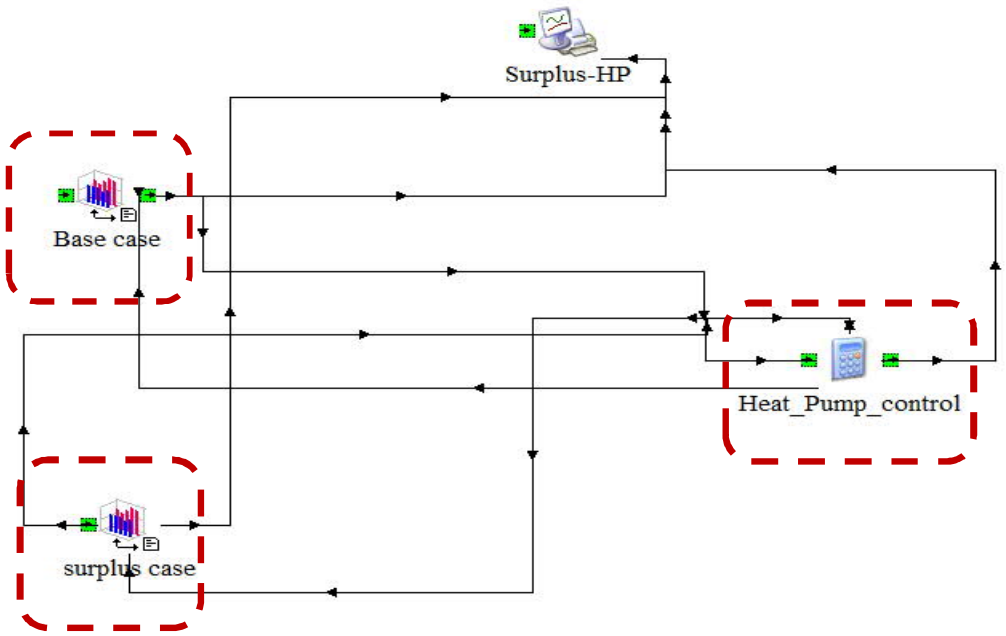

Figure 3-4: The Variable Speed Heat Pump model in TRNSYS

Based on three independent parameters that are given as input to the 3D interpolation components, the wished outputs are generated. The inputs and outputs for Base and surplus cases are seen in Table 3-2:

Table 3-2: Inputs and Outputs of each operation case of the variable speed heat pump model

Operation Scenarios	Inputs	Outputs
Base Case	Q_{req}	Q_{evap}
	T_{source}	$\dot{E}$
	T_{load}	Frequency
Surplus Case	$\dot{E}$	Q_{cond}
	T_{source}	Q_{evap}
	T_{load}	Frequency

Where Q_{req}, Q_{evap}, and Q_{cond} are heating demand of the building, transferred heat from source water by the evaporator and delivered heat to the building by the condenser. $\dot{E}$ stands for the electricity consumption of the compressor and T_{source} and T_{load} are the source and load sides water temperatures of the heat pump. Having the outputs of the Base and Surplus cases, the overall outputs of the variable speed heat pump are calculated. Same as the previous

simulation studies for single-speed heat pumps, in this section, the model of the variable-speed heat pump is coupled with stratified thermal storage, in order to monovalent supply of the heating demand of a certain building.

3.1.2. Thermal Storage Tank Model

The storage tank as an important part of the heating system plays a crucial role in indirect heating configuration, where the heat supply system, in this case, heat pump, is decoupled from the heat demand side by the thermal storage tank. This helps the heat pump to perform independently from heating demand profile and shifting hourly peak loads and consequently balancing consumption load. The stratification of the thermal storage as well as mixing fluid steams, entering fluid temperatures, heat transfer inside the storage tank and heat losses to the outside all have a considerable effect on the system performance. In this system both DHW and space, heating waters are stored in a single stratified thermal storage tank that connects the heat pump to the load side indirectly, depicted in Figure 3-5. The stratified storage tank is modeled in TRNSYS using type 534 developed and validated by Thermal Energy System Specialists (TESS). The tank is divided into the certain number of isothermal temperature "nodes" with constant volume in order to model stratification in storage tanks. In this study, ten isothermal nodes are defined and the maximum 40 K temperature difference in the storage tank is assumed, Figure 3-5. Each node interacts thermally with the nodes above and below through several heat transfer mechanisms such as fluid conduction and natural and forced movements. The heat storage tank has three ports where each port has two nodes for input and output fluid streams. The first port connects the heat pump to the storage tank, the second port includes the supply and return flows of the DHW and through the third port the storage tank is connected to the indoor heat distribution system for SH such as floor heating or radiator.

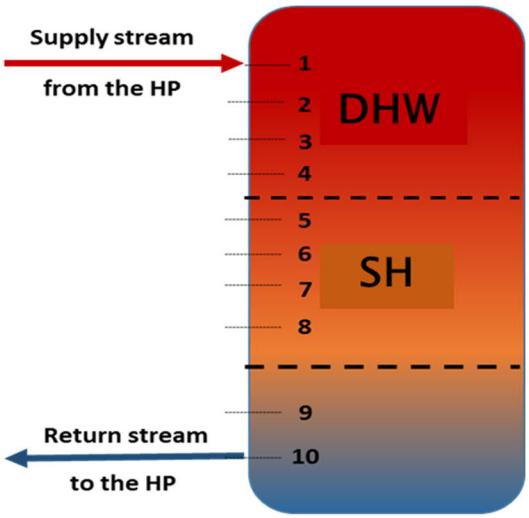

Figure 3-5: Stratified Storage tank with temperature nodes

The necessary storage volume to supply a certain hot water demand is calculated in the below Equation:

$$V_{TES}\left[\frac{l}{\frac{Pers.}{day}}\right] = \frac{\dot{Q}_w\left[\frac{W}{Pers.}\right]}{\rho_W\left[1\frac{kg}{l}\right].Cp_W\left[1.16\frac{W.h}{kg.K}\right].\Delta T_W[K]}$$ *Equation 3-5*

Where V_{TES} is the daily storage volume needed to supply the hot water demand ($\dot{Q}_w$) per person, the ΔT_W is defined as the temperature difference between supply flow and return flow of the storage tank that in the case of the stratified storage tank with a certain number of nodes as shown in Figure 3-5 is taken as temperature difference within the storage tank equal to the temperature difference of top and bottom nodes of the tank:

$$\Delta T_W[K] = T_{top\ node} - T_{bottom\ node}$$ *Equation 3-6*

$$= T_{node\ 1} - T_{node\ 10}$$

3.1.3. Temperature Control

Basically, for the thermal control of the heat pump unit, the hysteresis control method is applied. For this purpose, the on/off differential controller (Type2) is utilized in the TRNSYS simulation studio. Where the control function has a value of 1 or 0 (on or off). The value of the control signal is chosen as a function of the difference between upper and lower temperatures T_h and T_l, compared with two dead band temperature differences DT_h and DT_l. The new value of the control function depends on the value of the input control function at the previous timestep. The controller is normally used with the input control signal connected to the output control signal, providing a hysteresis effect. Aiming to control the Outlet temperature of the heat pump (T_{Load}) for DHW and SH purposes two controllers are applied. The outlet temperatures of the DHW and SH ports of the thermal storage tank, as well as the setpoint temperatures, are then provided as inputs of the controllers. Below Tables represent the inputs and outputs of each controller:

Table 3-3: Inputs and outputs of the temperature controllers

	Inputs	Outputs
DHW Controller	$T_h = T_{Setpoint,DHW}$	$Signal_{DH}$
	$T_l = T_{outlet,port\ DHW}$	
	$DT_{\frac{h}{l}} = \frac{+2}{-1}$	
SH Controller	$T_h = T_{Setpoint,SH}$	$Signal_{SH}$
	$T_l = T_{outlet,port\ SH}$	
	$DT_{\frac{h}{l}} = \frac{+2}{-1}$	

Based on both generated control signals of the controllers the setpoint temperature of the supplied flow to the storage tank (T_{Load}) will be then determined as it is seen in the Equation 3-7:

$$T_{Load,set} = \begin{cases} T_{Setpoint,DHW} = 60\,°C \;\; if \;\; Signal_{DHW} = 1 \;\; , \; Signal_{SH} = 0 \\ T_{Setpoint,SH} = 45\,°C \;\; if \;\; Signal_{DHW} = 0 \;\; , Signal_{SH} = 1 \\ T_{Setpoint,DHW} = 60\,°C \;\; if \; Signal_{DHW} = 1 \;\; , Signal_{SH} = 1 \end{cases}$$ Equation 3-7

3.2. Building Model

Based on statistics in the section 1.2 and in or order to evaluate the effect of different consumption profiles on the load management and wind power integration potential as well as sizing strategy of the heat pump heating system, the consumption profile of multi-family residential, also known as multi-dwelling unit (MDU), is considered; This building consists of twelve single-family units each 68 m^2 with 1.8 habitants/unit representing the average size of residential complexes in Berlin. Following the load profile of the building is calculated and explained in detail.

3.2.1. Load Profile of the Multi-Family Residential

In order to bust the energy-saving trend in Germany, since May 2014 the energy saving regulation (EnEV) [40] has been updated and new energy efficiency classification for buildings has been published, thereby four classes of multi-family residential with various energy demand are chosen to be investigated in the simulation. The heating demands and energy classes of these buildings are shown in Figure 3-6:

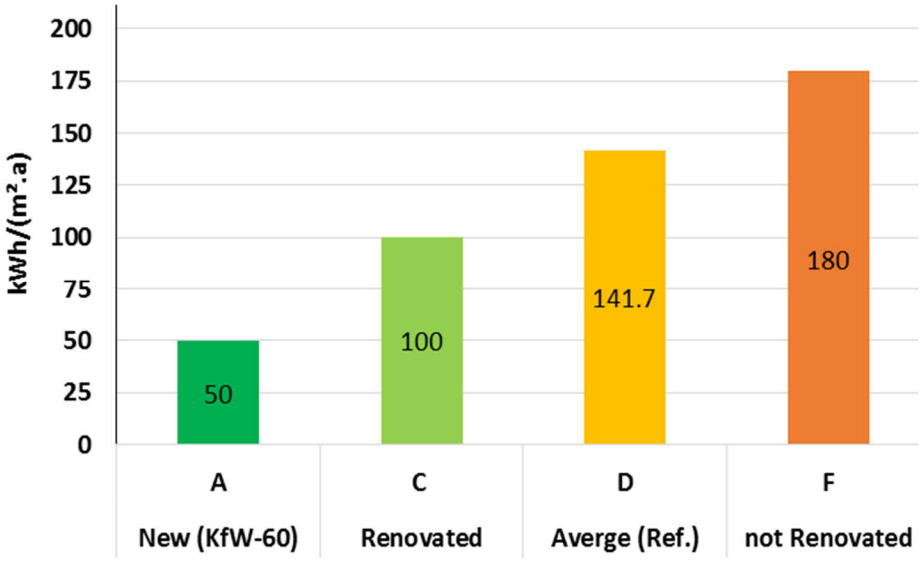

Figure 3-6: Energy consumptions of the investigated multi-family buildings

Since the specific annual energy demand of the multi-family residential is about 142 kWh/ (m². a), this building class is considered as the reference building for the base case scenarios in simulation models and further analysis. The SH and DHW demand profiles of the multi-family residential are calculated according to DIN EN 832 and VDI 4655 standards [41,42]; where the real measured data were applied to generate typical normalized daily load-profiles aiming to categorize the days which are repeating throughout the year. These certain days, named as day-type categories, are determined based on weather data considering sky coverage (cloudy/bright day) and the average daily ambient temperature. Taking in to account that there is no distinction between bright and cloudy days in summer, overall ten day-type categories are classified considering times of the year: Transition (T), Summer(S) and Winter (W) as well as Bright (B), Cloudy (C) and Workday (W) and Sunday (S). It is to be noticed that all public holidays are considered as Sunday. By using the normalized demand factors given in Table 3-3, the daily energy demand for space heating $Q_{Heiz,TT}$, domestic hot water $Q_{TWW,TT}$ and electricity W_{TT} of the building for each day-type category are calculated:

$$Q_{Heiz,TT} = F_{Heiz,TT} * Q_{Heiz,a} \qquad \textit{Equation 3.7}$$

$$Q_{TWW,TT} = F_{TWW,TT} * Q_{TWW,a} \qquad \textit{Equation 3-8}$$

$$W_{TT} = F_{EL,TT} * Q_{EL,a} \qquad \textit{Equation 3-9}$$

Where $\mathrm{Q_{Heiz,a}}$, $Q_{TWW,a}$ and $Q_{EL,a}$ are annual heating, domestic hot water and electricity demands of the building and $\mathrm{F_{Heiz,TT}}$, $F_{TWW,TT}$ and $F_{EL,TT}$ are factors for normalized daily energy demand for space heating, domestic hot water and electricity of each typical-day category, respectively.
As the demand varies depend on the ambient temperature and regional climate, the demand factors should vary depending on the climate region; Based on the historical climate data as well as recent measured data of each climate region in Germany and according to the DIN 4710 standard [43], a certain test reference year (TRY) is calculated and provided by DWD for each climate region (Figure 3-7); Berlin is located in the region 4 (Northern Germany-Lowland) determined as TRY4.

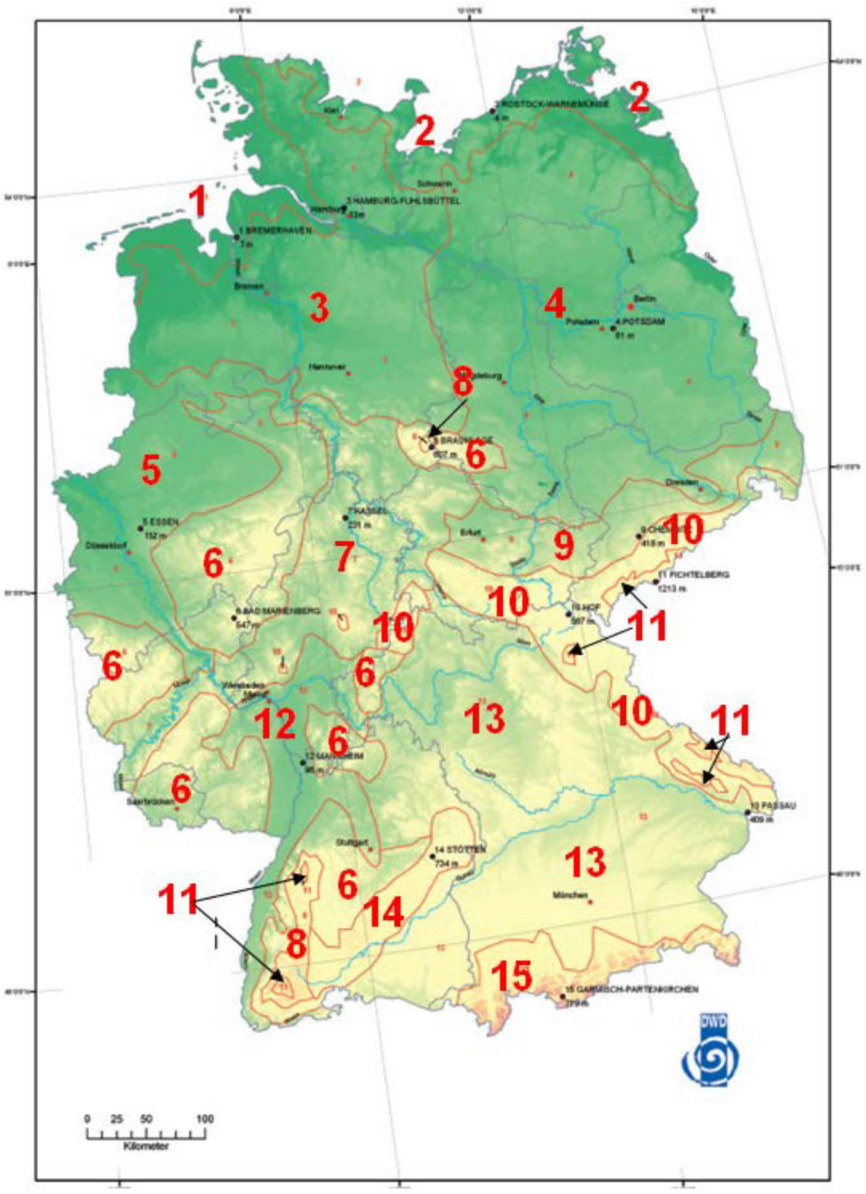

Figure 3-7: 15 climate regions in Germany according to DWD [43]

Table 3-4: Demand factors for all day-type categories for TRY4

	T-W-B	T-W-C	T-H-B	T-H-C	S-W-X	S-H-X	W-W-B	W-W-C	W-H-B	W-H-C
$T_{amb,ave}$ [℃]	11.10	10.20	10.60	9.50	17.50	17.40	-1.20	2.00	1.50	2.20
$F_{Heiz,TT}$	1.87E-03	2.21E-03	1.85E-03	2.02E-03	2.32E-04	2.33E-04	6.10E-03	4.94E-03	5.44E-03	4.24E-03
$F_{EL,TT}$	1.29E-05	2.91E-06	-1.40E-05	-1.40E-05	-3.89E-05	-4.09E-05	5.17E-05	1.88E-05	3.18E-05	-7.64E-08
$F_{TWW,TT}$	1.33E-05	4.38E-06	4.38E-06	1.72E-05	-5.30E-05	-4.41E-05	2.91E-05	2.81E-05	2.12E-05	1.53E-05

For the reference building with twelve 67.8 m² apartments and annual specific heating demand of 142 kWh/m².a the annual SH $Q_{Heiz,a}$, DHW $Q_{TWW,a}$ and electricity $Q_{EL,a}$ energy demands are:

Table 3-5: Annual demands of the reference building

$Q_{Heiz,a}$ [kWh]	$Q_{TWW,a}$ [kWh]	$Q_{EL,a}$ [kWh]
114526.4	10183	23840.2

Having the annual demands together with daily normalized factors, the daily demand of the buildings for each typical-day categories are calculated in Table 3-6:

Table 3-6: Daily Energy Demands for each day-type for the Ref. Building

Day Type Categories	SH Demand [kWh]	Electricity Demand [kWh]	DHW Demand [kWh]
T-W-B	215	69	30
T-W-C	254	66	28
T-H-B	213	61	28
T-H-C	233	61	30
S-W-X	27	54	21
S-H-X	27	54	23
W-W-B	702	80	31
W-W-C	569	71	31
W-H-B	626	74	30
W-H-C	489	65	30

Based on TRY-4 and the same process for calculating daily energy demand, by multiplying these daily demands by normalized demand factors for minute time steps, the energy demands for each minute and consequently the daily load profiles for each day-type category can be calculated; Sorting out the daily load profiles, monthly and annual load profiles of the building are generated. Due to the fact that at the time of executing this research work, the last published version of TRY is for the year 2011 whilst as input of the simulation models, the load profiles of the building based on the weather data of 2014 are required, it is necessary to adapt the TRY 2011 to generate new one for 2014 and accordingly sorting the day-type categories in new order to generate the updated load profiles of 2014 for the reference building. Having the climatic data of Berlin for 2014, the average daily ambient temperature, as well as daily sky coverage (cloud rate), are calculated as it is presented in Figure 3-8.

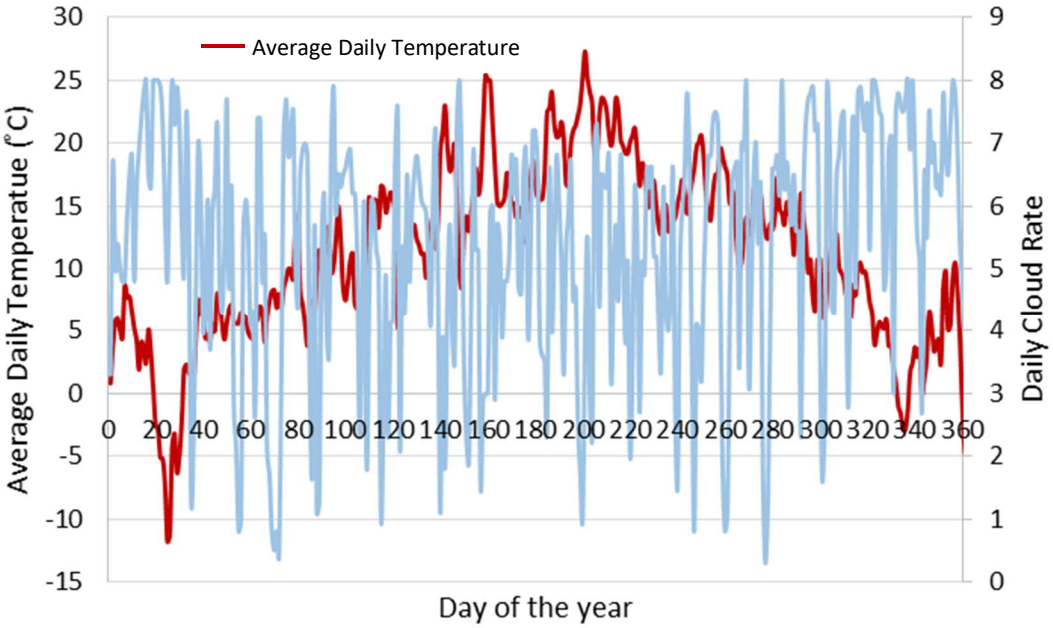

Figure 3-8: Weather data of Berlin-Dahlem for the year 2014

Considering the daily average weather data and the prioritized criteria's [44]: 1. Workday/Holiday 2. Season (ambient temperature) 3. Coverage rate (Cloud rate), each day of the year is assigned to the certain typical-day category. The allocation methodology is carried out in three steps considering the number of Workdays/Holidays of TRY4, taken by VDI standard, for adapting the calendar days of 2014 with these numbers. In the next step the temperature criteria given by DWD to assign the days of the year to the certain season should be redefined aiming to adapt the number of the days of each season to the number of the days of the seasons in TRY04 2011; as the final step the coverage rate of the sky is reassigned so that the entire number cloudy days does not exceed the one for TRY04 2011. The new distribution of the days for the year 2014 are given in Table 3-7:

Table 3-7: Distribution of the day-type categories for the year 2014

Day-Type-Category	T-W-B	T-W-C	T-H-B	T-H-C	S-W-X	S-H-X	W-W-B	W-W-C	W-H-B	W-H-C
Nr. Of the days	37	76	9	17	78	13	29	82	6	18

As it is described at the beginning of this part, the simulation is carried out in 15-minute time steps; Therefore, the normalized load data for the family house are averaged to quarter-hour data. By arranging the daily load profiles together according to the new test reference year (TRY4 2014), the weekly, monthly and annual consumption load profiles of the corresponding building are generated. Figure 3-9 illustrates the SH, DHW loads and the entire heating load as the sum of the SH and DHW for the reference building during the heating season (January-March and October-December):

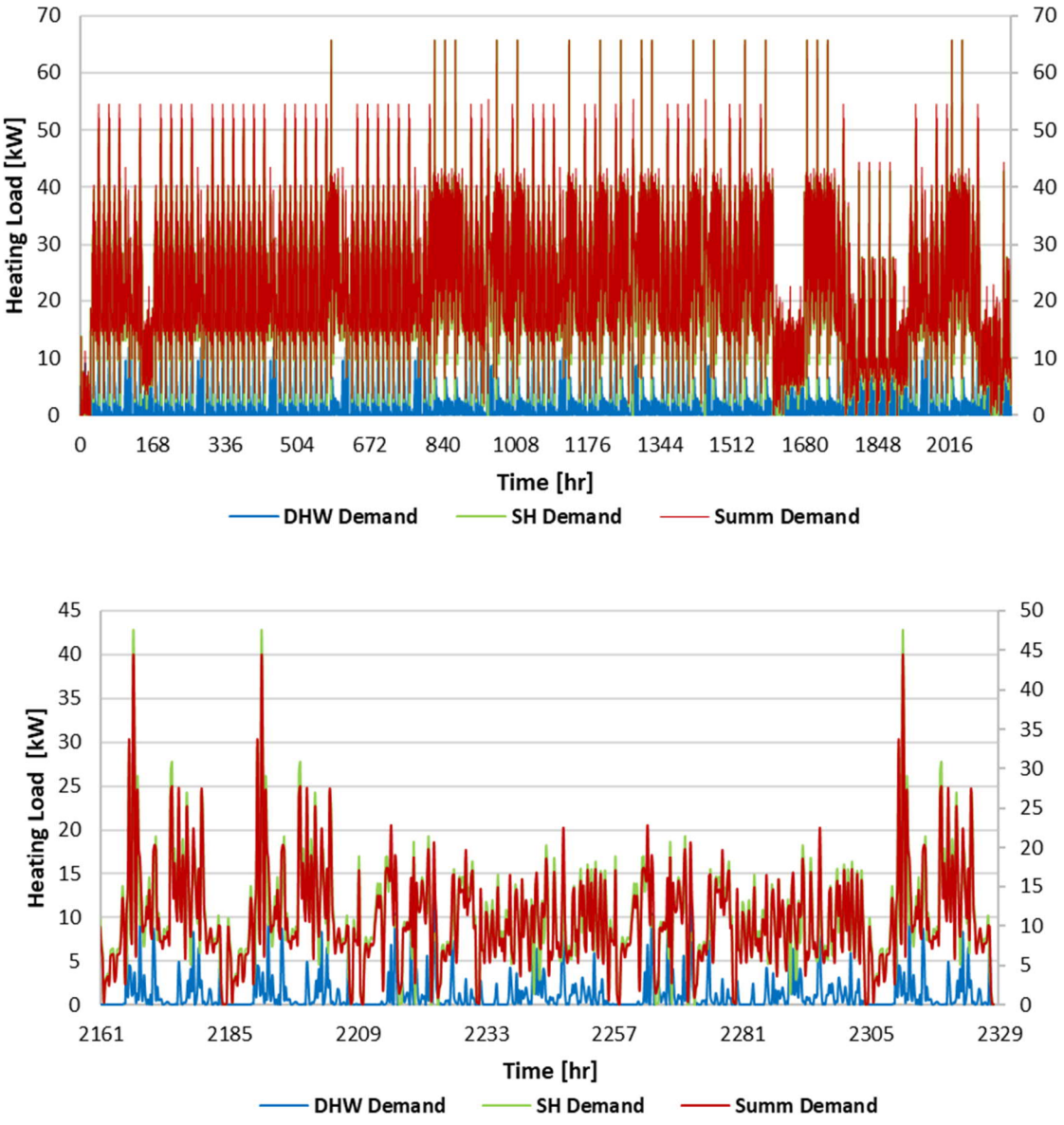

Figure 3-9: Heating load profiles of the Reference multi-family residential during heating season (a) January-March, (b) First week of October

Figure 3-10 indicates the load duration curves (LDC) for all considered demand levels during the heating season where the seasonal duration load of the reference building is specified by the red dashed line. The Peak- load, medium-load and base-load ranges in each LDC can be clearly seen in this diagram; For instance in case of reference building according to the LDC almost 260 hours, which is roughly 6% of the entire heating season, is within peak-load range; The rest of the period is dedicated to the medium-and base-load ranges.

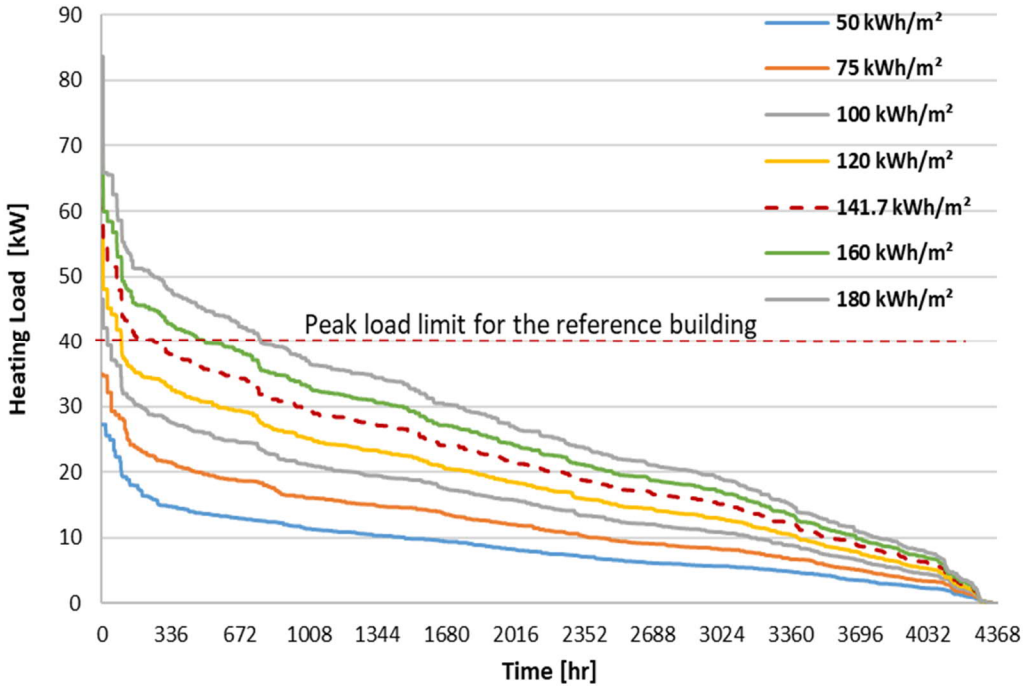

Figure 3-10: Seasonal heating load duration curve (LDC) of the considered demand levels

3.3. Load Management Strategy

Basically, the load management strategy lays on the hourly electricity generation and consumption profiles which are used to indicate the hourly available wind surplus for load shifting which is based on determined peak and off-peak hours. Within this developed scenario heat pump system is operated based on the hours where wind surplus electricity is generated and available in low voltage grid. As surplus rate is fluctuating throughout the year it might affect the operation trend of the heat pump, therefore the amount and distribution of surplus are deciding factors in developing the control scenarios; Followings are two reference profiles applied to develop the control strategy:

1. Standard load profile (SLP): a representative load profile by which the load of the consumers without registered power measurement in order to reduce the complexity of dealing with various types of unmeasured power consumption behaviors for power suppliers categorizing different groups of demands based on time-of-use, demand rate, and historical load data seems to be necessary. SLPs are determined as representative load profiles for residential and commercial sectors and are normalized for the consumers with annual electricity demand below 100,000 kWh; According to the paragraph 12 of the German Electricity Network Access Regulation (Strom

NZV[3]) these consumers are supplied by power utility based on their standard load profiles and a registered load profile measurement is not applied in this case. These profiles are then followed as load prognosis by power suppliers. In Germany SLPs published by Federal Association of Energy and Water Management (BDEW) are applied. In this study the normalized SLP for multi-family residential (H0) is selected as reference to determine off-peak and peak hours; This profile is presented in Figure 3-11.

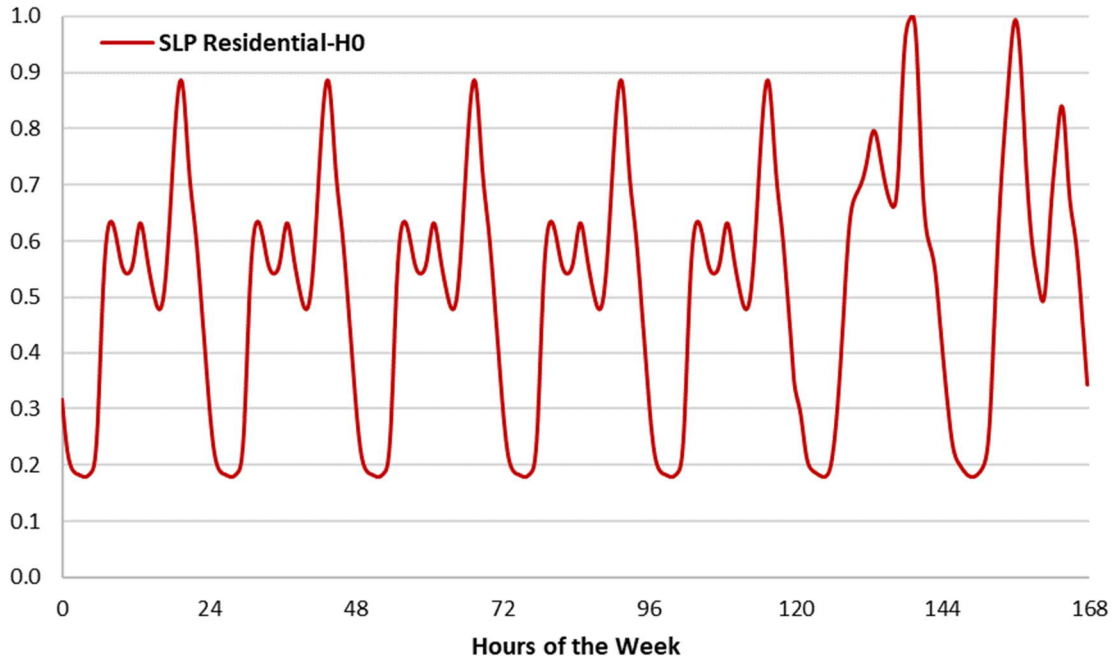

Figure 3-11: SLP for multi-family residential in the first week of January [7]

Considering the SLP off-peak load hours is determined as the periods where the electrical load is below the 60% of the maximum load.

2. Wind generation profile: is released by power distributer and represents the amount of wind power generated by wind miles throughout the year, to be integrated into different electricity networks, the fluctuations can be clearly seen in this profile. Figure 3-12 demonstrate the wind power generation profile in Eastern Germany in 2015:

[3] Stromnetzzugangsverordnung - StromNZV

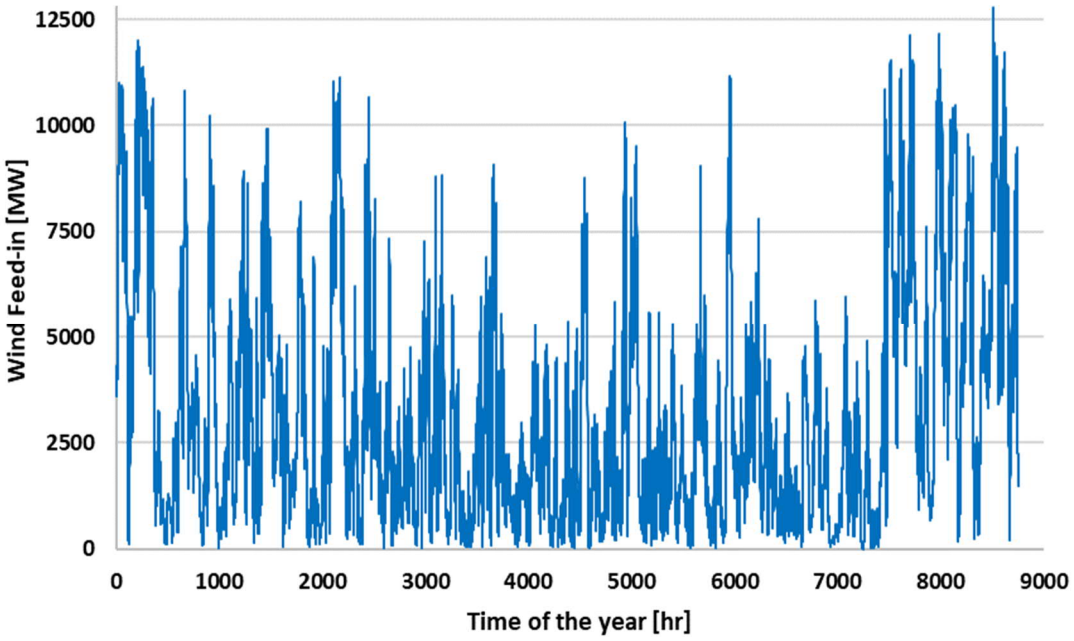

Figure 3-12: Wind power profile of Eastern Germany in 2015 [7]

Having the wind feed-in profile and calculating the daily wind feed-in, the daily average wind feed-in is determined and represented in Fig 3-13. Comparing the 0.25 minutes wind feed-in trend in each day with the average wind feed-in of the same day, the surplus wind power production is defined when average daily value is exceeded by wind feed-in trend.

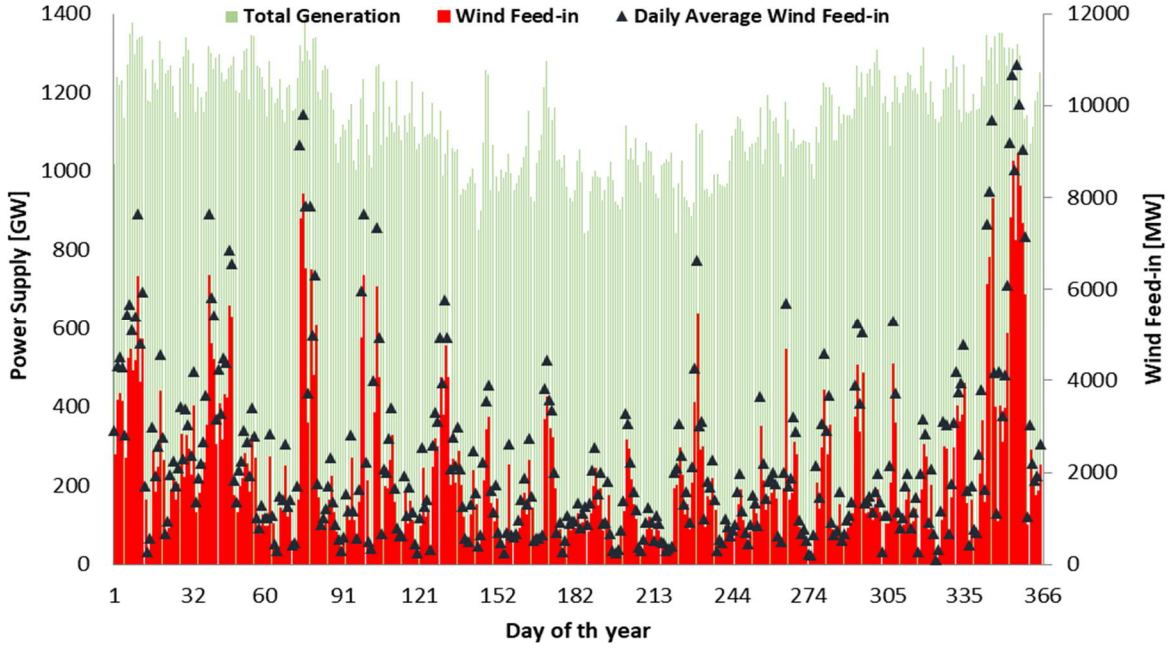

Figure 3-13: Daily Average Wind Feed-in 2015

Aiming integrate the surplus power through heat pump system and thermal storage, the surplus signal is defined, as the control signal for heat pump system, based on the SLP and wind feed-in profile; The 25 minutes operation signal indicates the off-peak periods where surplus wind power is available and can be integrated in the network. As it is seen in the Figure 3-14 the length of the surplus periods varies depending on the availability of the surplus hours.

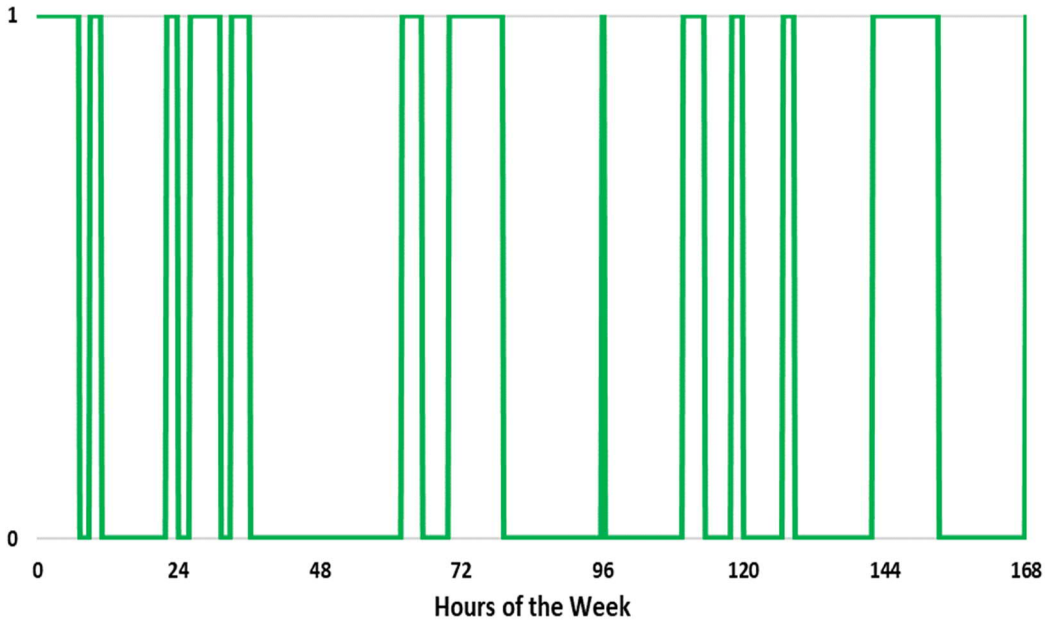

Figure 3-14: Surplus Signal for controlling the heat pump for the first week of January

3.3.1. Load Control Unit

The control scenarios are developed depending on on/off control for single speed heat pump or the capacity control for variable speed heat pump as well as standard load profiles and reference wind feed-in and network power profiles. The developed load control unit in this case consists of two main parts, the controller which is responsible to control the heating operation of the heat pump system through switching on/off in single-speed heat pumps or changing the compressor operational frequency in variable speed heat pumps based on the top node temperature of the thermal storage and the power feed-in conditions; the second part is a controller to adjust the charging and discharging steps of the thermal storage based on the timely demand by controlling the flow rate through hydraulic pumps in the primary or secondary cycles of the heating system. Therefore, the control signal is generated based on two groups of signals sent to the control unit: 1. Temperature signals from the top and bottom nodes of the heat storage tank and 2. The surplus signal calculated by the comparison of reference power and SLP profiles and indicates the appropriate time for operating heat pump to harvest surplus power. Figure 3-15 represents the flowchart of the control unit:

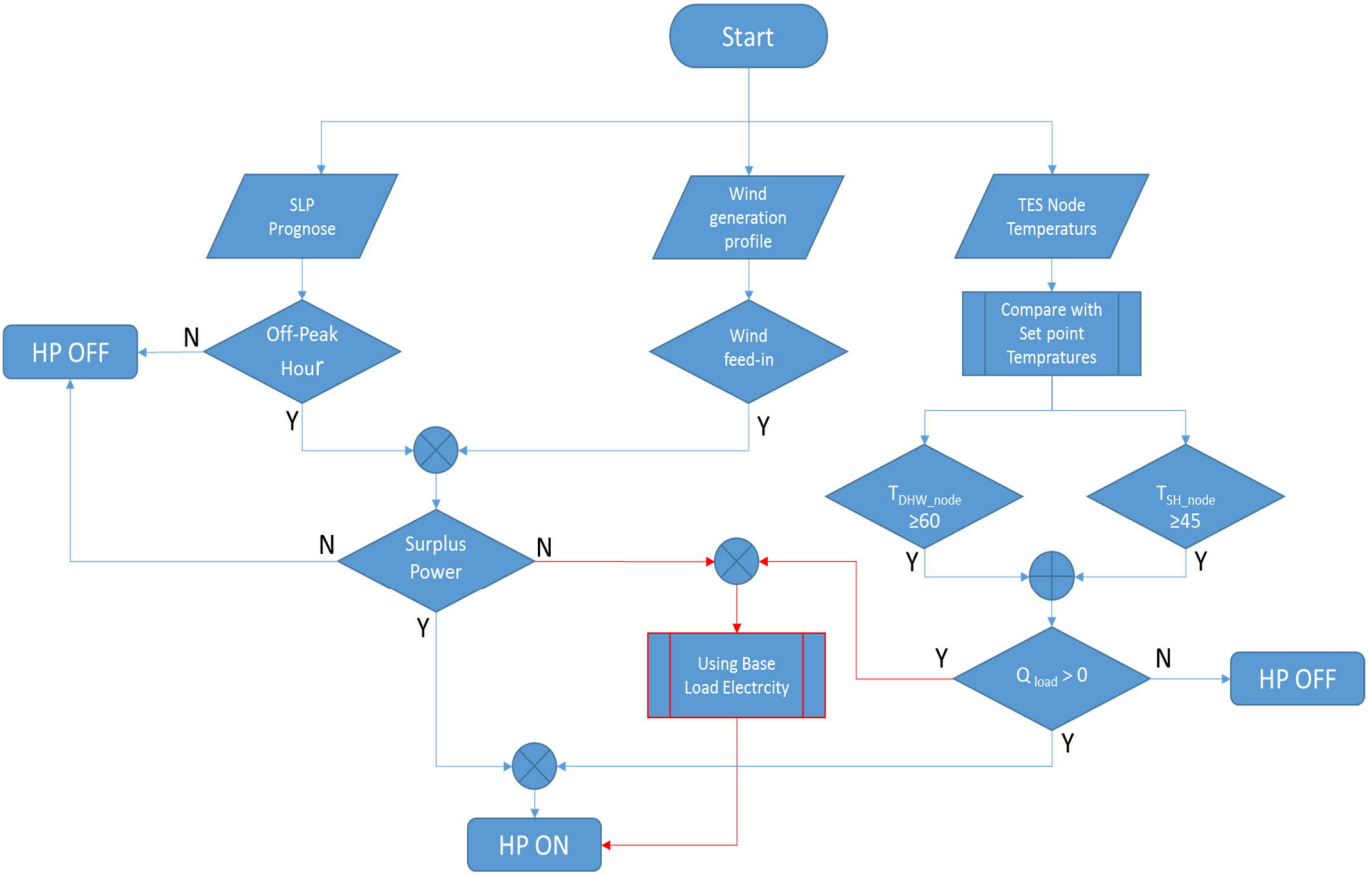

Figure 3-15: The Flowchart of the load management control unit

As it is seen in the flowchart Q_{load} and Surplus Power are the deciding signals for switching on/off heat pump in single-speed heat pumps; during the time that there is no surplus power available in the network but still heating demand exists, a base case-control scenario (shown in red lines) is incorporated, where the electricity demand of the heat pump is supplied by baseload power plant (conventional power).

3.4. Dimensioning of The Heat Pump Heating System

According to DIN 15450 standard [45], heat pumps must be planned in such a way that the highest possible seasonal performance factor (SPF) with respect to the selected heat source is achieved. The SPF of the designed heat pump must at least fulfill the national minimum rates given by heat pump manufacturers; In case of no available standard rates, the minimum values given in the attachment C of DIN 15450 should be applied. Other crucial criteria to be considered for sizing a heat pump is start-up cycles; it is important to avoid excessive start-up cycles. Normally, three start-up cycles per hour are standard, but this may differ depending on the manufacturer and the power network condition. Different experimental methods and instructions are recommended by the manufacturers for dimensioning the heat pump heating systems and heat storages depending

on the bivalent or monovalent (partial or full load) operation modes of the heat pump system and heat distribution system. In the following sections, these operation modes are explained.

3.4.1. Bivalent Operation Mode

Basically, in bivalent operation heat pump is used as a backup for a heating system such as oil or gas boilers to supply DHW. In most bivalent cases the heat pump is responsible to supply the space heating demand, where it is connected to the heat distribution system such as a floor heating or radiator, and the boiler covers the domestic hot water proportion of the heating demand. Depending on the part load covered by the heat pump heating system, it operates over the certain outdoor temperature called Bivalent Temperature (T_{biv}) provided by the manufacturer, at which the heat pump exactly meets the heating demand, below this temperature level the heat pump is switched off and the backup (Auxiliary) heater operates. In this case heating capacity of the heat pump is calculated depending on the maximum heat load of the building at standard ambient temperature (e.g. -12˚C) according to the DIN EN 12831[46] standard and the considered supply share of the heat pump. Typically, in this case the heating capacity of the heat pump can vary between 20%-50% of the maximum heating demand of the building to supply around 40%-80% of the entire annual heat demand.

3.4.2. Monoenergetic and Monovalent Operation Mode

Under monovalent and monoenergetic operation mode, the heat pump is seen as the main heating system that must supply the major part and in the best case the entire heating demand of the building. In monoenergetic operation, in order to cover the peak consumption loads a small electrical auxiliary heater is utilized, assisting the heat pump heating system to reach the peak load level. It is to be noticed that in this case the heat pump should be sized in the way that the proportion of the supplied heat by the auxiliary heater is minimized. Figure 3-16 represents the annual proportion of the heating energy demand that can be delivered by the heat pump depends on the dimensioning rate of the heat pump in monoenergetic mode; this is indicated as the ratio between heating capacity of the heat pump over the standard heating load of the building; As it is presented (blue line) for this case the suitable sizing of the heating capacity of the heat pump is about 70%-80% of the maximum heating demand of the building which ends up with supplying around 98% of the entire annual heat demand.

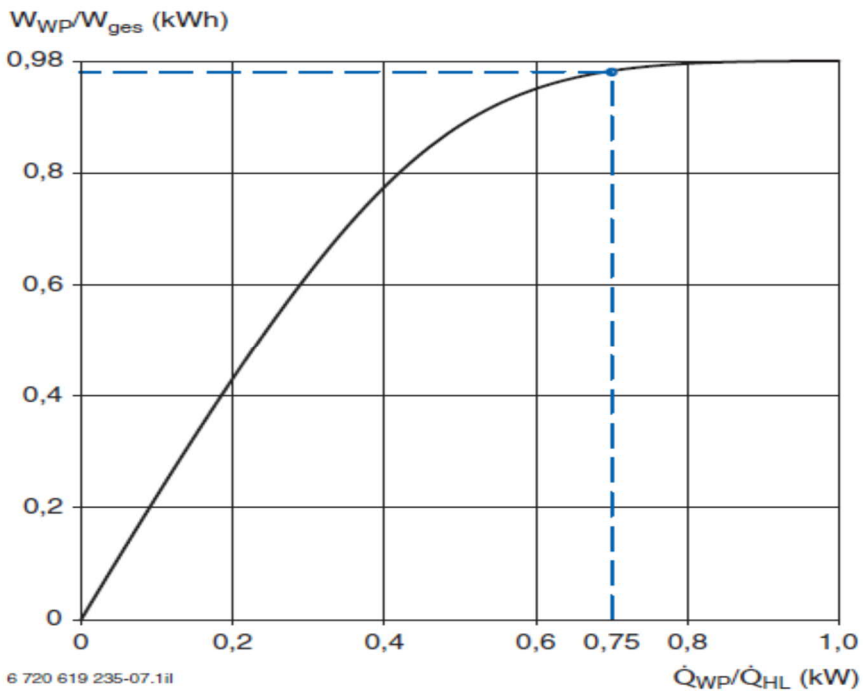

Figure 3-16: Dimensioning curve of the heat pump in monoenergetic operation [48]

Since in monovalent supply heat pump should operate more hours than bivalent mode, apart from individual control system of each system, the operating hours of the heat pump are restricted by power utility companies; During off-peak hours of the day where the electricity load decreases, the power utilities sell the electricity cheaper to the customer and in return during peak-hours for certain short periods of the time exclude the power consumption of the heat pumps. Thus, due to the regulations, the energy supplier has the right to disconnect the heat pump from the grid up to three times a day, each time for maximum 2 hours; The maximum length of the shut-down hours results in so-called "blocking hours"[4], the sum of the blocked hours during heating season is maximum 1110 hours. To bridge these blocked hours and supply the heating demand, using either an auxiliary heater or an appropriate storage tank seems to be necessary. Therefore, the number of blocked hours affects the dimensioning of the heat pump and the volume of the storage tank. This effect is characterized by a dimensioning factor (f_{extra}) derived from the number of blocked hours as shown in Equation 3-8:

$$f_{extra} = \frac{24\,h}{24\,h - (blocking\ hours\ per\ day)}$$ *Equation 3-8*

[4] Sperrzeiten

Aiming to operate the system in monovalent mode, the heating capacity of the heat pump and the heat storage volume are determined based on the maximum daily heating demand of the building and the dimensioning factor as follows:

$$\dot{Q}_{HP} = (f_{extra})\left(\dot{Q}_{DHW} + \dot{Q}_{SH}\right)_{max} \qquad \textit{Equation 3-9}$$

$$V_{TES} = \frac{((\dot{Q}_{DHW}+\dot{Q}_{SH})_{max}/24)(blocking\ hours)}{\rho_{water}*Cp_{water}*(T_{top-node}-T_{bottom-node})} \qquad \textit{Equation 3-10}$$

Where $\left(\dot{Q}_{DHW} + \dot{Q}_{SH}\right)_{max}$ is the maximum daily heating power demand and $\left(T_{top-node} - T_{bottom-node}\right)$ is the temperature difference between top and bottom of the storage tank; As a result, based on above equations in case of increasing daily blocking hours, larger heat pump and larger heat storage tank are required to cover the supply gaps. On the other hand, Increasing the size of the storage tank could result in reducing the number of operation hours of the heat pump, this would affect the thermal efficiency of the system indicated by Seasonal Performance Factors (SPF). SPF of the heat pump unit at the narrowest boundary level is defined in Equation 3-11, including only the compressor electricity consumption and excluding the parasitic losses in the system:

$$SPF = \frac{\int \dot{Q}\times dt}{\int \dot{E}\times dt} = \frac{\int_{0\ h}^{2160\ h} \dot{Q}_{hp}\times dt + \int_{6552\ h}^{8760\ h} \dot{Q}_{hp}\times dt}{\int_{0\ h}^{2160\ h} \dot{E}_{comp}\times dt + \int_{6552\ h}^{8760\ h} \dot{E}_{comp}\times dt} \qquad \textit{Equation 3-11}$$

Where $\dot{Q}_{hp}$ is the heating power delivered by heat pump at rated conditions, and $\dot{E}_{comp}$ is the total power consumption of the compressor at rated conditions, in this case the integral is calculated over the heating season divided into two periods: 1. January to March (0 - 2160 hours) and 2. October to December (6552 -8760 hours).

3.5. Dimensioning Methods

As it is discussed in the previous section the focus of the conventional sizing method for the heat pump heating system in monovalent operation is to meet the peak heat load of the building and consequently supplying the entire heating demand of the building; this method is also called "Thermally driven dimensioning[5]". However, considering the constraints of the low voltage power grid specifically during cold season and the large surplus potential of wind power, when it comes to load management and integrating wind energy, it is necessary to determine new measurement and reconsider the conventional dimensioning method by including the irregular blocking hours

[5] Wärmegeführte Dimensionierung

caused by fluctuation wind feed-in in sizing the heat pump system and heat storage, in this sizing strategy the main focus, besides supplying the heat load of the building, is to integrate surplus wind electricity and thereby reduce the conventional share of the electricity demand of the heat pump, this method is called "Electrically driven dimensioning[6]". Aiming to evaluate the wind integrating and load shifting potential of the heat pump system, it is necessary to determine new measurements. As the priority in the electrically driven dimensioning strategy is to supply the power demand of the heat pump by wind electricity, in this case the entire power demand of the heat pump system is supplied by two sources: 1. Surplus wind power and 2. Conventional (baseload) electricity. Therefore, the power consumption of the compressor ($\dot{E}_{comp}$) of the heat pump is divided into two sections and demonstrated in Equation 3-12:

$$\dot{E}_{comp}(kW) = \dot{E}_{comp,wind} + \dot{E}_{comp,baseload} \qquad \textit{Equation 3-12}$$

Where, $\dot{E}_{comp,wind}$ is the part of the compressor electricity demand taken from the wind surplus production and considered and $\dot{E}_{comp,baseload}$ is the part of the power that is provided by baseload power plants during the times where no wind generation is available. Through increasing the operation times of the compressor during the times where excess wind power is available it is possible to harvest more wind power and thereby reduce the share of baseload electricity. Aiming to quantify the capability of the heat pump system on adapting wind power, the wind integration factor is determined based on the Equation 3.12 as an indicator to demonstrate the fraction of the power consumption of the heat pump system that is provided by wind power generation; Thereby the ratio of the integrated surplus wind power to the entire power consumption of the heat pump is calculated over the considered heating season:

$$Wind\ Integration\ Facotr(WIF)\ [\%] = \frac{\int \dot{E}_{wind,comp}.dt}{\int \dot{E}_{comp}.dt} \times 100 \qquad \textit{Equation 3-13}$$

Aiming to evaluate the effect of oversizing the heat pump and thermal storage concerning the availability of the wind generation on the load shifting potential of the system, the dimension factor is developed as a ratio between storage tank volume (V_{TES}) and heating capacity of the heat pump($\dot{Q}_{hp}$):

$$Dimension\ Factor\ (DF)\ [\frac{m^3}{kW}] = \frac{V_{TES}}{\dot{Q}_{hp}} \qquad \textit{Equation 3-14}$$

Applying above parameters, the following steps are designed to be implemented in the simulation model to investigate the correlation between sizing the heat pump and thermal storage and adapting wind power feed-in and finally introducing this correlation as a new criterion in sizing HP and TES to maximize the adaptation rate of the surplus wind electricity:

[6] Stromgeführte Dimensionierung

1. Sizing heat pump and thermal storage based on thermally driven dimensioning
2. Running simulation applying base-load electricity scenario
3. Running simulation applying surplus electricity scenario and calculating WIF
4. Over sizing the system based on electrically driven dimensioning
5. Running simulation applying surplus electricity scenario and calculating WIF
6. Identifying the correlation between DF and WIF: $DF = f(WIF)$
7. Introducing the HP and TES sizes where maximum WIF occurs
8. Studying the effect of over dimensioning on SPF and operation hours of the HP

Section 3.7 will elaborate on the detailed simulation method as well as sizing strategy.

3.6. Simulation Cases

As mentioned in the previous chapter, three variants of the heat pump heating system are considered in the model as follows: 1) Single speed ground source HP 2) Single speed air source HP and 3) Variable speed air source HP. As shown in Figure 3-17 under the surplus load management strategy, three scenarios are considered for the three types of heat pump systems. In order to study the impact of different standard load profiles and heating demand rates on the adaptation of the wind energy, a typical multi-dwelling unit (MDU), which represent the majority of the multi-family buildings in the city of Berlin, has been considered for each variant of supply system. It is to be noted that the demand side of the load control unit is determined depending on the standard electrical load profile of this type of building.

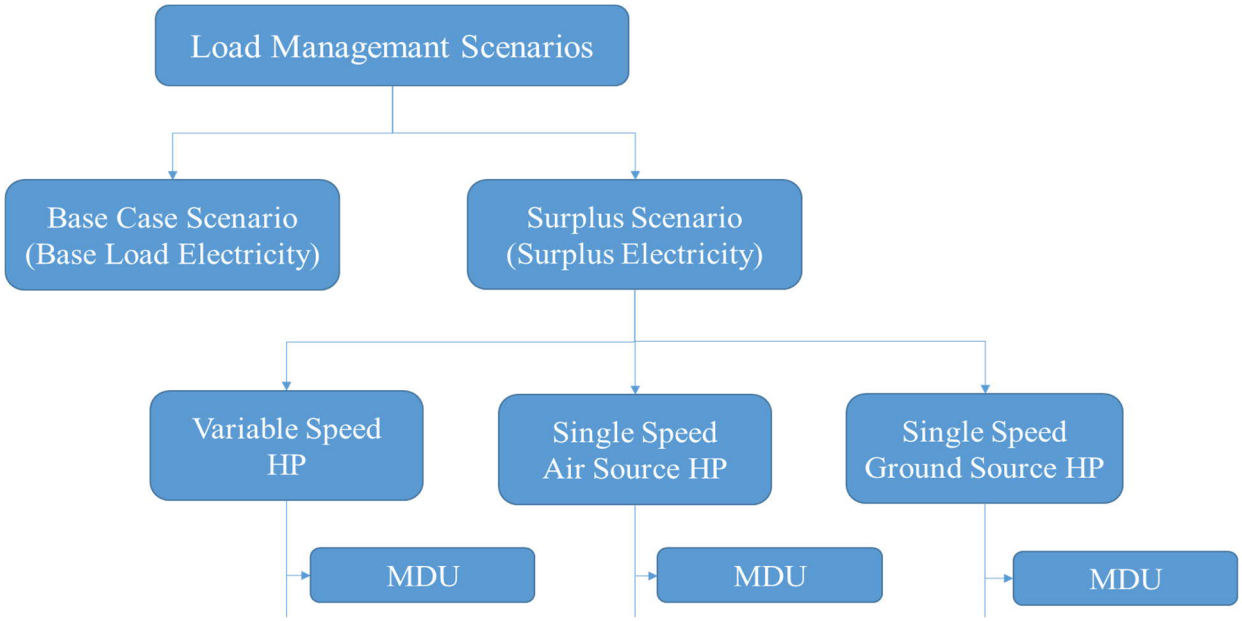

Figure 3-17: Simulation Cases: Load Management Strategy applied for different HP Types

3.7. Surplus Sizing Strategy of the System

To evaluate the impact of the sizing of the heat pump and thermal storage system within active load management on adaptation rate of the wind energy feed-in, the first step is to determine a baseline scenario in which heat pump and thermal storage are sized based on typical dimensioning method for monovalent supply with maximum six blocking hours per day. It is then necessary to develop a sizing strategy for the system, aiming to adapt the maximum possible wind power by the system. Based on the calculated surplus signals in the previous section, the daily surplus and blocking hours are calculated. According to Figure 3-18, the daily blocking hours vary between [6, 11] hours due to the fluctuating wind power generation.

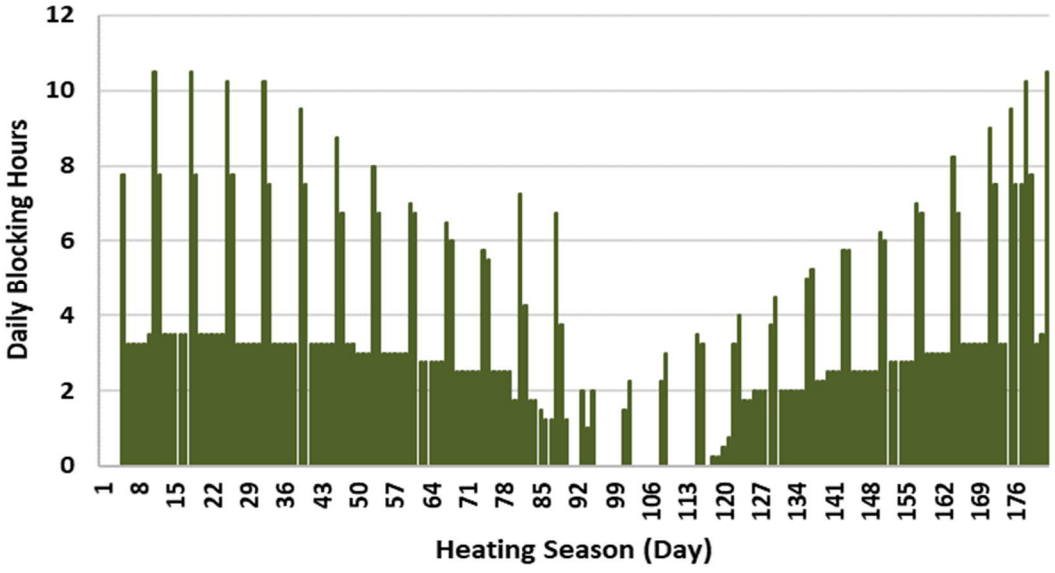

Figure 3-18: The variation of the blocking hours during the heating season of the year 2014

In order to benefit from the maximum share of wind power by oversizing the heat pump, the heating capacity of the heat pump is increased stepwise with the variation of daily blocking hours throughout the heating season and based on section 3.3. The exercise is conducted starting from the average blocking hours rate of 6 hours per day and progressing towards the worst-case scenario of 12 blocking hours, where the heat pump is operated in the coldest day of the winter ($T_{amb,min} = -14\,K$) with maximum daily heating demand and minimum daily availability of surplus power. The oversizing steps of the heat pump are calculated based on the sizing method in section 3.3 and represented in Table 3-8:

Table 3-8: Oversizing steps of the heat pump based on daily blocking hours

Daily Blocking hours [h]	Oversizing Factor (f_{ext})
2	1.1
4	1.2
6	1.5
10	1.7

Aiming to evaluate the impact of oversizing the storage tank on bridging blocking hours, each heat pump size is then simulated with increasing thermal storage volumes starting from minimum necessary thermal storage for the corresponding heating demand and 6 blocking hours per day. Increasing storage volume for each simulation case continues until saturation point where increasing the storage volume does not affect the maximum wind power adapted by the supply system. Hence the correlations between WIF from Equation 3-15 and DF from Equation 3-16 will be developed for each heating demand rate (each building category). Finally, comparing the correlations for all demand levels leads to a global correlation, where the wind power adaptation behavior of the system can be evaluated against dimensions of the system for each type of heat pump. Furthermore, to recognize the overall energy saving potential of the heat pump system within the load management concept, the baseline scenario is then compared with the reference building case in terms of electricity consumption and wind power share as well as the cycle length and SPF of the heat pump system. Figure 3-19 represents the heating curves of the considered buildings with certain demand levels where the reference building is depicted by the dashed line. The baseline sizing of the heat pump system for each demand level will be accomplished based on the peak load ($Q_{heating,bui,\ max}$) occurs at $T_{amb,min}$=-14 °C which is represented in below diagrams.

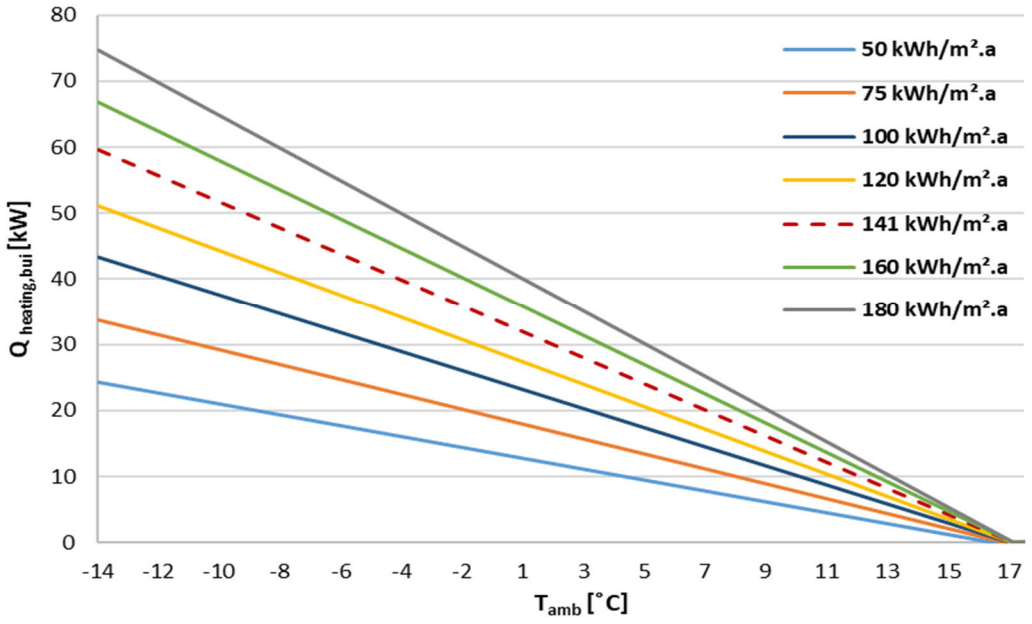

Figure 3-19: Heating curves for considered specific heating demand levels

4. Results and Discussions

In this chapter, the integration potential of the wind feed-in through the heat pump and storage tank for the considered multi-family buildings is evaluated. In the first step the surplus control scenario is incorporated in each heat pump model and compared with the operation of the heat pump under base-case control scenario. In the second step the oversizing strategy based on availability of the wind generation is carried out for each model and all demand levels, in order to investigate the impact of this strategy on the wind integration and to develop the correlations between WIF and DF for each simulation model that are determined as characteristic curves for wind integration in each case.

4.1. Model I: Ground Source Heat Pump Heating System

The first model consists of a ground source heat pump coupled with a stratified heat storage tank supplying a multi-family building. As it is explained in section 3.1.1, Type 927 for single stage ground source water-to-water heat pump is employed in this model which is provided by a reference file based on the technical datasheet of the Viessmann company given in [Appendix A]; This data file contains normalized heating capacity and power consumption of the GSHP at certain inlet and supply temperatures. The first step of the seasonal simulation is carried out for the reference building introduced in section 3.2. Considering the base-case scenario with the surplus scenario, where the building is supplied by GSHP with a rated heating capacity of 56 kW at standard operating conditions and 10 m^3 TES which is sized on the basis of 3*2 daily blocking hours, Figure 4-1 illustrated the simulation results during the first week of February where the operation of the GSHP under base-case and surplus scenarios are compared with each other; The green diagram indicates the surplus signals, the blue diagram represents the heat output of the heat pump under base-case operation scenario and red diagram shows the heat pump output within surplus operation scenario. It can be observed that by implementing surplus control scenario the average operating cycle of the heat pump is increased more than two times from 1.4 hours in base-case operation to almost 3 hours. Longer operating cycles result in increasing the amount of the surplus hours in the operation of the GSHP leading to the higher wind share of the power consumption, furthermore as it is seen in the figure, due to the less start-up cycles in the surplus operation the operation heat loss is reduced and more output heat is achieved which results in slightly better COP of the heat pump compared to the base-case operation. Due to the monovalent operation of the heat pump, there are still some hours where the heat pump is switched on despite the absence of surplus wind feed-in and supplying the heating circuit; On the other hand applying 10 m^3 storage tank results in bridging the supply gaps, where heat pump is switched off, through shifting the supplied heat.

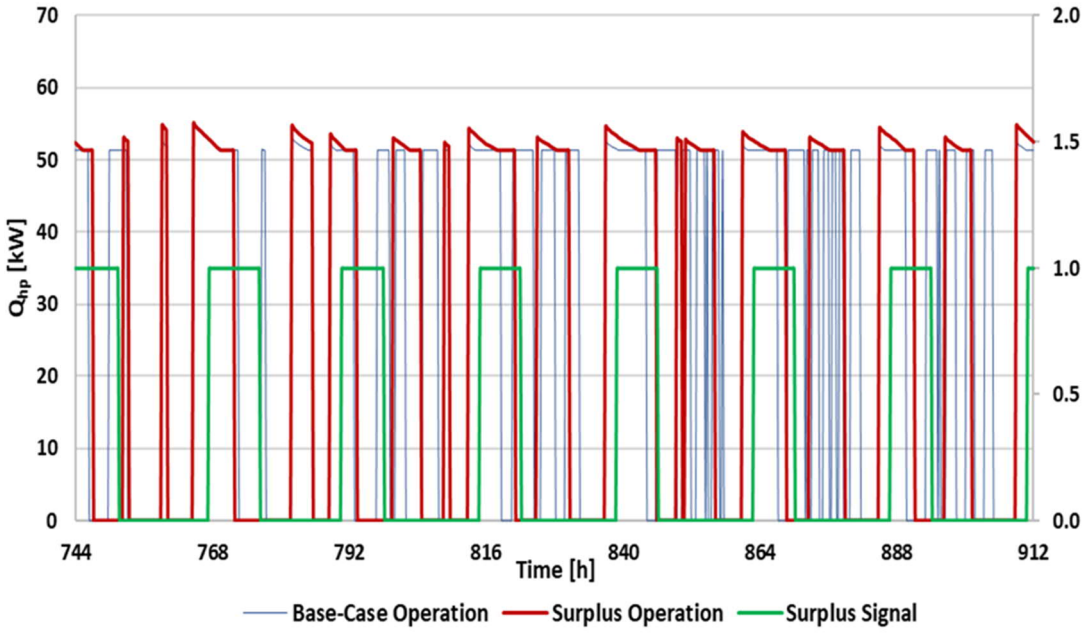

Figure 4-1: GSHP operation under Base-Case and Surplus scenarios in the first week of February

Evaluating the distribution of the power consumption of the heat pump for the entire heating season under considered scenarios, figure 4-2 indicates that the monthly base-load electricity consumption of the heat pump operating under surplus scenario (blue columns) is on average about 35% less than the case where heat pump operates under base-case scenario (red columns). This reduction is due to the flexible operation of the heat pump in surplus-scenario which enables replacing the baseload electricity through integrated wind feed-in.

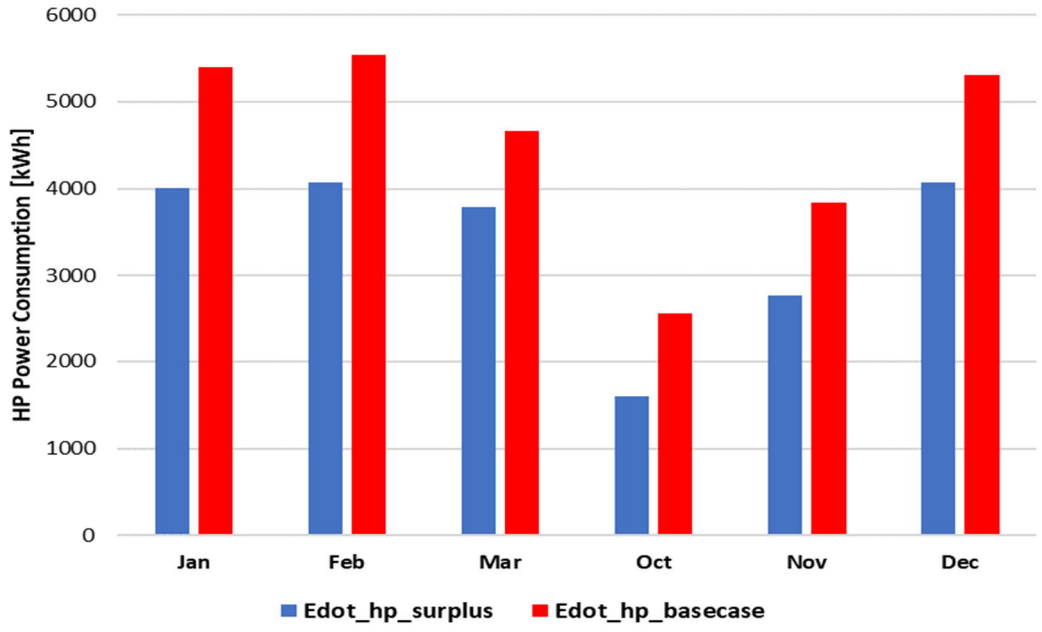

Figure 4-2: GSHP monthly baseload electric energy consumption in Base-Case and Surplus Operation Scenarios

In this stage, the oversizing of the GSHP and TES is carried out within several steps based on the daily blocking hours given in Table 3-8. Each certain GSHP size connected with a TES volume is defined by a Dimension factor (DF) which is explained in the previous chapter as the ratio between storage volume and heating capacity of the heat pump; Afterwards through running seasonal simulation for each DF of the system the corresponding WIF, as the indicator of the wind share of the entire power consumption of the heat pump, is calculated. In order to determine the maximum possible wind integration potential of each certain system size, the storage volume coupled to each heat pump will be further increased unless the WIF growth trend is saturated. The obtained WIF values are sorted out for each DF and listed in the Table 4-1 and illustrated in the Figure 4-3; As it is seen the GSHP is oversized within three steps, in order to include more system dimensions and thereby getting more accurate WIF diagram, the storage tank is enlarged within small steps; It can be observed that applying larger storage volume for oversized heat pumps at high DF of the system leads to reaching higher rates of WIF; Based on these results the highest WIF is roughly 70% that is obtained at DF 1.9 as extreme sizing scenario for the reference building where a 90 kW GSHP coupled with 150 m^3 is employed. Furthermore, it is realized that at DF below 1 coupling larger heat pumps (74 kW and 90 kW) with relatively low storage volume results in clearly fewer amounts of WIF compared with smaller heat pumps; This is the result of shorter operation cycle and less operation time in case of large heat pumps that avoids long operation during off-peak hours and harvesting wind surplus; For instance having 56 kW GSHP with 30 m^3 TES the cycle of operation is over 6 hours that results in WIF of 55% at DF 0.65, whilst at the same DF utilizing a 90 kW GSHP shortens the operation cycle to less than 3 hours that in overall reduces the off-peak operation time and results in 10% degradation of WIF. That is why the length of the operating cycle of GSHP is an important parameter to be noticed beside DF of the system within oversizing scenario; Based on the simulation results an average cycle length of 4 hours can be a practical criterion to be considered in order to keep the wind share of the power consumption over 50%.

Table 4-1: Variation of adaptation rate of the GSHP by changing the system dimensions for the reference building

	Wind Integration Factor for each GSHP size			
Dimension Factor [m³/kW]	**56 kW**	**65 kW**	**74 kW**	**90 kW**
0.2	39.0%	34.4%	30.2%	34.4%
0.3	41.9%	39.5%	36.9%	39.7%
0.4	48.3%	41.9%	39.9%	40.7%
0.5	49.2%	43.1%	43.9%	42.3%
0.6	53.8%	45.9%	47.0%	44.0%
0.7	55.4%	49.9%	51.9%	45.3%
0.8	55.3%	54.9%	53.6%	47.0%
0.9		59.6%	56.9%	48.4%
1.0		60.8%	60.5%	49.4%
1.1		61.8%	63.8%	53.8%
1.2			65.3%	58.2%
1.3			65.8%	60.5%
1.4			65.2%	62.5%
1.5				64.2%
1.6				66.5%
1.8				68.3%
1.9				69.7%

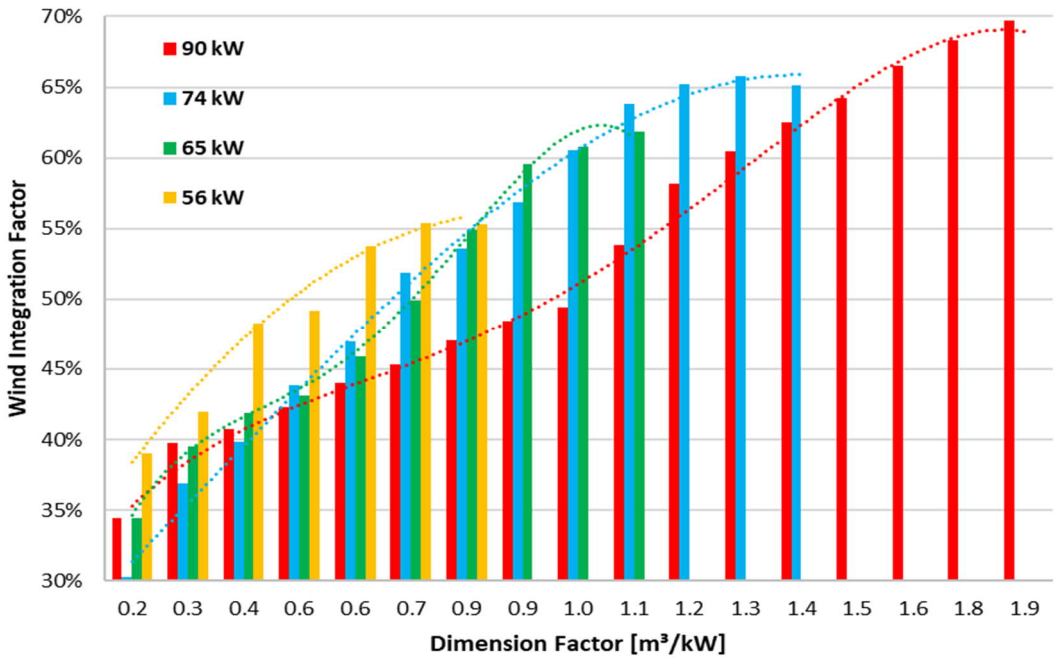

Figure 4-3: The growth of the adaptation rate of wind feed-in for different dimensions of the GSHP and TES for the reference case

The final step is to generate a uniform correlation between WIF and DF from above results to be applied as the reference characteristic curve for the estimation of the wind integration potential for certain dimensions of GSHP with TES for the reference building. For this purpose, the highest WIF amounts in each size of heat pump compared to the previous size are selected; Putting

together all the considered values the correlation between WIF and DF is generated through logarithmic regression and indicated in Figure 4-4 and Equation 4-1:

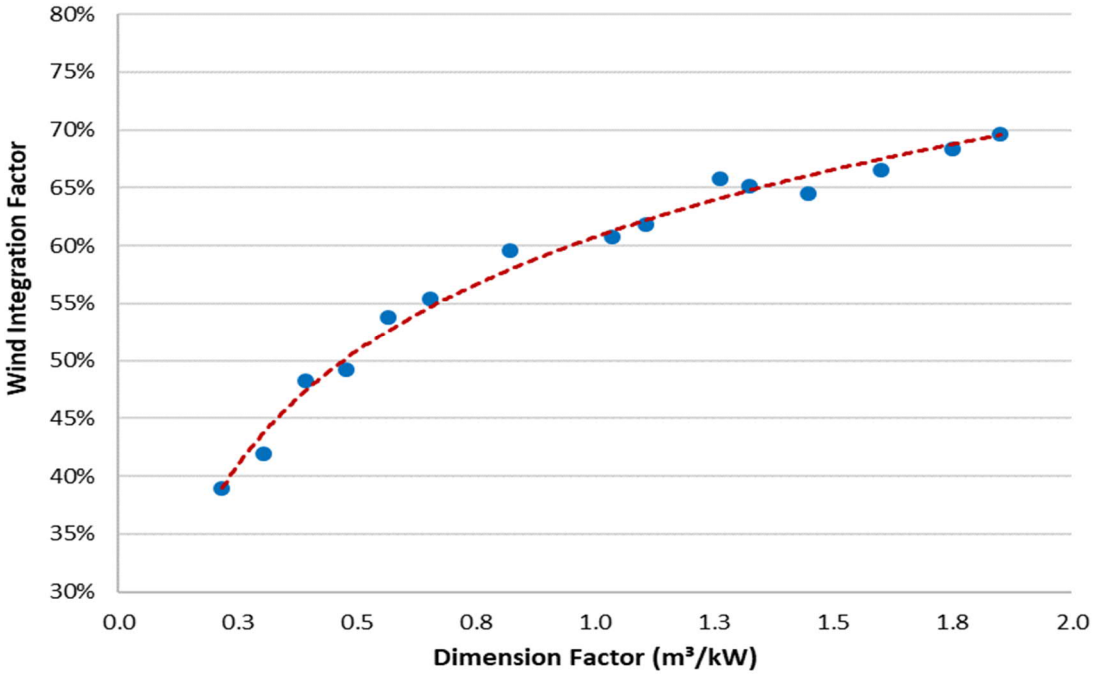

Figure 4-4: Logarithmic regression of the results for the reference simulation case

$$WIF = 0.143 * Ln(DF) + 0.61 \qquad \textit{Equation 4-1}$$

Figure 4-4 indicates that for the DF's more than 0.6 where WIF is over 50%, the growth rate of WIF is almost linear; This means that at DF's less than 0.6 the low storage volume is a crucial restriction that strongly reduces the operating cycle of the heat pump and results in significant decrement of the wind integration potential of the heat pump.

Aiming to include other demand classes of the multi-family building in this investigation and finally develop a general correlation that is valid for the entire types of the multi-family building, the same steps are done for the reference building are carried out for the entire demand levels to generate the corresponding characteristic curve for each demand profiles. Figure 4-5 demonstrates the reference diagrams of the growth rate of wind adaptation against DF of the system for the considered annual heating demand levels of multi-family residential. As it is observed for the demand levels lower than reference demand the saturation point of the diagrams is shifted to the right side, this implies that the maximum WIF of the system is quite lower in these cases and occurs at larger DF; On the other hand, at demand classes more than the reference level, which represent not renovated buildings, the maximum WIF increases and obtained at relatively lower DF of the system. For instance, for 50 kWh/m². a heating demand, which represents the demand class of a new building, the maximum achieved WIF is 60% at DF

2.5, whereas for 180 kWh/m² demand class maximum WIF of 72% is reached at DF 1.6. Same as the case for the reference building, it is seen in all diagrams that moving from the saturation point down to roughly DF 0.6 the WIF shows almost linear behavior versus DF of the system, this proves ones more that in order to obtain at least 50% wind share of the power consumption in a system, the volume of the heat storage tank should at least 40% of the heating capacity of the selected heat pump in case of highest demand level and around 90% of the heating capacity of the heat pump for the lowest demand level; In other word the storage tank should be sized in the way that the entire blocking hours bridged and thereby the operating cycle of the heat pump does not become shorter than the average cycle length. In general, it can be also concluded that due to the faster growth rate of the wind integration of the system at high demand levels, applying the oversizing strategy of GSHP and TES is more effective for high heating demands rather than low ones.

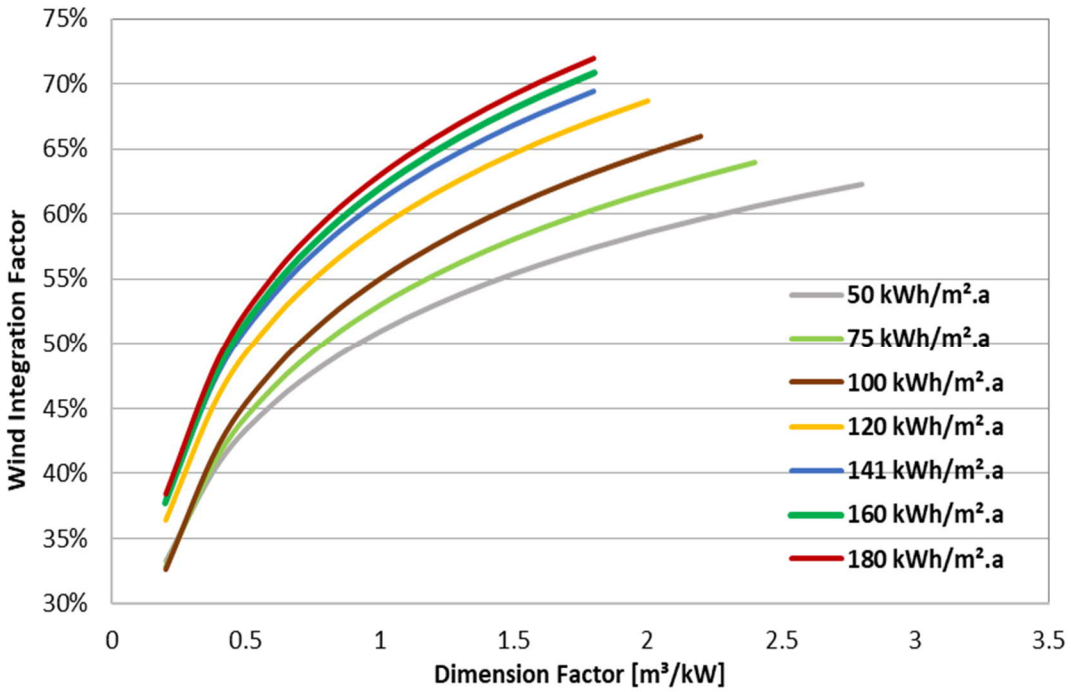

Figure 4-5: Wind adaptation curves for different system dimensions and heating demand levels

Having above diagrams, which are the logarithmic regressions of the results in each case, the general correlation between WIF and DF for the DIF's over 0.2 as the minimum system sizes to cover 2 blocking hours, can be used to estimate the wind integration potential of GHSP with TES for multi-family buildings:

$$WIF = a_1 * Ln(DF) + a_0 \quad ; \; 0.2 < DF$$ *Equation 4-2*

Where: $\begin{cases} 0.11 \leq a_1 \leq 0.16 \\ 0.51 \leq a_0 \leq 0.65 \end{cases}$

The detailed values of these constants for the considered demand level are given in the below table:

Table 4-2: Constant of the reference Equation 4-5 for the considered demand levels

$Q_{heating}$ $[\frac{kWh}{m^2.a}]$	a_1	a_0
50	0.115	0.51
75	0.125	0.53
100	0.139	0.55
120	0.141	0.57
141	0.143	0.61
160	0.151	0.62
180	0.153	0.63

Aiming to evaluate the impact of heating demand change on the wind integration potential of the GSHP system, the dispersion of WIF for the considered spectrum of demand classes is depicted in Figure 4-6. It can be seen that increasing the demand level results in the higher median and maximum values of the WIF where the median is raised by 8% and the maximum is boosted by 10% between lowest and highest heating demands, however the overall variation of WIF range amounts to 5% between least and most demand levels.

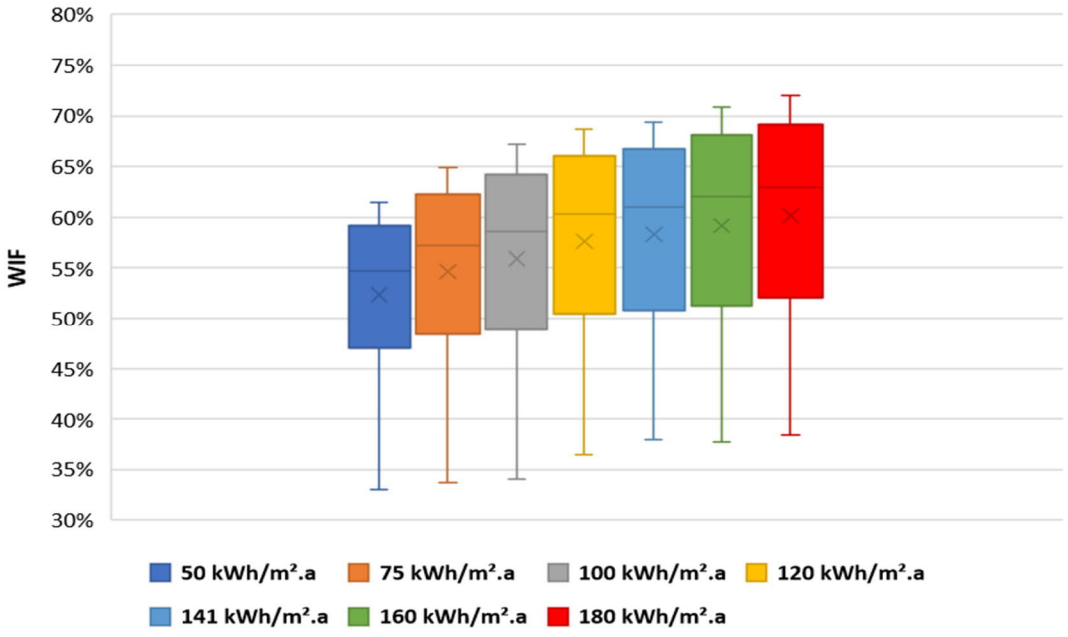

Figure 4-6: Distribution of the Wind Integration Factor of the GSHP system for the considered demand levels

In order to include the impact of the heating demand of the building ($Q_{heating}$) on WIF, considering the Table 4-2 and through linear regression represented in Figure 4-7, the correlations between the coefficients (a_0 and a_1) and $Q_{heating}$ are produced.

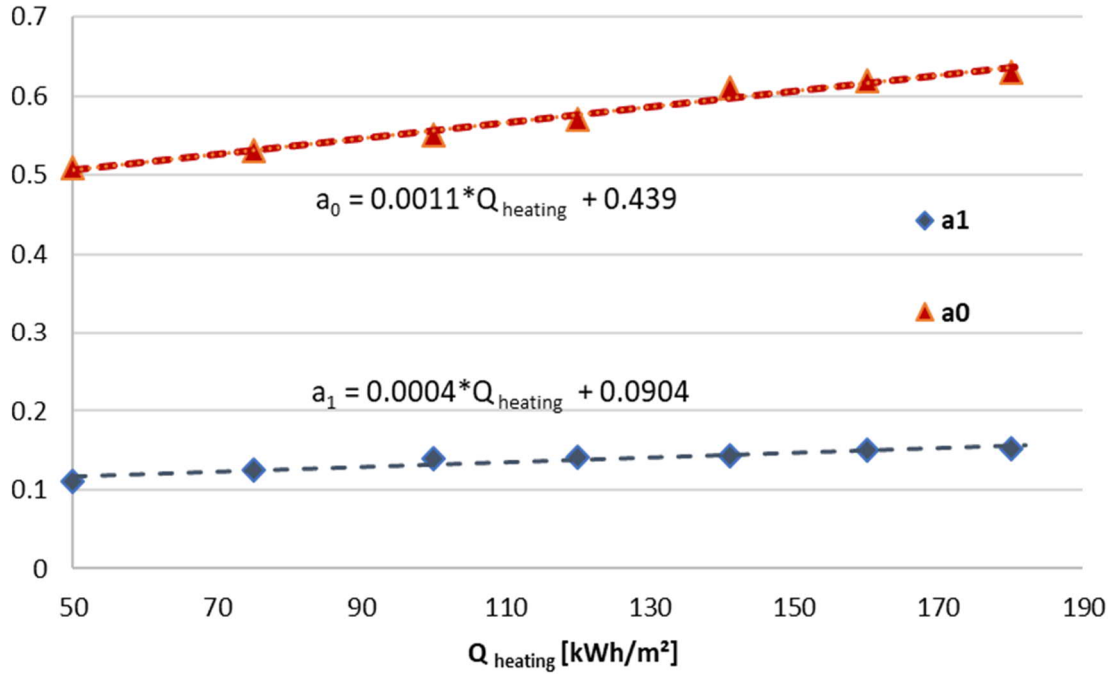

Figure 4-7: Correlation between a_0 and a_1 coefficients and heating demand of the building ($Q_{heating}$)

Substituting the coefficients in the Equation 4-2, WIF can be reproduced as the function of DF and $Q_{heating}$ as follows:

$$WIF\ [\%] = \left(0.04 * Q_{heating,bui} + 9.04\right) * Ln(DF) + 0.11 * Q_{heating,bui} + 43.9 \qquad \textit{Equation 4-3}$$

The Equation 4-3 can be then introduced as the reference correlation for surplus sizing of the GSHP system.

Aiming to recognize the effect of the surplus control scenario together with over dimensioning strategy on the thermal performance of the GSHP and TES system, the trend of SPF of the system for the entire considered dimension factors (DF) is investigated in case of the reference building. Figure 4-8 illustrates the impact of enlarging storage tank for each size of the heat pump on the SPF of the system; It is seen that utilizing larger storage tank for the same heat pump results in degradation of the SPF due to the longer charge/discharge cycle of the TES and therefore higher heat loss from the tank. On the other hand oversizing heat pump in case of higher daily blocking hours along with large storage tank leads to higher full-load operation hours and accordingly higher power consumption which together with heat loss of the thermal storage reduce the SPF; For instance, it is shown that for 56 kW heat pump increasing thermal storage volume by 200%

(30 m³) increases the full load operation to 1870 hours (10,27 hr/day) and reduces SPF by 14.6% to 3.69; In case of having 90 kW GSHP applying 140 m³ storage tank, as extreme oversizing case, rises the seasonal operation time to 1219 hours (6.7 hr/day) and decreases SPF by more than 30% to 3.17 compared to base case dimensions of the system where SPF is 4.73.

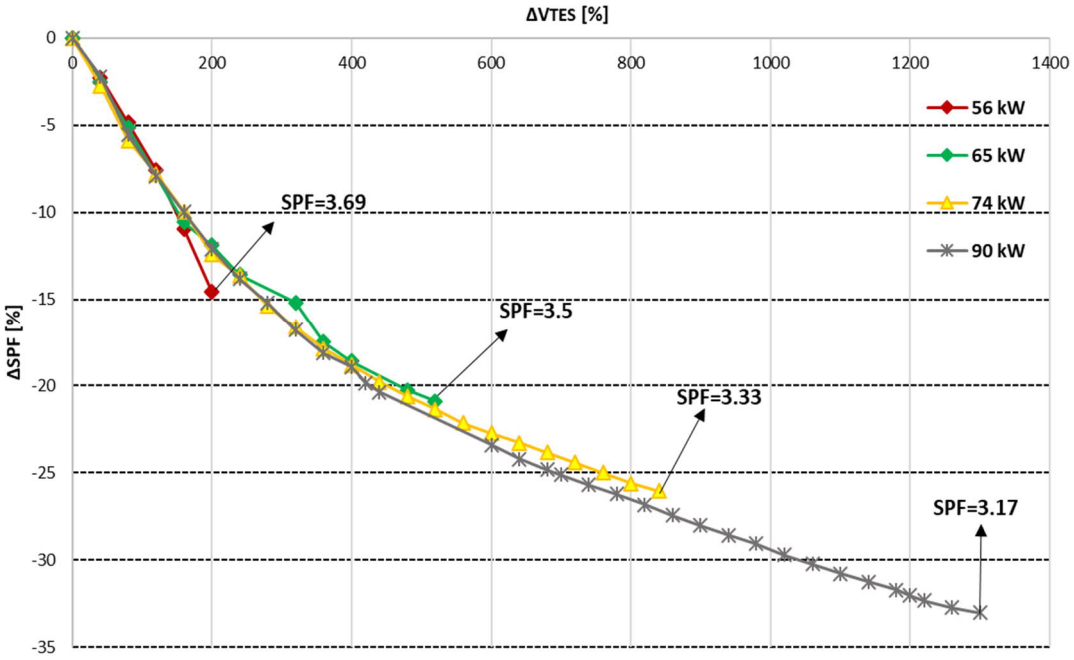

Figure 4-8: the impact of changing storage volume for each GSHP on SPF for the reference building

Figure 4-9 demonstrates the comparison of the thermal and electrical performances of the heat pump system through comparing WIF with SPF rates for each size of the GSHP in the reference building where WIF_{max} is reached; It can be observed that in the base case dimensions (green column), where a 56 kW GSHP is accompanied with 10 m³ storage tank, the SPF is 4.32 and WIF is roughly 40%; Connecting 30 m² storage tank to the identical HP increases WIF by 15% whilst SPF falls down to 3.7 ; For the extreme oversizing scenario where a 90 kW GSHP coupled with a 140 m³ storage volume the WIF reaches almost 70% which is about 30% growth compared with

base case DF whilst the SPF is reduced further to 3.17. In average the growth rate of WIF is roughly 5% more than the reduction rate of the SPF.

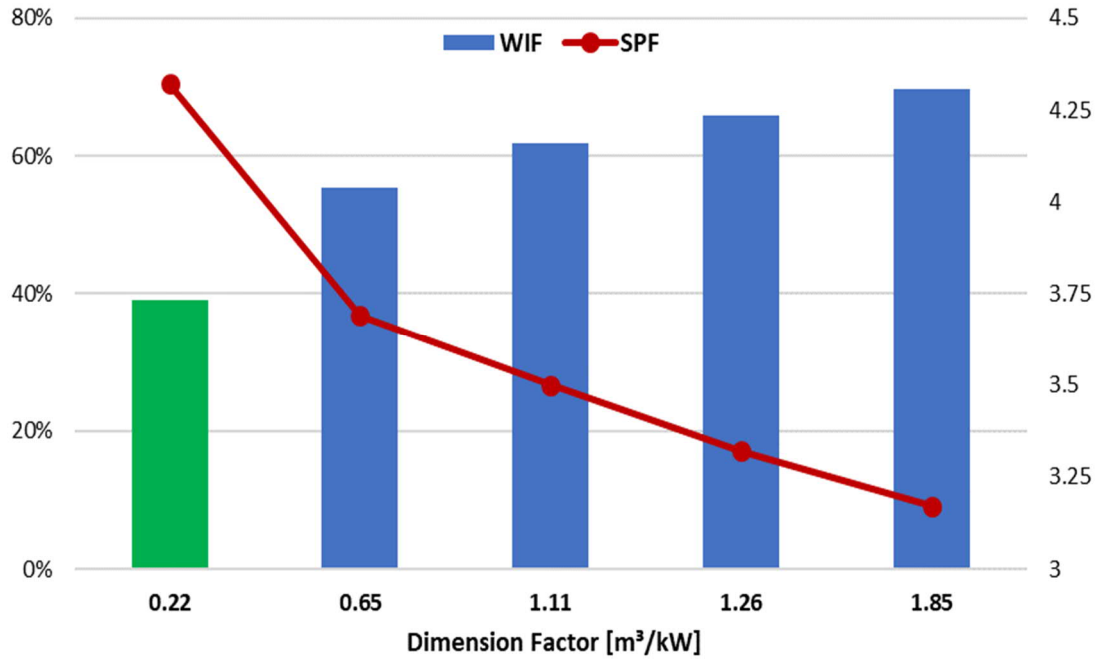

Figure 4-9: Variation of the SPF of the GSHP by oversizing the system for the reference building

Overall from the results presented in Figures 4-8 and 4-9 it is concluded that reaching high share of wind energy through oversizing strategy of the heat pump system, has negative impact on the thermal performance of the system specifically for extreme cases where blocking hours that should be bridged by thermal storage tank is longer than 6 hours due to the long charging and discharging cycles also imposed by wind surplus availability and limited heat demand of the building.

Figure 4-10 represents the distribution of the baseload and surplus hours of the entire seasonal operation time of the GSHP at the same DF's of the system for the reference building. It is seen that by enlarging storage volume for a 56kW heat pump at DF 0.65, due to the longer operating cycle the share of the surplus hours is boosted by 15%. In general, it is seen that oversizing the GSHP and TES under surplus scenario at high DF, despite shortening the entire operating time, leads to longer operating cycle that is increasing the share of the surplus hours of the entire operation.

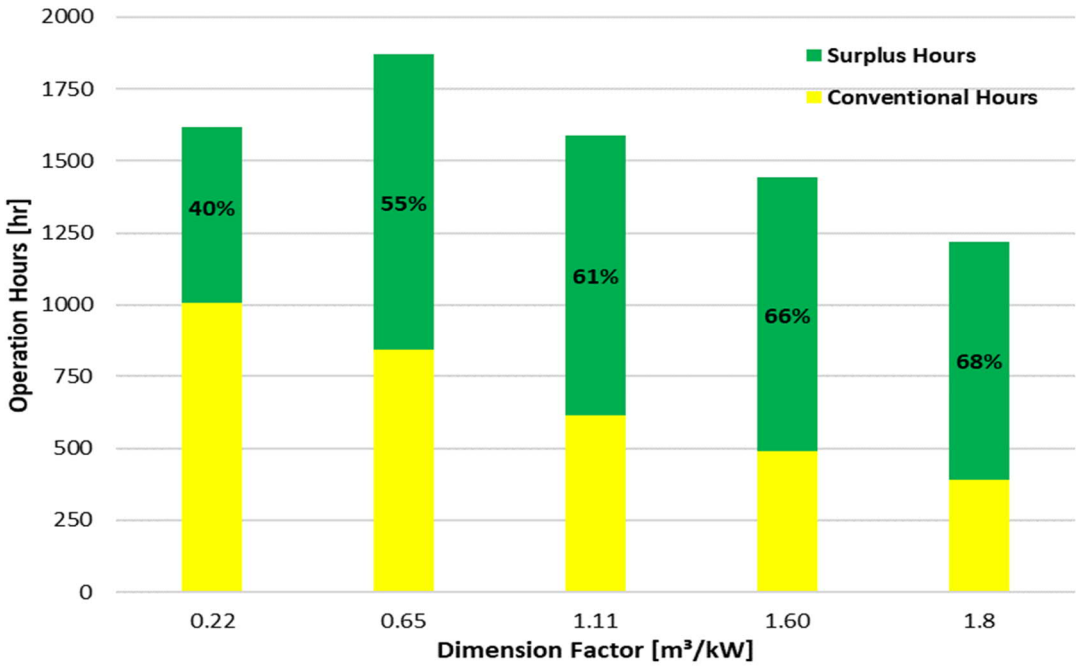

Figure 4-10: Distribution of the operation hours of GSHP for the reference building

4.2. Model II: Air Source Heat Pump Heating System

In this case, the reference model is an ASHP accompanied by a TES that supplies the average size multi-family building in Berlin. For implementing the model in TRNSYS environment, Type 941 is chosen which represents single-stage air-water heat pump. At standard operation conditions according to the standard EN 14511 and manufacturer's datasheet ($T_{Inlet\ air}$=2°C/$T_{Supplied\ Water}$=35 °C and ΔT=5° C) [Appendix A], the coefficient of performance (COP) of a 56 kW ASHP is 3.4 which is quite lower than the COP of the same size GSHP which is around 4.5 at standard condition. The low outdoor temperature in Berlin during the heating season [Figure 3.8] and monovalent supply of the building including DHW at $T_{Supplied\ Water}$= 60° results in worse COP of the ASHP under these operating conditions than the nominal COP which leads to the considerably higher power consumption of the heat pump. Same as the previous section in order to evaluate the performance of the heat pump under developed surplus control scenario and compare it with base case-control scenario, in the first step a 56 kW ASHP accompanied by 10 m³ TES is considered, both are sized based on 2 daily blocking hours given by power utility. Figure 4-11 compares the operation of the ASHP under base-case and surplus scenarios during first week of February; As it is seen operating the ASHP under surplus scenario results in longer operating cycle, which is in average 3 hours, and consequently higher wind share in the power consumption of the heat pump; Moreover having less number of operating cycles causes less start-up losses in

the compressor which results in better COP and higher supplied heat of the ASHP which can be also seen by comparing red and blue diagrams in the below figure.

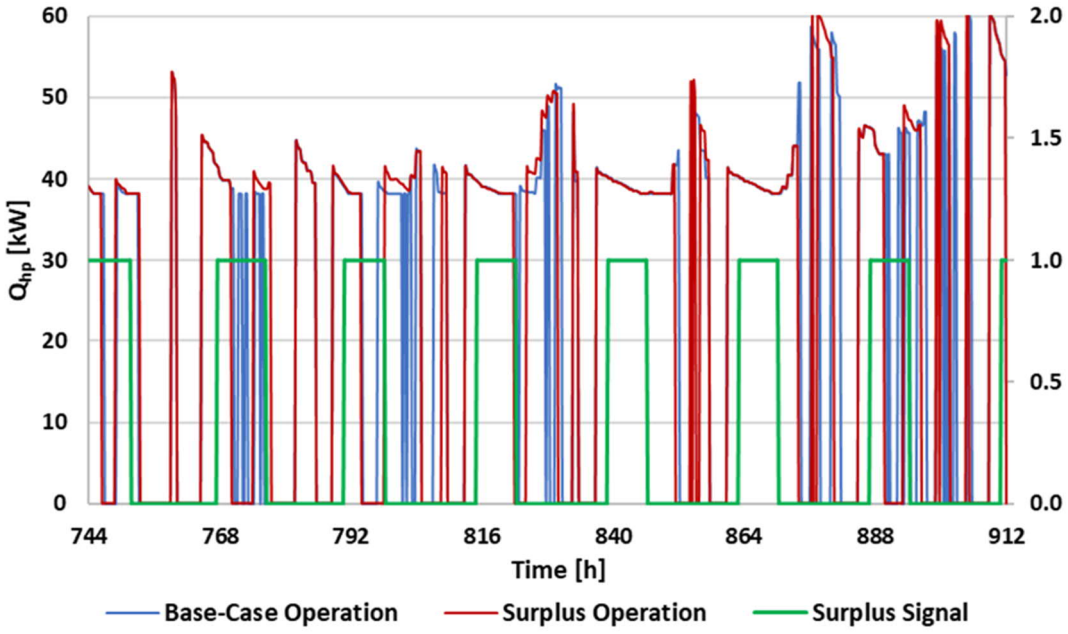

Figure 4-11: ASHP operation under Base-Case and Surplus scenarios during the first week of February

The power consumption of the heat pump system for the entire heating season is compared for both base case and surplus scenarios; As it is shown in Figure 4-12 on the basis of monthly consumption, the electricity consumption of the heat pump supplied by based load power plants within base case scenario is reduced on average by 42% through operation under surplus scenario and replaced by the wind feed-in.

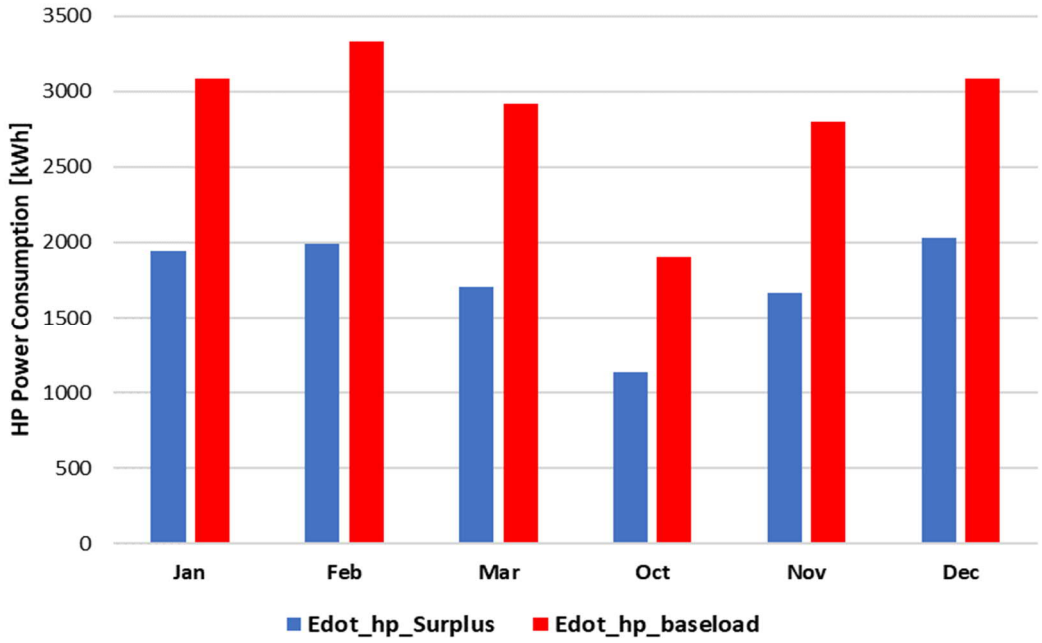

Figure 4-12: ASHP monthly base-load electricity consumption in Base-Case and Surplus Operation Scenarios

In the next stage, the wind integration potential of the reference system is investigated within the oversizing strategy of ASHP and TES. The wind integration performance of each size of the heat pump is investigated through increasing the capacity of the thermal storage tank starting from minimum storage volume that bridges the operation gaps of the heat pump to the maximum volume where the highest WIF of the system is achieved. Due to the restricted sizes for large ASHP, in this case the Oversizing of the systems is investigated within two steps aiming to calculate the corresponding WIF for each DF of the system. Seasonal simulations are carried out for each DF. Changing the DF of the system reflects on the operating cycle (number of startups and shutdowns) as well as the power consumption of the system as deciding parameters that affect the WIF of the ASHP system.

Figure 4-13 demonstrates the wind integration behavior of the ASHP system for different DF's for the reference building. As it is seen the ASHP is oversized within two steps where for each heating capacity the thermal storage is enlarged in several steps. It is observed that at low DF's, smaller heat pump systems achieve better WIF than oversized heat pumps due to the longer operating cycle and consequently longer off-peak operating hours; For instance, when 56 kW ASHP coupled with 11 m^3 storage tank is served, which represents DF 0.2, WIF amounts to 43%, while at the same DF a 70 kW ASHP results in roughly 3% less WIF. According to the simulation results the operating hours of the ASHP system can reach up to 8 hours when it is associated with proper size thermal storage and can be falling down to almost 1.5 hours for 70 kW heat pump coupled with a 10 m^3 storage tank, this implies the crucial role of the DF in case of oversizing ASHP. Up to DF=1 the rest of the heat pumps obtain worse WIF than 56 kW heat pump but afterward due to

deployment of larger storage tanks the off-peak operating hours of 56 kW are reduced and WIF of the system is saturated accordingly; On the other hand the operating cycle and off-peak hours of the oversized heat pumps increase and lead to higher amounts of WIF. It is also seen that the maximum WIF amounts to 72.5 % which is achieved at DF=1.6 where a 70 kW ASHP and a 120 m³ tank are utilized.

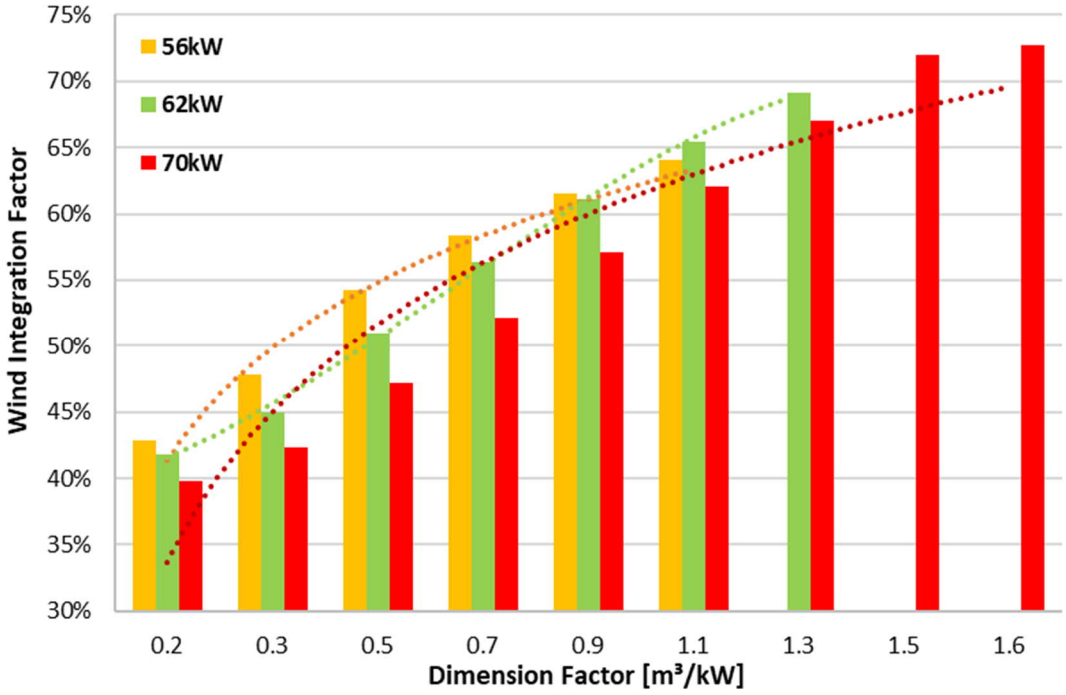

Figure 4-13: The growth of adaptation rate of wind feed-in for different dimensions of the ASHP and TES for the reference case

Based on the maximum WIF values of each heat pump in the above Figure, the growth trend of the WIF is produced and depicted in Figure 4-14. This diagram gives a practical estimation of wind integration performance through over dimensioning an ASHP system for a building with a heating demand equal to the reference building. It is understood that in order to integrate over 50% of the power consumption of the system from wind-feed the minimum DF of 0.5 is required; However, it is recognized that within the period where DF is between [0.6, 1.6] the WIF is increased by 17% with a linear growth rate. Thereby the part can be introduced as the optimal oversizing period for ASHP.

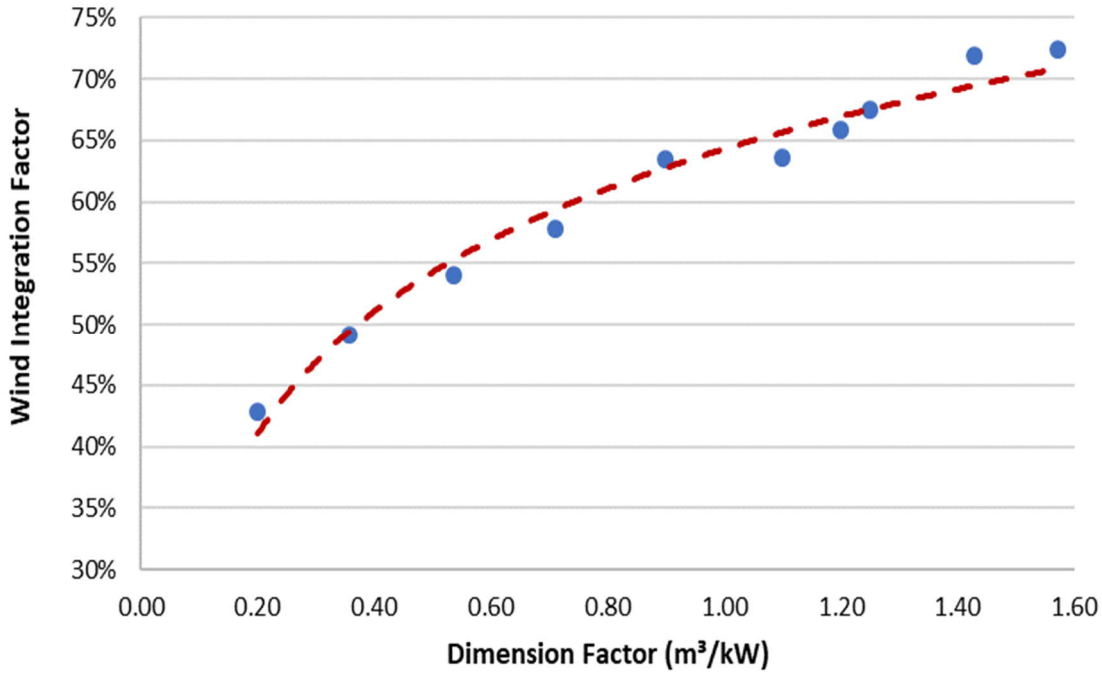

Figure 4-14: Logarithmic regression of the results for the reference simulation case

As it is seen the ratio between WIF and DF can be well estimated by a logarithmic regression represented by the red dashed line; This graph can be then employed as the characteristic sizing diagram for wind integration potential of ASHP system with DF over 0.2 as the minimum required system size for a 2 hours supply gap for the reference building; applying logarithmic regression the correlation can be formulated as follows:

$$WIF = 0.147 * Ln(DF) + 0.64 \ ; 0.2 < DF$$ *Equation 4-4*

In the next step in order to achieve a general correlation that is valid for all demand levels of the multi-family building, the same analysis as the previous step is carried out for the spectrum of certain demand levels that are incorporated in the ASHP model. The outcoming results of the logarithmic regression for the entire heating demand profiles are defined as wind integration characteristic curves for all considered demand levels illustrated in Figure 4-15; It is seen that starting from DF 0.2 as minimum sizing requirement for monovalent supply of the multi-family building, the curves are relatively closer together and the average WIF is less than 40% indicating that standard size of ASHP system does not relatively offer considerable wind integration potential for all building types; However by continuing the oversizing of the system it is observed that the from DF=0.6 the entire diagrams show almost linear behavior and the difference between diagrams becomes larger, this trend continues up to the saturation point where the maximum possible WIF is achieved, at this point the maximum difference of 10% is achieved between the WIF for lowest and highest demand levels; Same as the previous model it is seen that for low demand buildings the WIF curve is saturated at higher DF unlike the high demand buildings where maximum WIF occurs at relatively lower DF of the ASHP system, this is due to the less number of

daily startup cycles and higher power consumption for the system with large DF that results in longer operation during off-peak (surplus) hours. As an example, the heating demand of 50 kWh/m².a representing the new building, maximum WIF of 65 % occurs at dimension factor of 2.6; Whilst for the annual demand of 180 kWh/m², WIF curve is saturated at 75% at DF of 1.4. In other words in a multi-family building with 50 kWh/m².a demand, oversizing ASHP system by 13 times results in roughly 32 % growth of wind share of the power consumption whilst for a building with 180 kWh/m².a demand the same increase of the wind share can be achieved by 8 times enlarging the system dimensions; Comparing these cases it can be concluded that employing oversizing strategy is more effective for the multi-family building with high pick demands.

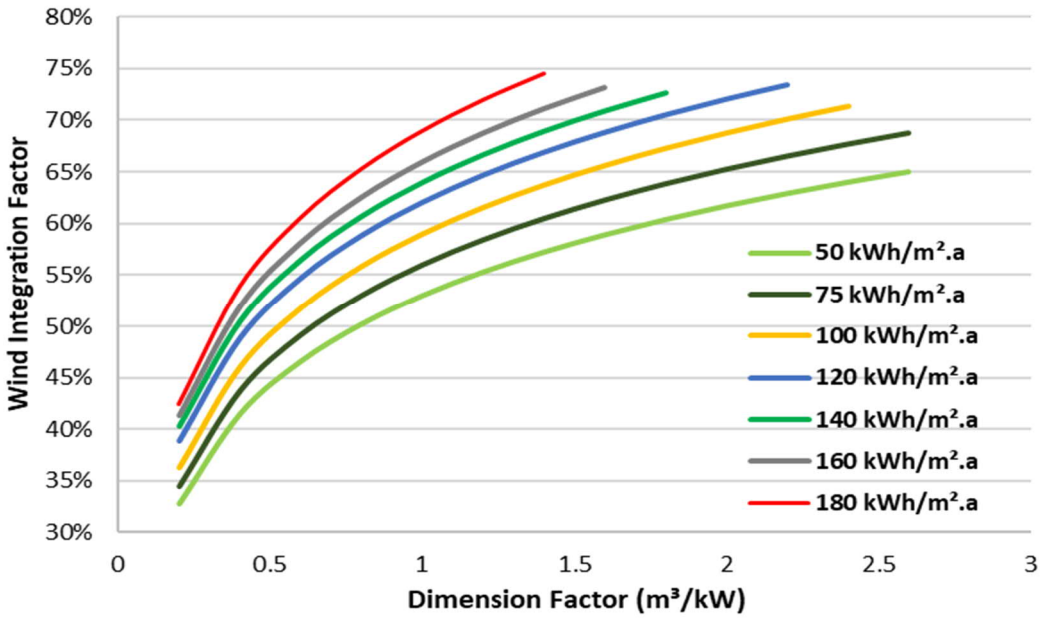

Figure 4-15: Wind adaptation curves for different system dimensions and heating demand levels

Same as the GHSP model, through logarithmic regressions, shown in the above figure the general correlation valid for all demand levels is realized; Equation 4-5 represents this correlation to estimate the wind integration potential as well as sizing of the AHSP with TES for multi-family building:

$$WIF = a_1 * Ln(DF) + a_0$$ *Equation 4-5*

Where: $\begin{cases} 0.126 \leq a_1 \leq 0.165 \\ 0.53 \leq a_0 \leq 0.69 \end{cases}$

The detailed values of these constants for each demand level are given in the below table:

Table 4-3: Constant of the reference Equation 4-5 for the considered demand levels

$Q_{heating}$ $[\frac{kWh}{m^2.a}]$	a_1	a_0
50	0.126	0.53
75	0.134	0.56
100	0.141	0.59
120	0.144	0.62
141	0.147	0.64
160	0.153	0.66
180	0.165	0.69

To have a better understanding of the impact of heating demand change on the wind integration potential of the ASHP system the WIF distribution for each demand level is depicted in below Figure:

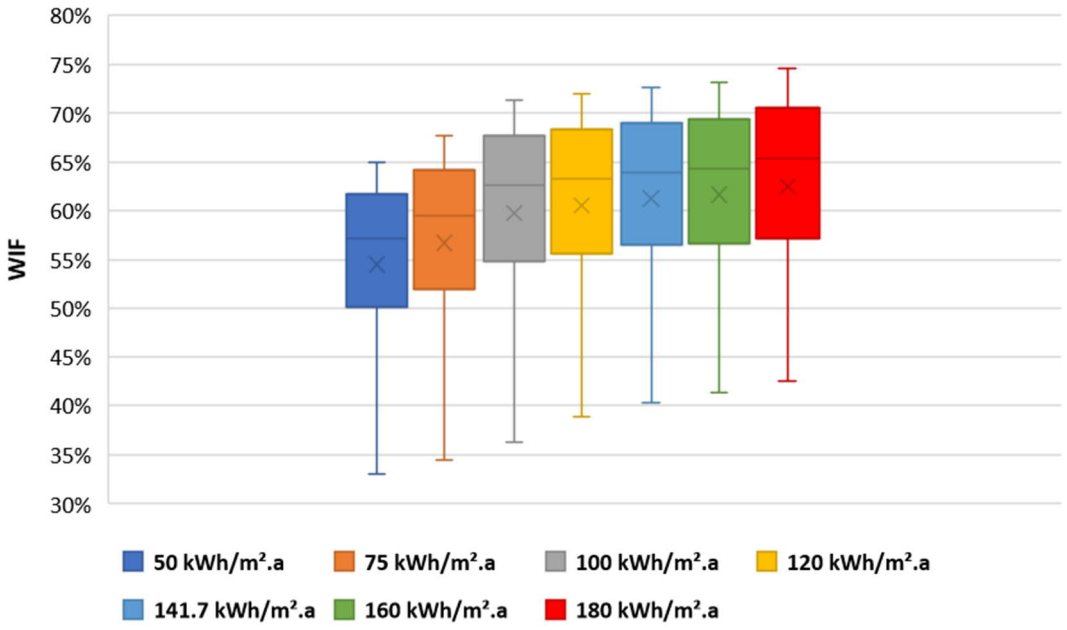

Figure 4-16: Distribution of the Wind Integration Factor of the ASHP system for the considered demand levels

It is observed that increasing the demand level results in the higher median and maximum values of the WIF where the difference between highest and lowest achieved WIF is roughly 10%, however the average WIF changes by 8% in the same period. Considering the WIF ranges of demand levels which varies less than 3% between lowest and highest demand classes, indicates that disregarding maximum and minimum values of WIF within the oversizing scenario of ASHP

system, the distribution of the WIF growth is not influenced considerably by heating demand of the building.

Aiming to include the impact of the heating demand of the building ($Q_{heating}$) on WIF, considering the Table 4-3 and through linear regression represented in Figure 4-17, the correlations between the coefficients (a_0 and a_1) and $Q_{heating}$ are produced.

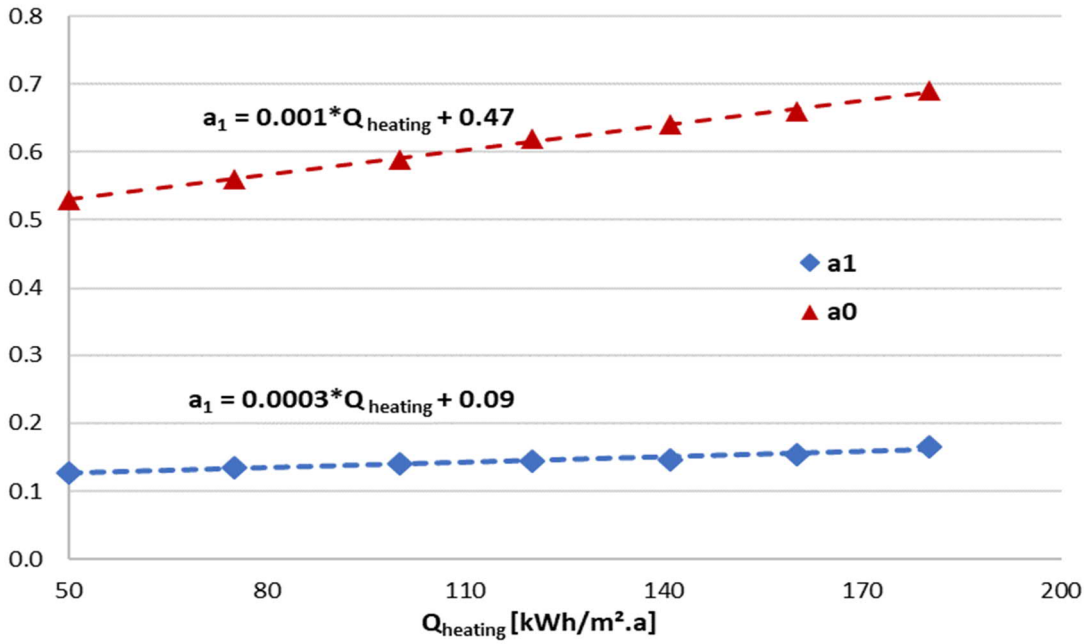

Figure 4-17: Correlation between a_0 and a_1 coefficients and heating demand of the building ($Q_{heating}$)

substituting these coefficients, Equation 4-6 is recognized as the reference correlation for surplus sizing of the ASHP system:

$$WIF[\%] = \left(0.03 * Q_{heating,bui} + 9.01\right) * Ln(DF) + 0.12 * Q_{heating,bui} + 47 \qquad \textit{Equation 4-6}$$

To evaluate the impact of the over dimensioning the system on the thermal performance of the ASHP system, the SPF of the system is calculated for the entire considered dimensions for the case of the reference building.

Figure 4-18 represents the SPF changes of each ASHP size against increasing the thermal storage volume. As it is seen in general by increasing the storage volume the SPF of the system is constantly degraded due to the restricted heating generation by heating load and particularly high heat loss from the storage tank in long discharging cycles. In baseline scenario where a 56 kW ASHP is coupled with a 10 m³ storage tank, the SPF amounts to 3, enlarging the thermal storage by 500% at extreme case (60 m³ tank) results in to roughly 8% reduction of the SPF whilst extends the heat pump operation to almost 2160 hours which increases the WIF by 21%. Utilizing larger sizes of ASHP it is seen that decrement rate of the SPF for larger storage tanks is getting

worse, for instance for the case where a 62 kW ASHP and a 75 m³ are used, SPF is 10% less than the case with 10 m³ storage tank. For the extreme case where the storage tank of a 70 kW ASHP is increased by 12 times, SPF falls to 2.42 which means 15.5 % reduction compared to the base size of the storage tank; This implies that despite increasing the wind integration performance of the ASHP system, the surplus sizing scenario has negative impact on the thermal efficiency of the system.

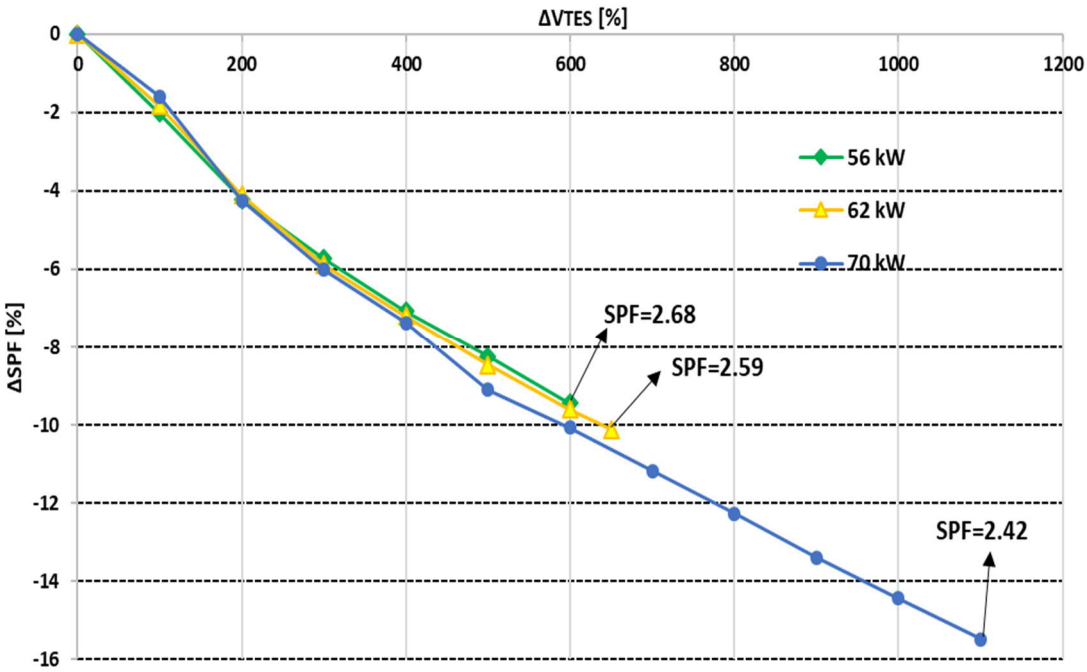

Figure 4-18: the impact of changing storage volume for each ASHP on SPF for the reference building

To have a clear comparison between wind integration performance and thermal performance of the system, Figure 4-19 presents a comparison between behaviors of SPF and WIF for the reference building at DFs of the system where maximum WIFs are achieved. The green column represents the baseline scenario where the system is harvesting the least wind share amounts to 42%, it is seen that increasing DF despite the constant degradation of SPF, maintains constant increase of WIF of the system; For extreme sizing case at DF of 1.57 the WIF of the system is enhanced by 30% and reaches the maximum value of 72% whilst SPF is reduced by 17% to 2.45. This means that the growth rate of the WIF of the system is substantially more than the degradation rate of SPF.

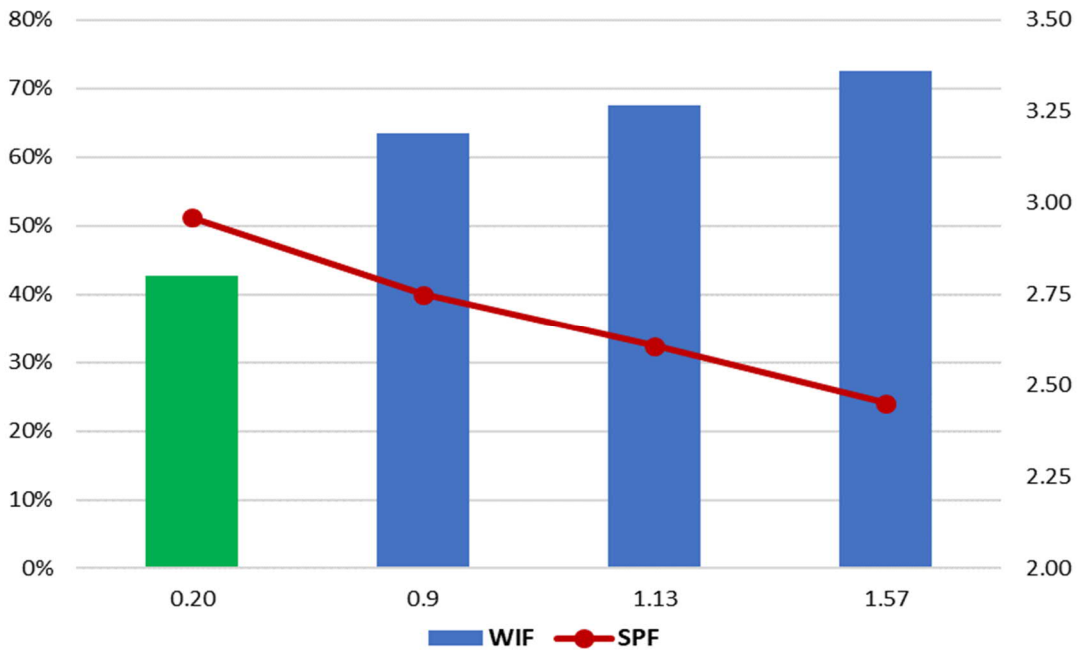

Figure 4-19: Variation of the Seasonal Performance Factor (SPF) of the ASHP by oversizing the system for the reference building

Figure 4-20 represents the distribution of the operation hours of the ASHP system for the same DFs in reference building. The standard system represented by DF= 0.20, 817 hours of the entire 1927 full load operation hours are within the surplus period, which corresponds 43% of the entire seasonal operation; Applying large storage tank for the identical heat pump at DF 0.9 leads to longer operation and longer cycle which consequently increase the surplus hours to 63% of the total operation period. Despite reduced operation hours at higher DF due to the oversized heat pumps based on the higher blocking hours, as operation cycle increased up to 7 hours at DF 1.57, the surplus period of the operation time extends accordingly; The surplus hours at DF reaches to 1325 hours which corresponds 71% of the overall operation.

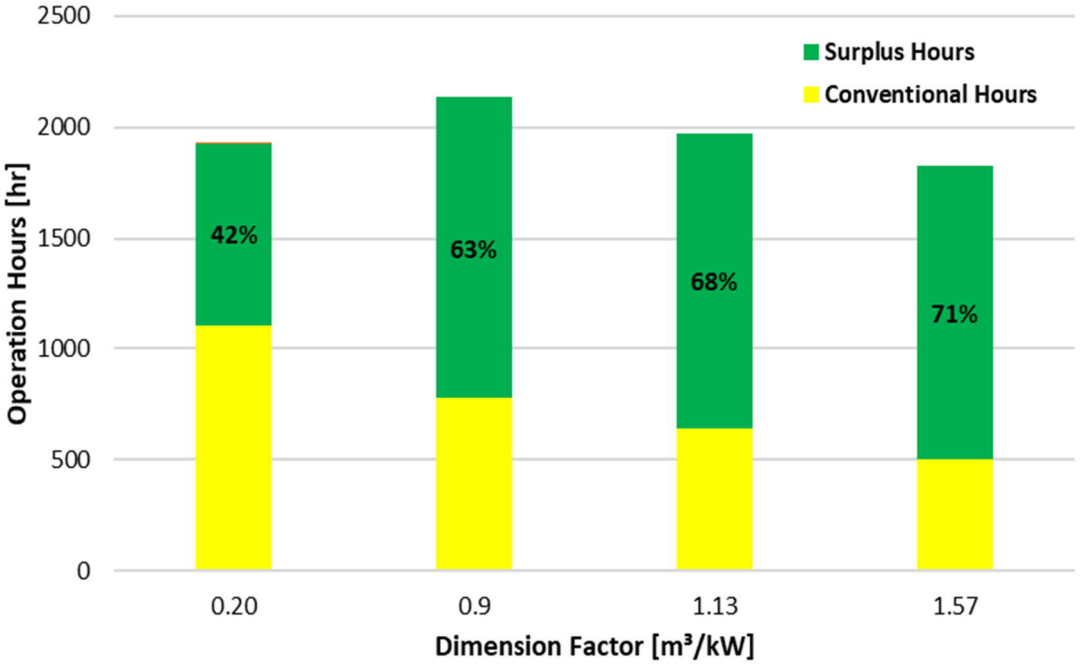

Figure 4-20: Distribution of the operation hours of ASHP for the reference building

4.3. Comparison between Models I and II

Figure 4-21 demonstrates the wind adaptation diagrams of ground source and air source heat pumps for the reference building:

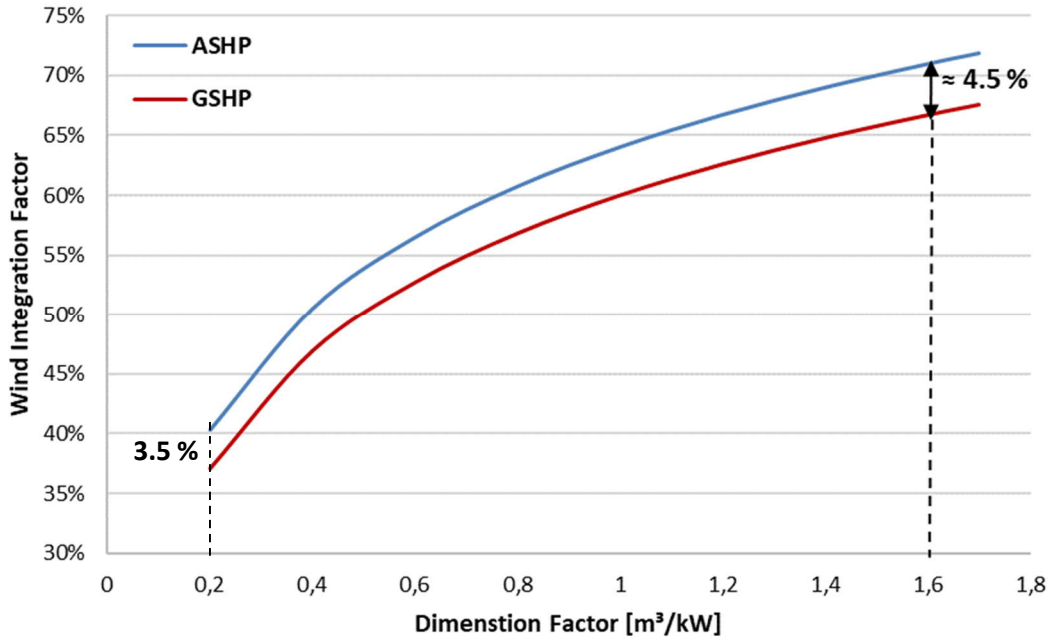

Figure 4-21: WIF comparison between GSHP and ASHP for the reference building

Comparison between the WIF diagrams indicates that at the same DF, ASHP is able to integrate higher share of wind power than GSHP; This is due to the lower COP of the ASHP which results in higher power consumption and longer operating hours than GSHP with the same heating capacity ; For instance considering the standard sized system (DF=0.2) there is a difference of 3.5% between the WIF of ASHP and GSHP, by increasing the DF it is seen that despite a little increase in difference the gap between the curves is almost constant throughout the extreme oversized system at DF 1.6; The small continues growth rate in difference between diagrams at extreme cases is due to the strong degradation of the average COP and accordingly higher power consumption in oversized ASHP which become worse in extreme cases. Figure 4-22 compares the SPF of the GSHP with ASHP for the reference building; As it is expected at the same system dimensions the SFP of the GSHP is quite higher than ASHP; It can be observed that the reduction rate of SPF in both heat pumps is almost identical and the difference between SPFs at all points is roughly 1.4.

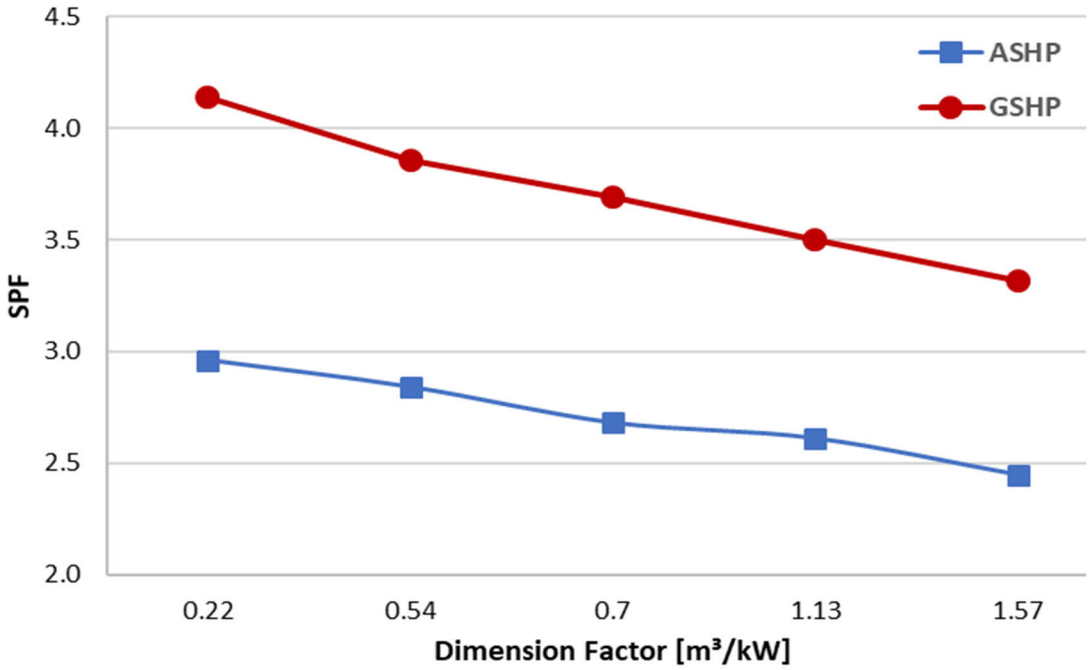

Figure 4-22: SPF comparison between GSHP and ASHP for the reference building

4.4. Model III: Variable Speed Heat Pump Heating System

Aiming to study the operation of the variable speed heat pump (VSHP) under different conditions with time, load and power constraints as well as analyzing the potential of this type of heat pump in adapting surplus wind power for heating purposes, heat profiles of multi-family buildings with different demand ranges are implemented in the TRNSYS model. Following section will investigate

the effect of heating load as well as thermal storage volume on adapting surplus wind power by this type of heat pump system, in this case typical heating load profiles of four multi-dwelling units with different annual specific energy demand levels (50, 100, 141 and 180 kWh/m². a) are supplied by a variable speed heat pump with nominal capacity of 55 kW at 50 Hz complemented by thermal storage tank. Figure 4-23 represents the performance map of this heat pump at different frequency ranges of the multi-speed compressor under corresponding operation conditions:

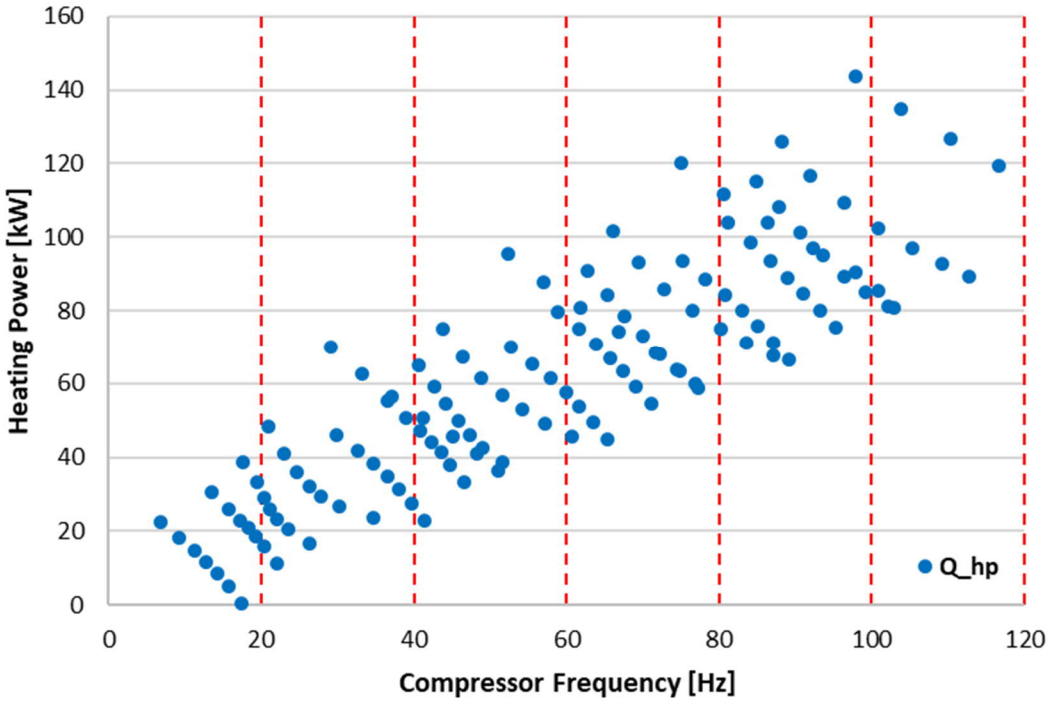

Figure 4-23: Heating capacities of variable speed heat pump at different compressor frequencies

At the first step, the effect of increasing thermal storage volume on the operation of the heat pump as well as the IWF is investigated for the MDU with annual specific heating demand of 50 kWh/m².a; In this case the thermal storage is increased within 6 steps, starting from 10 m³ storage tank which is almost the necessary volume for bridging the minimum daily operation hours gap of the heat pump (blocking hours) under the surplus operation scenario and ending with 60 m³ storage as the worst case for covering the maximum possible operation gap of the heat pump (see Figure 3-18). Figure 4-24 illustrates the simulation results for this case, as it can be observed for the first case where VSHP is equipped by 10 m³, total heat pump operation hours is 749.3 for the entire heating period; Considering the fact that the selected heat pump capacity (55 kW) is almost twice larger than the maximum daily peak load of the building (27.3 kW), almost 630 operation hours are included in low-frequency range of the compressor (less than 50 Hz) and only 34.5 hours are within high-frequency range (50 Hz and more); this results in wind share of 23%. As it is seen increasing thermal storage volume in the next steps is leading to the longer part-load operation hours while full-load operation time is reduced; The reason is larger storage

tank is able to supply the peak loads more frequently in each discharging cycle compared with small storage tanks; On the other side since the larger storage tanks bridges over more daily blocking hours, the heat pump can operate longer during surplus hours and harvest more wind power which leads to higher WIF up to 32 % at 60 m³ storage tank, at this point as the maximum possible daily blocking hours covered by storage tank and thereby maximum surplus share of the heat pump operation hours are achieved, oversizing the volume does not enhance wind power share of the heat pump power consumption; in other words the WIF reaches the saturation point at 60 m³ storage tank in this case.

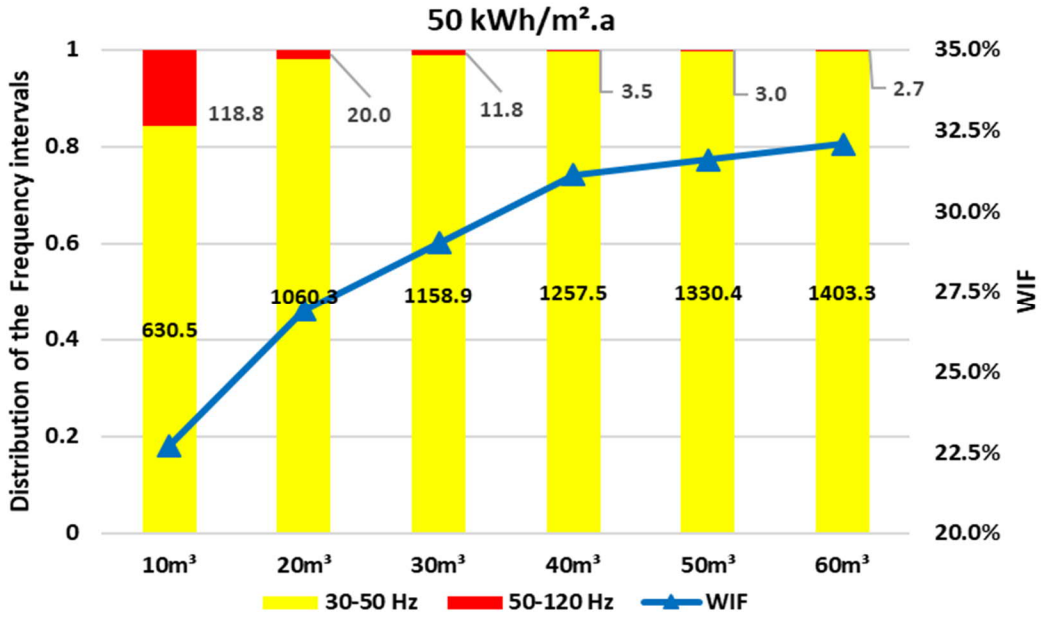

Figure 4-24: Impact of increasing the storage volume on the compressor frequencies and integrated wind power for the specific annual heating demand of 50 kWh/m². a

For the next step, the same seasonal simulation is carried out for the specific annual heating demand of 100 kWh/m².a representing the renovated building with a daily peak load of 46.5 kW. Having two times more heating load than the previous case, according to the results seen in Figure 4-25, the number of heat pump operation hours for a certain storage volume is significantly more than the same volume supplying 50 kWh/m².a building. Furthermore as it is seen for the 10 m³ storage tank, about 0.15 of the entire seasonal performance of the heat pump (216.5 hours) is under full load condition (high frequency range operation), which indicates that due to the lower capacity of the small storage tank and consequently short discharge, the operation gap of the heat pump cannot be covered entirely in extreme cases and therefore heat pump has to operate relatively longer and more often in high-frequency range to charge the storage tank and supplying the peak heating loads accordingly. By adding up the thermal storage volume it is seen that despite increasing the overall operation hours of the heat pump, the high-frequency share of the operation is gradually getting lower as large storage tank can cover more peak loads as well as

longer operation gaps. Due to the increase of the operation hours and longer covered gaps by enlarging storage volume, as it is mentioned before, heat pump can harvest more wind surplus power up to 70 m³ where almost 39% of the power consumption of the heat pump is utilized by wind electricity, as the maximum rate of the WIF in this case.

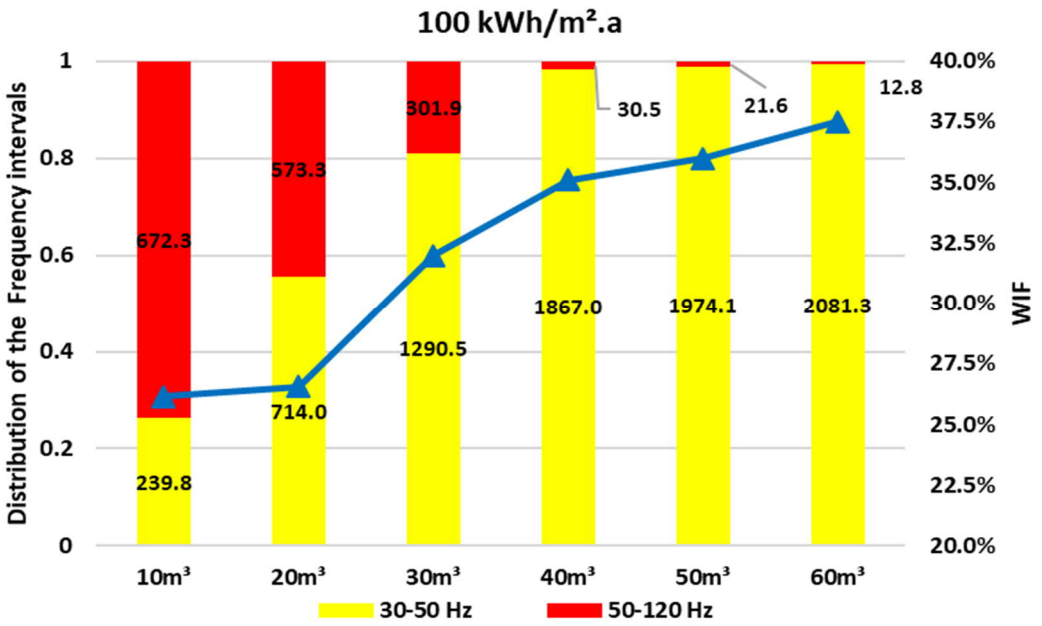

Figure 4-25: Impact of increasing the storage volume on the compressor frequencies and integrated wind power for the specific annual heating demand of 100 kWh/m². a

Next simulation case is to utilize the identical variable heat pump with thermal storage to supply the reference building with 141 kWh/m².a heating demand. Considering the maximum daily peak load of the building (66 kW), it is seen that the nominal heating capacity of the heat pump (55 kW) is below the peak load which results in substantially longer full load operating hours within high operation frequencies; the difference can be clearly seen specifically for relatively small storage volume, where the thermal storage is not able to bridge the operation gaps and supply the demand and thus needs to be charged more often. The simulation results presented in Figure 4-26 prove the above statement, for instance for the case with 10 m³ storage tank about 70% (1085 hours) of the entire operation period (1434 hours) of the heat pump is within the high-frequency range; Applying larger tank increases the part-load operation hours (low frequency range), since the peak demands are more frequently supplied by the storage tank; Nevertheless, contrary to the previous cases, larger storage tanks don't result in flexible operation of the heat pump and consequently higher adaptation rates of the wind power; As it is seen the WIF reduces slightly from 45% at 10 m³ storage tank to about 41% at 60 m³ storage tank; the reason is higher operation hours and thereby longer operation cycles (roughly 3 hours in average) of the heat pump, this means that the number of working hours within the baseload periods where heat pump is supplied by conventional electricity is rising which results in lower WIF.

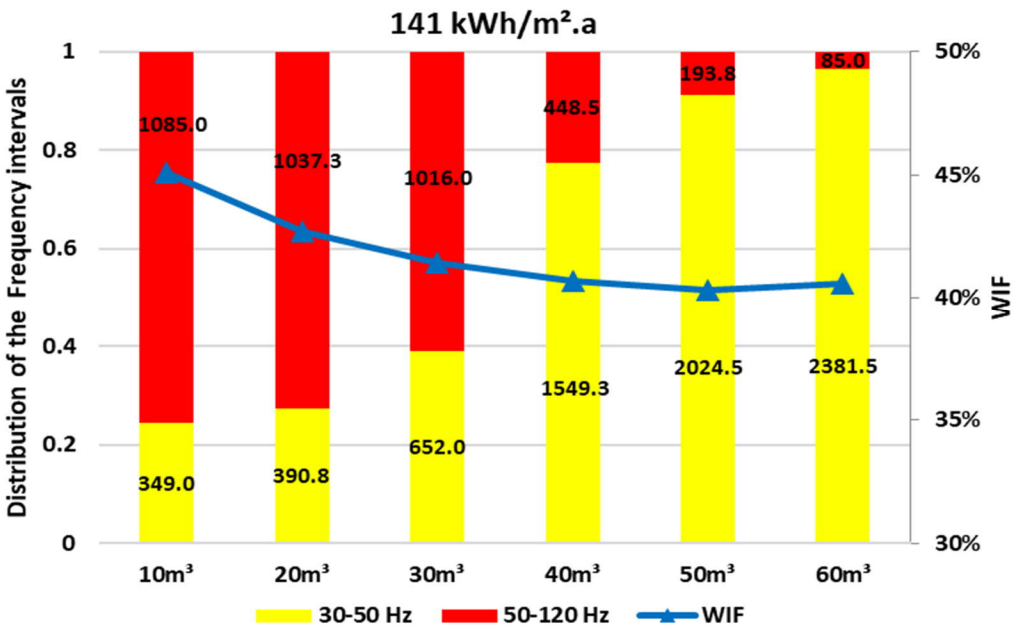

Figure 4-26: Impact of increasing the storage volume on the compressor frequencies and integrated wind power for the specific annual heating demand of 140 kWh/m². a

As the final case a building with 180 kWh/m².a heating demand is considered representing a non-renovated multi-family building to be supplied by the identical variable speed heat pump; Figure 4-27 shows that in the base case (10 m³ storage tank) due to the same reason mentioned for the reference case, heat pump performs roughly 70 % (1071 hours) of the entire operation hours (1428 hours) under high frequencies followed with 51.41% WIF. Complimenting heat pump by larger storage volumes results in deterioration of wind adaptation rates because of longer operation cycles and lower off-peak operation hours that covers surplus hours; Since the peak load of the building is quite higher than the previous case and the number of operation cycles are more, the reduction of the WIF (10% reduction) is clearly stronger than the case before (less than 5% reduction). Thereby it can be concluded that for the buildings with the peak demand more than the nominal capacity of the VSHP, applying an oversized storage tank has a negative impact on wind power integration.

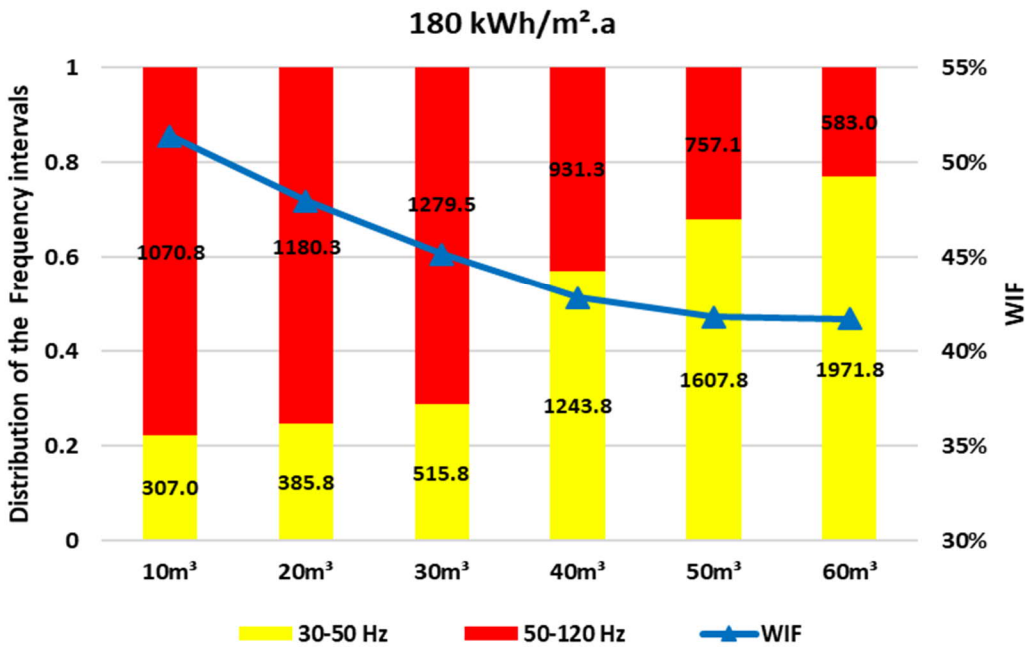

Figure 4-27: Impact of increasing the storage volume on the compressor frequencies and integrated wind power for the specific annual heating demand of 180 kWh/m². a

Considering worse case scenarios for all demand levels where changing thermal storage size does not change the WIF anymore, Figure 4-28 gives a clear comparison between WIF saturation points and operation hours for different heating loads, for instance for the building with 50 kWh/m² annual demand, due to the over-dimensioned system, almost all the 1536 operation hours of the heat pump are located in low-frequency range (part load). In this case maximum, 32.67 % power consumption is drawn from the wind feed-in. by increasing the heating load, since thermal storage needs to be charged more frequently the operation hours of the heat pump under full load (high frequency) are increased that results in higher wind adaptation rate. This continues up to the annual heating demand of 180 kWh/m².a where WIF reaches almost 42%. Putting together the simulation results of all cases for VSHP, the impact of increasing thermal storage volume and heating load of the building on the wind integration capability of the identical VSHP is presented in Figure 4-28.

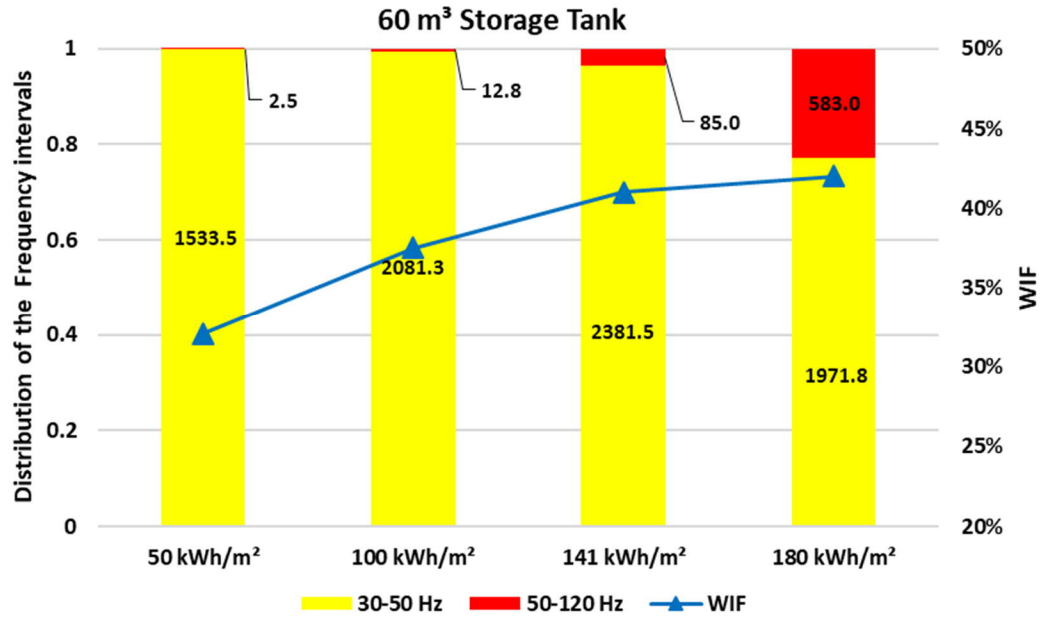

Figure 4-28: the impact of increasing demand level for the identical system dimensions on the operation hours and WIF of the VSHP

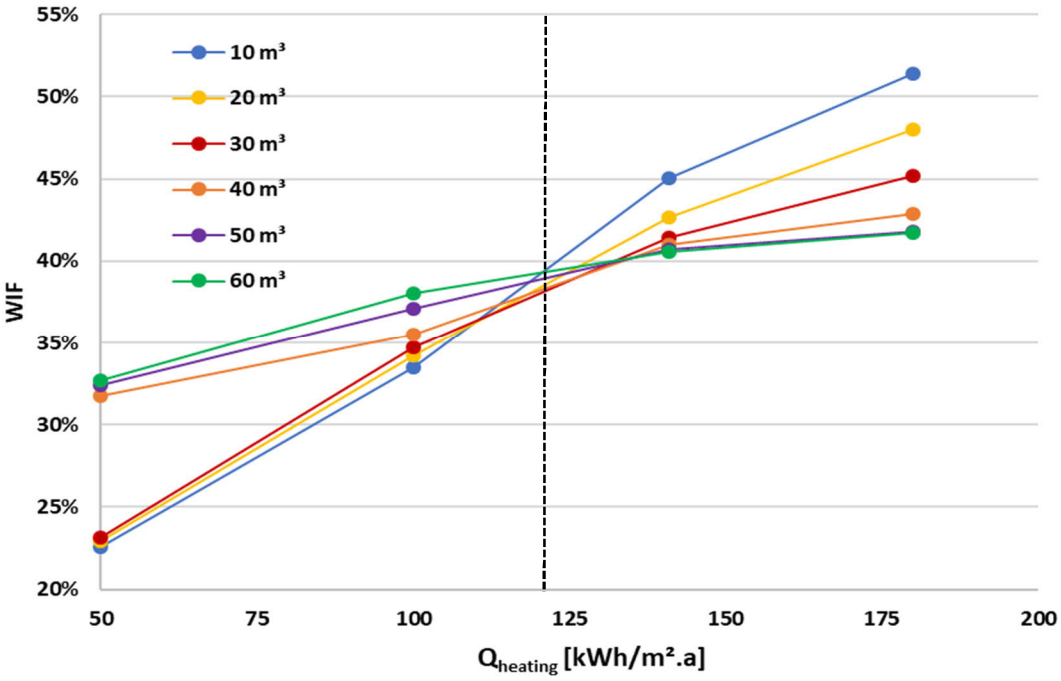

Figure 4-29: the impact of increasing storage volume and heating load on the WIF

Figure 4-29 illustrates the impact of increasing thermal storage volume on the wind integration for considered heating demands; as it is seen for the new and renovated buildings, where heating

demand is lower than nominal heating capacity of the VSHP, enlarging the storage volume results in higher WIF indicating the higher wind power ratio in the power consumption of the VSHP; the reason is, as explained previously, in this case enlarging the heat storage volume leads to significantly covering peak load hours and thereby heap pump is enabled to operate longer during off-peak hours that results in higher wind share. For the higher heating load where the nominal heating capacity of the VSHP is close to peak heating demand (shown in dotted line), utilizing larger storage tanks does not make any considerable change in WIF since the heat pump operates longer under full load condition and during peak hours and using larger thermal storage does not improve the situation. For the heating loads larger than 125 kWh/m².a Where the rated heating capacity of the heat pump is exceeded, the full load operation hours of the heat pump is increasing significantly; Escalating the storage volume in this case despite the previous cases has negative impact on the wind integration as it reduces WIF; This occurs due to the long operation cycles of the heat pump beyond off-peak hours to charge larger storage tanks. Overall in case of utilizing VSHP, it is understood that for higher demand levels, increasing the thermal storage volume is less effective in integrating wind power by the heat pump system and in worse case increases the conventional power consumption of the heat pump.

Aiming to achieve a clear image of the impact of utilizing various storage volumes as well as changing the heating loads on the compressor performance and consequently wind power adaptation of the VSHP, as by increasing the heating loads VSHP capacity is increased until it reaches the nominal heating capacity where VSHP operates under full load condition, the heat pump capacity ($\dot{\mathrm{Q}}_{\mathrm{hp}}$) in strongly affected by heating load of the building $\left(\dot{Q}_{heating}\right)$ and thereby the modified dimension factor (DF) for VSHP is written as below equation:

$$\dot{Q}_{hp} = f\left(\dot{Q}_{heating}\right) \xrightarrow{yields} DF_{VSHP}[\frac{m^3}{kW}] = V_{TES}/\dot{Q}_{heating} \qquad \textit{Equation 4-7}$$

Figure 4-30 shows the simulation results for the case where the identical VSHP system is performed under increasing $\mathrm{DF}_{\mathrm{VSHP}}$. For the worst-case scenario where heat pump is accompanied by a 60 m³ thermal storage tank supplying the MDU with 50 kWh/m² annual demand, due to the over-dimensioned system, almost all the 1536 hours operation of the heat pump is in low-frequency range; In this case 32.67 % power consumption is drawn from the wind feed-in. By increasing the demand level as it is shown, as the full-load operation of the heat pump is more frequently needed to supply peak demands, the overall working hours as well as the number of high-frequency operation hours is rising, which results in higher wind adaptation rate. This continues up to the annual heating demand of 180 kWh/m².a where WIF reaches almost 42%.

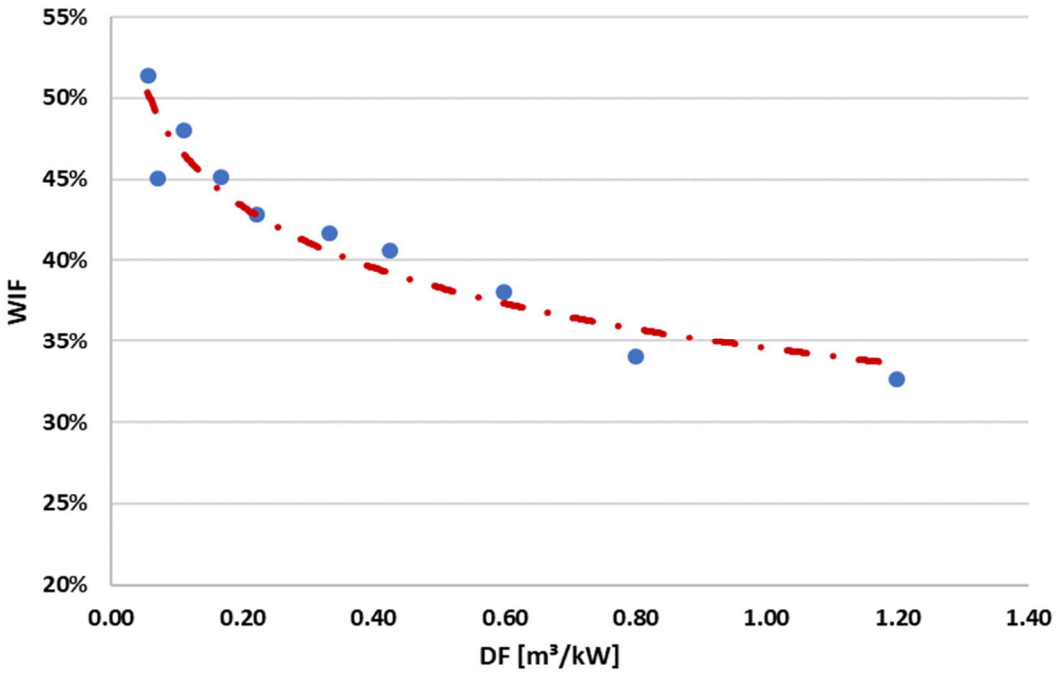

Figure 4-30: Variation of the compressor frequencies and integrated wind power for the same storage volume and different demand levels

Applying logarithmic regression, the correlation between WIF and DF for VSHP is written as:

$$WIF = -0.0055 * Ln(DF) + 0.35 \qquad \textit{Equation 4-8}$$

As it is can be observed from Figure 4-30 and above correlation the downtrend of WIF is saturated by almost 33% at DF=1.2 representing the fact that further increasing storage (larger than 60 m³) does not reduce the WIF anymore. Moreover, in order to achieve the optimum wind integration performance by the VSHP in case of large demands, standard-sized thermal storage should be utilized.

Figure 4-31 illustrates the effect of increasing thermal storage volume on the SPF of the heat pump with thermal storage for the considered heating demand levels. For all cases, the storage tank is enlarged from 10 m³ to 60 m³. As it can be observed by increasing the storage tank, the SPF of the system is reduced for all demand levels; The highest SPF degradation occurs in the case where the variable speed heat pump system supplies the building with 50 kWh/m² annual demand, in this case by utilizing 60 m³ storage tank the SPF is reduced by roughly 35%; The reason is the extremely high heat loss of the thermal storage due to the long discharge cycle of the thermal storage for low demand level. In case of the annual demand of 180 kWh/m², due to the high heating demand which is more than nominal capacity of the heat pump, the entire charge heat to the storage tank is required to cover the demand and thereby the discharge cycle of the

storage tank is clearly shorter that results in lower heat loss of the thermal storage; Thereby SPF is decreased by almost 22% which is the least SPF degradation among all cases.

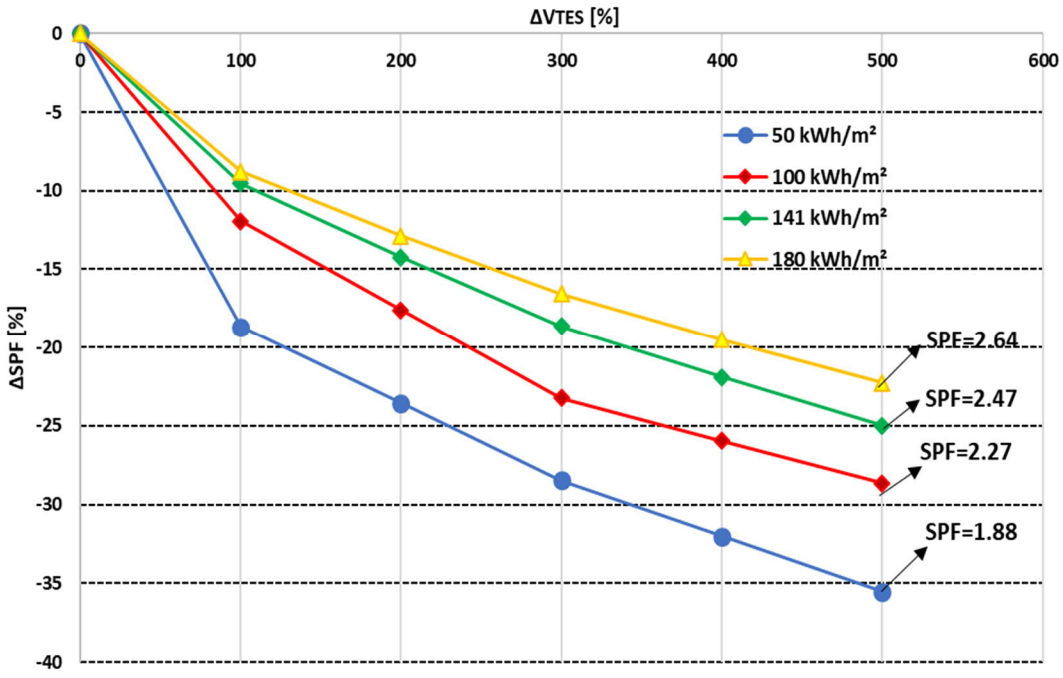

Figure 4-31: The impact of increasing the thermal storage volume on SPF

4.5. Comparison of all simulation cases

In this section the wind integration and thermal performances of all considered types of heat pump heating systems are compared within considered sizing and surplus control circumstances for the reference building with the annual specific heating demand of 141 kWh/m².a. ; In the first step the comparison is made based on base-line sizing scenario at the 0.2 DF where a 56 kW heat pump associated with 10 m³ thermal storage supplies the reference building, the results are presented in the Table 4-4:

Table 4-4: Baseline scenario- performance comparison for heat pumps in the reference simulation case

Type of the heat pump	Adapted Wind Energy [MWh]	WIF	Total Operation [hr]	Off-Peak Operation [hr]	Ave. Cycle Length [hr]	SPF
Single- speed GSHP	8.1	39%	1617	610	3	4.3
Single-speed ASHP	11	42%	1927.4	817	3.5	2.9
Variable speed ASHP	7.6	45%	1434	647.25	2.85	3.3

The above results prove that at baseline dimensions of the system the highest WIF belongs to the VSHP, however, due to the quite shorter full load operation time in VSHP compared with single stage heat pumps, the power consumption and consequently the adapted wind energy by this type of the heat pump is less than other types. Because of the highest full-load operation and power consumption in single-speed ASHP, this type integrates the most amount of wind energy under surplus control and extreme sizing scenario; On the other hand considering the thermal performance of the heat pumps, as single-speed GSHP generates the highest output heat during 1617 operation hours, it delivers the highest SPF (4.3) among all types; The lowest SPF belongs to the ASHP, this is mostly due to the considerably lower average COP of this and significantly high power consumption heat pump within surplus scenario during heating-period. Furthermore, this table implies that within the surplus control scenario at standard operating conditions using VSHP instead of ASHP will improve both thermal and wind integration performances in the surplus scenario.

In the second step, the performance of the heat pumps is evaluated and compared under the extreme sizing scenario where dimension factor 1.6 is applied. In this step for the case of single-speed heat pumps both heat pump and thermal storage are oversized while for the case of variable speed ASHP the identical heat pump is coupled with maximum oversized thermal storage.

Table 4-5: Extreme sizing scenario -performance comparison for the heat pumps in the reference simulation case

Type of the heat pump	Adapted Wind Energy [MWh]	WIF	Total Operation Hours	Off-Peak Operation Hours	Ave. Cycle Length [hr]	SPF
Single- speed GSHP	19	67 %	1442	953	6.6	3.32
Single-speed ASHP	23.1	72 %	1828.2	1282.6	7.2	2.45
Variable- speed ASHP	14.5	40 %	2464	959.5	2.6	2.47

Considering the results in the Table 4-5, the maximum wind integration potential is presented by single-stage ASHP which harvests 72% of the entire power consumption from wind feed-in which is roughly 23 MWh wind energy for the entire heating season, this is substantially more than the case with GSHP and variable-speed ASHP; In contrast to the single-speed heat pumps, where enlarging storage tank has a negative impact on the wind integration capability of the variable speed ASHP; On the other hand, the operation of the single-speed heat pumps is more stable than variable-speed heat pump as the number of startup and shutdowns in variable-speed heat pump is high and the operating cycles are extremely short; The reason is the high-frequency

change sequences based on the availability of surplus wind power and charging cycles of large storage tank. In terms of thermal performance of the heat pump systems, it is observed that due to the substantial increase of the power consumption in one side and higher heat loss of the storage tank on the other side, oversizing strategy has in general a negative effect on the SPF for all types, however same as the previous case stable operation and low operating hours of the single-speed GSHP causes the highest SPF among considered heat pumps.

5. Summarizing Discussions and Outlook

5.1. Summarizing Discussions

In this present work, the possibility of adapting wind feed-in in power network through different technologies of heat pump system associated with thermal energy storage that is used to supply the heating demand of multi-family building in Berlin has been numerically investigated. For this purpose, after developing the simulation model of the entire system in TRNSYS [32], in the first step, based on the availability of the wind generation and the standard electrical load profile of the multi-family building a surplus control scenario for operating the heat pump system was introduced and implemented in the model as an alternative to the conventional operation of the heat pump system; The comparison between the performances of the surplus and conventional control scenarios shown in Figure 4.2 proved that through operating GSHP system under standard sizing and surplus control scenario for the reference building, in average 35% of the power consumption of the system is supplied from wind generation, this number is over 40% in the ASHP system. In the second step, in order to maximize the wind-share of the power consumption of the investigated heat pump systems, an oversizing scenario of heat pump and thermal storage tank based on the oversizing factor, which is driven from the daily blocking hours, has been applied within the surplus control scenario. Aiming to characterize the wind power integration potential of the heat pump system, (WIF) as the wind share of the power consumption of the heat pump and dimension factor (DF) as the ratio between thermal storage volume and heating capacity of the heat pump were determined in this study; Considering the results of the seasonal simulations for all cases the correlations between these factors for each type of the heat pump and different demand levels of the multi-family building have been developed; This leaded us to the characteristic diagrams as a reference for dimensioning heat pump and thermal storage in relation with measuring the wind integration potential of the system. Summarizing the methodology of this study the flowchart in Figure 5-1 represents the procedure of oversizing the single-speed heat pump for multi-family building under surplus control algorithm. In other words, knowing the daily average surplus hours, the peak heating load of the building and type of the heat pump, the system dimensions to achieve maximum wind share will be suggested by this algorithm. For instance, in case of using a GSHP for a renovated multi-family building with 100 kWh/m².a specific demand and peak load of 47 kW, having maximum 6 blocking hours per day, according to the reference diagram (Figure 4-5) in order to provide at least 50% of the power consumption from wind-feed in (WIF=50%), the storage tank volume must be at least 70% of the heating capacity of the selected heat pump (DF=0.7 m³/kW), this means a 63 kW GSHP coupled with 44 m³ TES is suitable for this case; It can be calculated directly by employing the reference correlation for GSHP given in the Equation 4-3 as follows:

$$\left\{\begin{matrix} Q_{heating} = 100\ \left[\frac{\mathrm{kWh}}{m^2.a}\right] \\ WIF = 50\% \end{matrix}\right\}$$

$$\xrightarrow{Eq.\ 4-3} \mathrm{WIF} = (0.0004 * 100 + 0.09)(\mathrm{Ln}(\mathrm{DF})) + 0.001 * 100 + 0.44$$

$$\rightarrow \boxed{DF \approx 0.7\ [\frac{m^3}{kW}]}$$

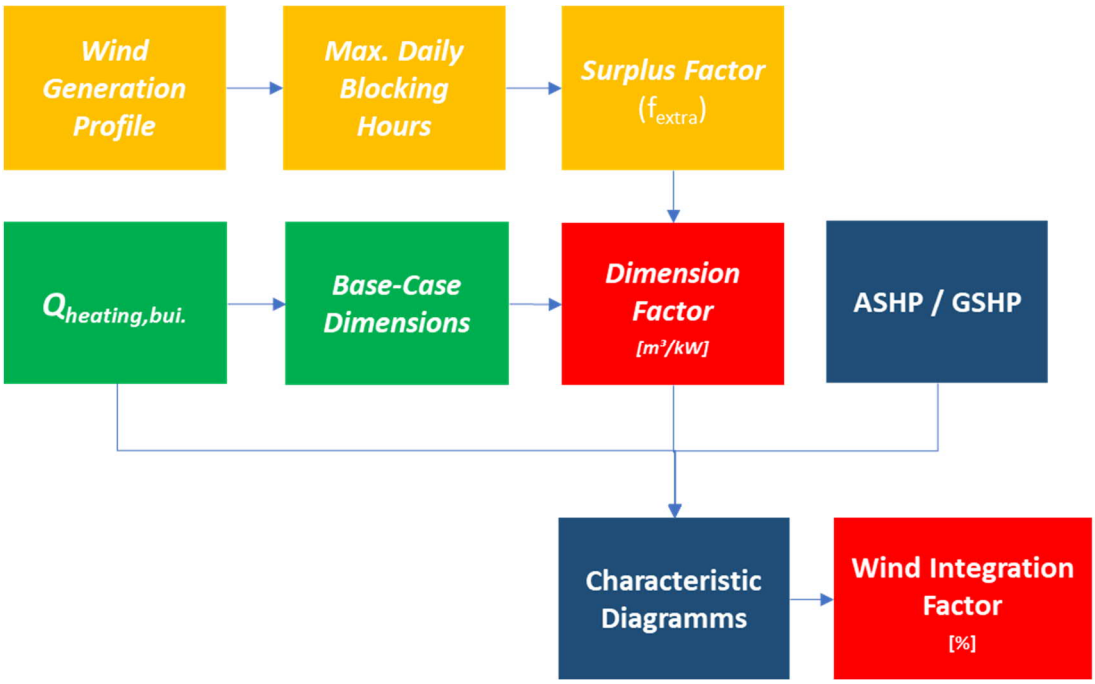

Figure 5-1: Oversizing Procedure for single-speed heat pumps supplying multi-family building

As an example for the case of ASHP, for the same multi-family building based on the reference diagram presented in the Figure 4-15 and the Equation 4-5, in order to achieve the maximum wind share of 73% at extreme sizing scenario, the DF of the system should not be less than $1.5\ [\frac{m^3}{kW}]$ which means the storage tank must be 1.5 times more than the capacity of the heat pump. The simulation results for both air-source and ground-source single-speed heat pump systems indicated that startup cycle of the heat pump and the off-peak operation hours are deciding parameters within the surplus oversizing approach, as an example the average cycle length of GSHP under surplus scenario for the reference building is around 3.5 hours; That means roughly 3 startups per day which are quite longer than conventional operation where heat pump starts 3-5 times in an hour [34]. In general, it is seen that in the buildings with demand levels over average such as none-retrofitted buildings where the wind shares of the power consumption have been boosted by roughly 34% where WIF has reached up to 75% in case of applying ASHP, the surplus oversizing scenario has been more effective than low demand buildings.

The second part of the study was dedicated to the air source variable-speed heat pump where the capacity control approach introduced in [23], [24] have been applied together with the surplus control scheme. In this case, due to the variable capacity of the heat pump which is maintained by variable operating frequencies of the compressor, the impact of oversizing the heat storage volume on the performance of the heat pump and consequently wind integration potential of the system has been evaluated for different demand levels. Analyzing the simulation results in this case, it was observed that for the buildings with the peak heating load lower than the nominal capacity of the heat pump, since a major part of the heat pump operation time is located within part-load range (low-range frequencies: 30-50 Hz) employing larger storage tank increases the part-load operation time and resulted in more flexibility that facilitated the increasing wind share of power consumption of the compressor up to 40%; In contrary to the high demand buildings, where the pick-load was higher than the nominal capacity of the heat pump and therefore due to the long full-load operation which mostly located out of off-peak period; Since the operation in this case is less flexible Implementing oversized storage tank for such buildings resulted in longer operation out of off-peak period and consequently reduced WIF. therefore, the operation flexibility and the reduction trend of WIF became worse when the demand was increased. Figure 4-30 and Equation 4-7 gave a clear image of the degradation rate of the WIF of the system in VSHP for increasing heating demand; 20% reduction of WIF of the system in case of implementing 60 m^3 storage as the saturation point of the diagram in this figure, implies the negative impact of the oversizing algorithm for the VSHP. However, it is to be noticed under standard operating conditions, the VSHP delivers quite better thermal and electrical performance than single-stage ASHP.

5.2. Conclusions

- Applying oversizing algorithm based on the availability of wind electricity alongside with surplus control strategy for single-speed heat pump systems with thermal storage causes the flexible operation of the system, which results in delivering solid potential in integrating the wind energy and thereby reducing the fossil fuel share of the power consumption in the heating network.
- Despite the highest WIF achieved by ASHP, due to the significantly better SPF and less baseload power consumption for the identical heat capacity, as well as performance stability, the GSHP fits better in this operation and sizing scenario.
- The situation of the power distribution network and the intraday wind excess production plays crucial roles on the way to calculating blocking and surplus time periods and consequently establishing the surplus algorithm for the heat pump.
- Due to utilizing the synthetic load profiles of the multi-family building in the simulation models, the impact of the thermal storage effect of the building, which can specifically change the load profile and heating curve of the old buildings and consequently influence the operation of the heat pump system, is neglected in this research.
- Oversizing the thermal storage tank in case of peak demands does not offer extra flexibility to the VSHP and therefore is not recommended particularly when the heat pump is undermentioned.
- Knowing the WIF and SPF trends of the heat pump system for the entire investigated sizes, helps to find out the optimum design point of the system, where the integrated wind energy is maximized, and the degradation of the thermal performance is minimized.

5.3. Outlook and Future Research Potentials

As utilizing Power-to-Heat technologies and specifically heat pumps play a key role in integrating intermittent renewable energies and thereby strongly reducing the fossil fuel share of the heating market, smart control scenarios of the heating systems are significantly important in developing smart decentralized energy grid where the energy suppliers and consumers are characterized based on their instant supply and demand balances and match to each other through a power aggregator. The feasibility of Integrating renewable electricity through heat pumps by such proposed solutions strongly depends on the network infrastructure and power exchange structure. Modifying feed-in Tariff system in Germany that is currently inflexible and constant for all consumption hours, as well as applying smart power meters for the consumers is one the important prerequisites to economically quantify and justify the surplus load management and sizing strategies and motivating consumers to use such smart heating systems; Beside the cost-

effectivity analysis, there are other parameters such as grid support coefficient of the heat pump and building that could be studied to highlight the impact of the smart control and off-peak sizing strategies on the grid stability. Furthermore, developing a predictive control system that interacts with the wind generation forecasts is one of the necessities that should be developed as a supplement for the proposed sizing strategy for heat pump and heat storage. Implementing building models with different heat distribution systems will be significantly helpful to investigate the flexibilities of the entire system in coordination with the energy-saving potential of the system as well as integrating renewable electricity. In this regard since none-residential building types such as shopping centers have a crucial load in energy consumption, they should be investigated in terms of the potential of the load shifting and integrating renewable electricity. Finally, as cooling demand is recently considerably rising by increasing the ambient temperature and thereby the energy consumption in this sector is getting higher, extending the same studies for cooling by the heat pump and cold storage is highly recommended.

Bibliography

[1] D.Fraile, A.Mbistrova, WindEurope Business Intelligence (2017), “Wind power 2016”

[2] Bundeskartellamt Bundesnetzagentur (2014), “Monitoringbericht 2014“

[3] R.Paschotta, (2014), „Ausfallarbeit“ (https://www.energie-lexikon.info/ausfallarbeit.html)

[4] Federal Ministry for Economic Affairs and Energy (BMWi) Public Relations, Second Monitoring Report (2014), “The Energy of the Future”

[5] J.Niendorf -Senatsverwaltung für Stadtentwicklung (2011), “Berlin-Wohnenswerte Stadt”

[6] Auswertung Kraftwerksliste Bundesnetzagentur nach Bundesland (2014), (https://www.bundesnetzagentur.de/.../Kraftwerksliste/Kraftwerksliste_2014_1.xlsx)

[7] Stromnetz Berlin/fact, figures and dates, (https://www.stromnetz.berlin/en/facts-figures-dates.htm)

[8] B.Bach, J.Werling, T.Ommen, M.Münster, J.M. Morales, & B.Elmegaard, Energy 107 (2016) 321e334, “Integration of large-scale heat pumps in the district heating systems of Greater Copenhagen”

[9] Bundesministerium für Wirtschaft und Technologie (BMWi)Öffentlichkeitsarbeit, „Energie in Deutschland“ Trends und Hintergründe zur Energieversorgung (2013)

[10] F.Karlsson, (2007), “Capacity Control of Residential Heat Pump Heating System”

[11] Mathiesen, B. V., Blarke, M., Hansen, K., & Connolly, D. (2011). “The role of largescale heat pumps for short term integration of renewable energy”

[12] M. Economidou, B. Atanasiu, C. Despret, and J. Maio, “Europe’s buildings under the microscope,” Brussels (2011)

[13] Poulsen, C. S. (2007). Varmepumper – status sommeren 2007 i og uden for Danmarks grænser (Heat pumps - status summer of 2007 in and outside Denmark), Danish technological institute

[14] EU (2010), “Directive 2010/31/EU of the European Parliament and of the Council of 19 May 2010 on the energy performance of buildings,” in Official Journal of the European Union, pp. 13–35

[15] Bundesverband Wärmepumpe e.V. (2016), BWP-Branchenstudie 2015, Szenarien und politische Handlungsempfehlungen (heat pump market’s data in Germany until 2015 and prognosis until 2030)

[16] D.Patteeuw, K.Bruninx , A.Arteconi , E.Delarue, W.D’haeseleer,L.Helsen, Applied Energy 151 (2015) 306–319 “Integrated modeling of active demand response with electric heating systems coupled to thermal energy storage systems”

[17] M.Miara, D.Günther, Z.L. Leitner, and J.Wapler, Energy Technol. 2014, 2, 90 – 99”Simulation of an Air-to-Water Heat Pump System to Evaluate the Impact of Demand-Side-Management Measures on Efficiency and Load-Shifting Potential”

[18] W.J.A. van Leeuwen, M. Bongaerts, G.M.A. Vanalme, UPEC 2011 · 46th International Universities' Power Engineering Conference · 5-8th September 2011 “Load Shifting by Heat Pumps using Thermal Storage”

[19] D.Fischer, F.Rautenberg, T.Wirtz, B.Wille-Haussmann, H.Madani, International Congress on Refrigeration, At Yokohama, Volume: 24 (2015) “Smart Meter Enabled Control for Variable Speed Heat Pumps to Increase PV Self-Consumption“

[20] Y.Wang, Q.Chen, Energy 85 (2015) 609e619 “A direct optimal control strategy of variable speed pumps in heat exchanger networks and experimental validations“

[21] H.Madani, J.Claesson, P.Lundqvist, Energy and Buildings 65 (2013) 1–9 “A descriptive and comparative analysis of three common control techniques for an on/off controlled Ground Source Heat Pump (GSHP) system”

[22] Jong Won Choi a, Gilbong Lee b, Min Soo Kim, Applied Thermal Engineering 31 (2011) “Capacity control of a heat pump system applying a fuzzy control method”

[23] H.Madani, J.Claesson, P.Lundqvist, Applied Thermal Engineering 31 (2011) “Capacity control in ground source heat pump systems Part I: modeling and simulation”

[24] F.Karlsson, Fahlen, internaional journal of refrigeration 30(2007) Pages 221-229 “capacity controlled ground source heat pump for hydronic heating system”

[25] F.Karlsson, Fahlen, Energy and Building (2007) “Variable speed heat pump for hydronic heating system-energy saving potential and considerations for control”

[26] H.Madani, J.Claesson, P.Lundqvist, internaional journal of refrigeration 34(2011) 1934e942, “Capacity control in ground source heat pump systems part II: Comparative analysis between on/off controlled and variable capacity systems**”**

[27] Matteo Dongellini*, Claudia Naldi, Gian Luca Morini, Applied Thermal Engineering 90 (2015) 1072e1081, “Seasonal performance evaluation of electric air-to-water heat pump Systems “

[28] K.Hedegaard, B.Vad Mathiesen, H.Lund, P.Heiselberg, Energy 47 (2012) 284e293 “Wind power integration using individual heat pumps e Analysis of different heat storage options”

[29] K.Hedegaard, M.Münster, Energy Conversion and Management 75 (2013) 673–684 “Influence of individual heat pumps on wind power integration – Energy system investments and operation

[30] D.Fischer, K.B. Lindberg, S.Mueller, E.Wiemken, B.Wille-Haussmann “Potential for Balancing Wind And Solar Power Using Heat Pump Heating And Cooling Systems”

[31] S.Luigi, S.Massimiliano, T.Chiara, Energy Building 2015;90:15–28 “Demand response management by means of heat pumps controlled via real time pricing”

[32] TRNSYS : Transient System Simulation Tool: http://www.trnsys.com/

[33] DWD- climate data center (cdc): https://www.dwd.de/DE/leistungen/cdcftp/cdcftp.html

[34] I.Sarbu, C.Sebarchievici, Energy and Buildings 70 (2014) 441–454, “General review of ground-source heat pump systems for heating and cooling of buildings “

[35] Senatsverwaltung für Stadtentwicklung und Umwelt. Grundwassertemperatur und Temperaturjahresgang 2011. http://www.stadtentwicklung.berlin.de/umwelt/umweltatlas/da214_02.

htm#Abb2, Mai 2015

[36] Berlin Environmental Atlas 02.14 Groundwater Temperature (Edition 1999) https://www.stadtentwicklung.berlin.de/umwelt/umweltatlas/ed214_02.htm

[37] BINE Informationsdienst. Erdgekoppelte Wärmepumpen für Neubauten, http://www.bine.info/publikationen/publikation/erdgekoppelte-waermepumpen-fuer-neubauten/auswertung/, 2010.

[38] F.Karlsson, Building service engineering, Department of Energy and Environment, Chalmers University, Sweden (2007), “Capacity Control of Residential Heat pump Heating Systems”

[39] Amt für Statistik Berlin-Brandenburg. https://www.statistik-berlin brandenburg.de /webapi/jsf/tableView/tableView.xhtml

[40] Energieeinsparverordnung - EnEV (2014). http://www.enev-online.com /enev_2014_volltext/enev_2014_verkuendung_bundesgesetzblatt_21.11.2013_leseversion.pdf

[41] EUROPEAN STANDARD DIN EN 832 (Jun 2003) “Thermal performance of buildings - Calculation of energy use for heating”

[42] VEREIN DEUTSCHER INGENIEURE-VDI 4655 (May 2008), “Reference load profiles of single-family and multi-family houses for the use of CHP systems”

[43] Handbuch (September 2014), “Testreferenzjahre von Deutschland für mittlere, extreme und zukünftige Witte-rungsverhältnisse “

[44] A. Wieczorek, technische Universität Berlin, Herman Rietschal Institut (September 2015), Masterarbeit “Simulation und Bewertung eines aktiven Lastmanagements einer Wärmepumpenanlage mit Wärmespeicher in einem Energienetz“

[45] DIN EN 15450:2007-12. Titel (Deutsch): “Heizungsanlagen in Gebäuden-Planung von Heizungsanlagen mit Wärmepumpen“, Titel (English): “ Heating Systems in Buildings- Design of Heat Pump Heating Systems“

[46] DIN EN 12831-1:2017-09. Titel (Deutsch): “Energetische Bewertung von Gebäuden - Verfahren zur Berechnung der Norm-Heizlast“, Titel (English): “Energy Performance of Buildings - Method for Calculation of the Design Heat Load - Part 1: Space heating load“

[47] VIESSMANN group, Planungsanleitung der Wärmepumpe VIESSMANN group

[48] Buderus- Ausgabe 2013/11, Sole-Wasser Wärempump Plannungsunterlagen

[49] L.Gelažanskas, K.A.Gamage, Sustainable Cities and Society, Volume 11, 2014, 22-30 “Demand side management in smart grid: A review and proposals for future direction“

[50] Lorenz GmbH & Co. Behälter und Apparatebau KG Ingenieurbüro für Schweißen, Schneiden und verwandte Verfahren

Appendixes

A: Datasheets of the heat pump systems of the Viessmann company [48]

Ground-water heat pump system (VITOCAL 300-G, 351.B42)

Technische Daten Wasser/Wasser-Wärmepumpen

Typ BW/BWS in Verbindung mit „Umbausatz Wasser/Wasser Wärmepumpe“		351.B20	351.B27	351.B33	351.B42
Leistungsdaten nach EN 14511 (W10/W35, Spreizung 5 K)					
Nenn-Wärmeleistung	kW	25,4	34,7	42,2	52,3
Kälteleistung	kW	21,1	29,3	35,7	43,8
Elektr. Leistungsaufnahme	kW	4,50	5,70	6,80	9,00
Leistungszahl ε (COP)		5,70	6,10	6,20	5,80
Sole (Primärzwischenkreis)					
Inhalt	l	9	11	14	14
Nennvolumenstrom (Spreizung 3 K)	l/h	6400	9500	10300	14000
Durchflusswiderstand bei Nennvolumenstrom	mbar	145	80	120	320
	kPa	14,5	8,0	12,0	32,0
Mindestvolumenstrom (Spreizung 5 K)	l/h	4800	6500	7700	10500
Durchflusswiderstand bei Mindestvolumenstrom	mbar	90	42	77	124
	kPa	9,0	4,2	7,7	12,4
Max. Vorlauftemperatur (Soleeintritt)	°C	25	25	25	25
Min. Vorlauftemperatur (Soleeintritt)	°C	7,5	7,5	7,5	7,5
Heizwasser (Sekundärkreis)					
Inhalt	l	8	9	13	13
Nennvolumenstrom (Spreizung 5 K)	l/h	4300	5700	7300	9000
Durchflusswiderstand bei Nennvolumenstrom	mbar	68	53	105	154
	kPa	6,8	5,3	10,5	15,4
Mindestvolumenstrom (Spreizung 12 K)	l/h	1800	2400	3050	3750
Durchflusswiderstand bei Mindestvolumenstrom	mbar	11	13	23,0	33
	kPa	1,1	1,3	2,3	3,3
Max. Vorlauftemperatur (Spreizung 8 K)	°C	65	65	65	65
Max. Vorlauftemperatur (Spreizung 12 K)	°C	70	70	70	70

Ground-source heat pump (VITOCAL 350-G, 352.A076)

Technische Daten

Betrieb: Sole-Wasser

Typ BW		**352.A027** **352.A027 SA**	**352.A034** **352.A034 SA**	**352.A056** **352.A056 SA**	**352.A076** **352.A076 SA**	**352.A097** **352.A097 SA**
Leistungsdaten nach EN 14511 (B0/W35, 5 K Spreizung)						
Nenn-Wärmeleistung	kW	27,2	34,3	56,1	76,0	96,9
Kälteleistung	kW	20,8	26,4	43,4	58,8	74,6
Elektr.-Leistungsaufnahme	kW	6,4	7,9	12,8	17,3	21,9
Leistungszahl ε (COP)		4,2	4,4	4,4	4,4	4,41
Sole (Primärkreis)						
Inhalt	l	4	5	10	13	18
Nenn-Volumenstrom dT 3K	m^3/h	6,7	8,3	13,7	18,7	23,9
Durchflusswiderstand	mbar	150	160	170	190	190
Min. Volumenstrom	m^3/h	4,5	5,2	8,6	12,0	15,0
Max. Eintritt	°C	25	25	25	25	25
Min. Eintritt bei Nenn-Volumenstrom	°C	-7	-7	-7	-7	-7
Heizwasser (Sekundärkreis)						
Inhalt	l	4	4,5	8	10	13
Nenn-VolumenstromdT 5K	m^3/h	4,8	5,9	9,8	13,2	16,8
Durchflusswiderstand	mbar	200	200	200	200	220
Min. Volumenstrom	m^3/h	2,5	3,0	5,0	6,7	8,5
Max. Eintritt	°C	73	73	73	73	73
Min. Eintritt bei Nenn-Volumenstrom	°C	30	30	30	30	30

Air-water heat pump (AWHO 351.A20)

Typ AWHI 351.A/AWHO 351.A (400 V-Geräte)

Innenaufgestellte Wärmepumpen

Typ		**AWHI 351.A10**	**AWHI 351.A14**	**AWHI 351.A20**
Leistungsdaten Heizen nach EN 14511 (A2/W35)				
– Bei Volumenstrom Sekundärkreis	l/h	2400	3300	3700
– Bei Durchflusswiderstand	mbar	200	370	450
	kPa	20	37	45
Nenn-Wärmeleistung	kW	10,60	14,50	18,50
Elektr. Leistungsaufnahme	kW	2,9	4,2	5,8
Leistungszahl ε (COP)		3,60	3,50	3,20
Leistungsdaten Heizen nach EN 14511 (A7/W35, Spreizung 5 K)				
Nenn-Wärmeleistung	kW	12,70	16,70	20,60
Elektr. Leistungsaufnahme	kW	3,1	4,2	6,1
Leistungszahl ε (COP)		4,00	3,80	3,40
Wärmegewinnung				
Max. Ventilatorleistung	W	110	170	270
Max. Luftmenge	m^3/h	3500	4000	4500
Max. zul. Druckverlust (zu- und abluftseitig)	Pa	37	45	61
Min. Lufteintrittstemperatur	°C	–20	–20	–20
Max. Lufteintrittstemperatur	°C	35	35	35
Anteil Abtauzeit/Laufzeit	%	2 bis 5	2 bis 5	2 bis 5
Heizwasser (Sekundärkreis)				
Inhalt	l	5,0	5,5	6,0
Mindestvolumenstrom	l/h	1100	1450	1700
Durchflusswiderstand Verflüssiger (mit der Anschlussverrohrung, Lieferumfang)	mbar	50	90	120
	kPa	5,0	9,0	12,0
Max. Vorlauftemperatur (bei 5 K Spreizung)				
– Bei Lufteintrittstemperatur –20 °C	°C	55	55	55
– Bei Lufteintrittstemperatur –10 °C	°C	65	65	65
Elektrische Werte Wärmepumpe				
Nennspannung			3/N/PE 400 V/50 Hz	
Max. Nennstrom	A	10	14	18,3
Anlaufstrom (mit elektronischer Anlaufstrombegrenzung)	A	23	26	30
Anlaufstrom (bei blockiertem Rotor)	A	64	101	99
Absicherung	A	3 x B16A	3 x B20A	3 x B25A
Absicherung Ventilator		T 6,3 A H	T 6,3 A H	T 6,3 A H
Nennspannung Steuerstromkreis			1/N/PE 230 V/50 Hz	
Absicherung Steuerstromkreis		T 6,3 A H	T 6,3 A H	T 6,3 A H
Kältekreis				
Arbeitsmittel		R407C	R407C	R407C
Füllmenge	kg	4,0	4,5	5,2
Verdichter	Typ		Scroll Hermetik mit Einspritzung	
Abmessungen				
Gesamtlänge	mm	946	946	946
Gesamtbreite	mm	880	1030	1200
Gesamthöhe	mm	1870	1870	1870
Gesamtgewicht	kg	287	297	361
Zul. Betriebsdruck	bar	3	3	3
	MPa	0,3	0,3	0,3
Anschlüsse				
Heizungsvor- und -rücklauf	G	1½	1½	1½
Kondenswasserschlauch (Ø innen/außen)	mm	25/32	25/32	25/32

Außenaufgestellte Wärmepumpen

Typ		**AWHO 351.A10**	**AWHO 351.A14**	**AWHO 351.A20**
Leistungsdaten Heizen nach EN 14511 (A2/W35)				
– Bei Volumenstrom Sekundärkreis	l/h	2400	3300	3700
– Bei Durchflusswiderstand	mbar	200	370	450
	kPa	20	37	45
Nenn-Wärmeleistung	kW	10,60	14,50	18,50
Elektr. Leistungsaufnahme	kW	2,9	4,2	5,8
Leistungszahl ε (COP)		3,60	3,50	3,20

B: Normalized diagrams of heating capacity and power input of the considered GSHP and ASHP

GSHP

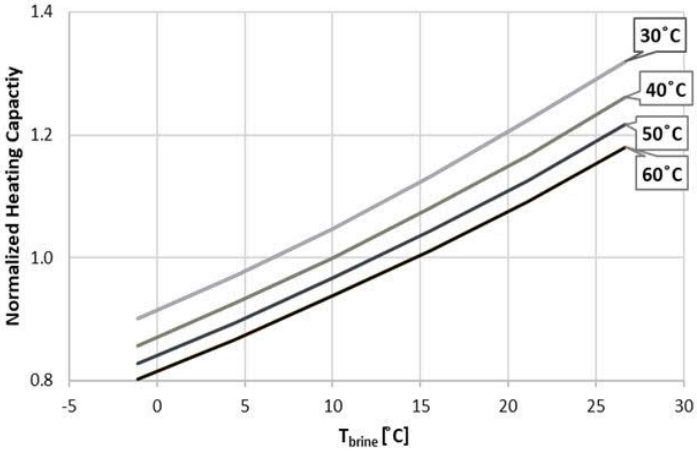

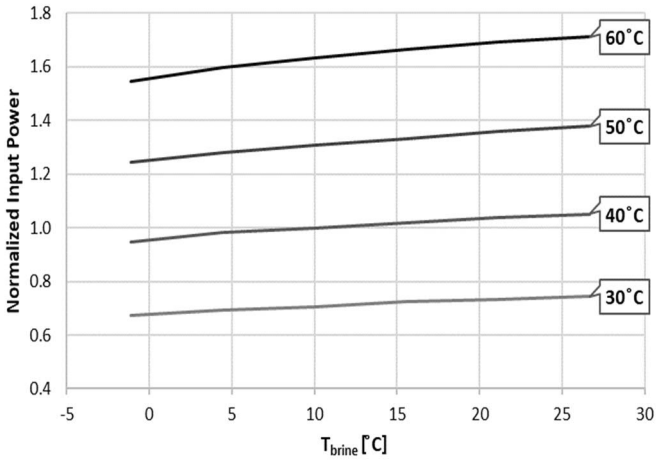

ASHP

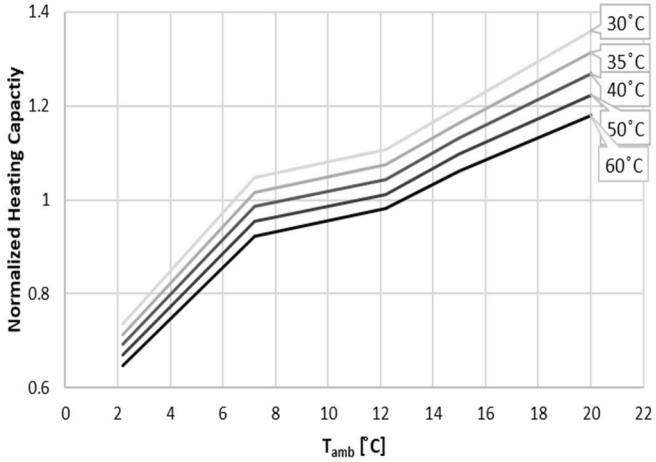

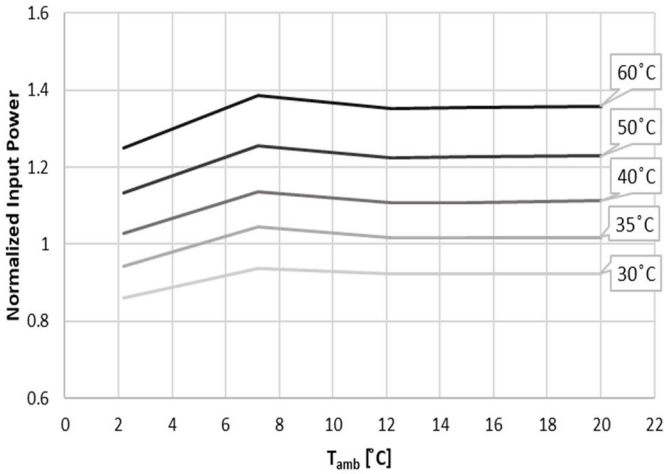

C: Dimensions of the thermal storage tank [50]

Preise einschließlich 15 frei platzierbaren Anschlüssen ½" – 2", Anschlüsse gerade oder schräg.
Anschlußlänge bis 250 mm, Betriebsdruck 3 bar, Betriebstemperatur bis 110°C

Ø	Zylindrische Behälterhöhe in mm 2000	3000	4000	5000	6000	7000	8000	
1200	2560	3560	4560	5560	6560	7560	8560	Höhe
	2700	3800	5000	6200	7300	8500	9700	Inhalt
	1.992,00	2.504,00	3.012,00	3.527,00	4.035,00	4.548,00	5.058,00	Preis
1300	2600	3600	4600	5600	6600	7600	8600	Höhe
	3200	4500	5900	7300	8700	10000	11400	Inhalt
	2.282,00	2.863,00	3.447,00	4.033,00	4.611,00	5.195,00	5.776,00	Preis
1400	2637	3637	4637	5637	6637	7637	8637	Höhe
	3700	5300	6900	8500	10100	11700	13300	Inhalt
	2.853,00	3.510,00	4.168,00	4.826,00	5.484,00	6.141,00	6.798,00	Preis
1500	2680	3680	4680	5680	6680	7680	8680	Höhe
	4400	6200	8000	9800	11700	13500	15300	Inhalt
	3.162,00	3.907,00	4.635,00	5.372,00	6.109,00	6.854,00	7.583,00	Preis
1600	2730	3730	4730	5730	6730	7730	8730	Höhe
	5000	7100	9200	11300	13300	15400	17500	Inhalt
	3.645,00	4.469,00	5.293,00	6.117,00	6.941,00	7.765,00	8.589,00	Preis
1700	2770	3770	4770	5770	6770	7770	8770	Höhe
	5700	8100	10400	12800	15100	17500	19800	Inhalt
	4.358,00	5.269,00	6.180,00	7.092,00	8.003,00	8.914,00	9.825,00	Preis
1800	2810	3810	4810	5810	6810	7810	8810	Höhe
	6500	9200	11800	14400	17000	19700	22300	Inhalt
	4.913,00	5.903,00	6.894,00	7.892,00	8.874,00	9.904,00	10.934,00	Preis
1900	2850	3850	4850	5850	6850	7850	8850	Höhe
	7300	10300	13200	16100	19100	22000	25000	Inhalt
	5.341,00	6.442,00	7.544,00	8.645,00	9.746,00	10.847,00	11.948,00	Preis
2000	2890	3890	4890	5890	6890	7890	8890	Höhe
	8200	11500	14700	18000	21200	24500	27700	Inhalt
	5.856,00	7.052,00	8.256,00	9.461,00	10.657,00	11.861,00	13.057,00	Preis
2200	2980	3980	4980	5980	6980	7980	8980	Höhe
	10200	14100	18100	22000	25900	29900	33800	Inhalt
	6.933,00	8.462,00	9.999,00	11.533,00	13.066,00	14.602,00	16.132,00	Preis
2500	3100	4100	5100	6100	7100	8100	9100	Höhe
	13600	18700	23800	28900	34000	39000	44100	Inhalt
	8.645,00	10.554,00	12.456,00	14.373,00	16.274,00	18.176,00	20.078,00	Preis

Höhe in mm, Inhalt in l, Preis in €/Behälter zuzüglich ges. MwSt. ab Werk

D: Simulation Layouts in TRNSYS environment

Single Speed ASHP and GSHP Models (Type 941, Type 927)

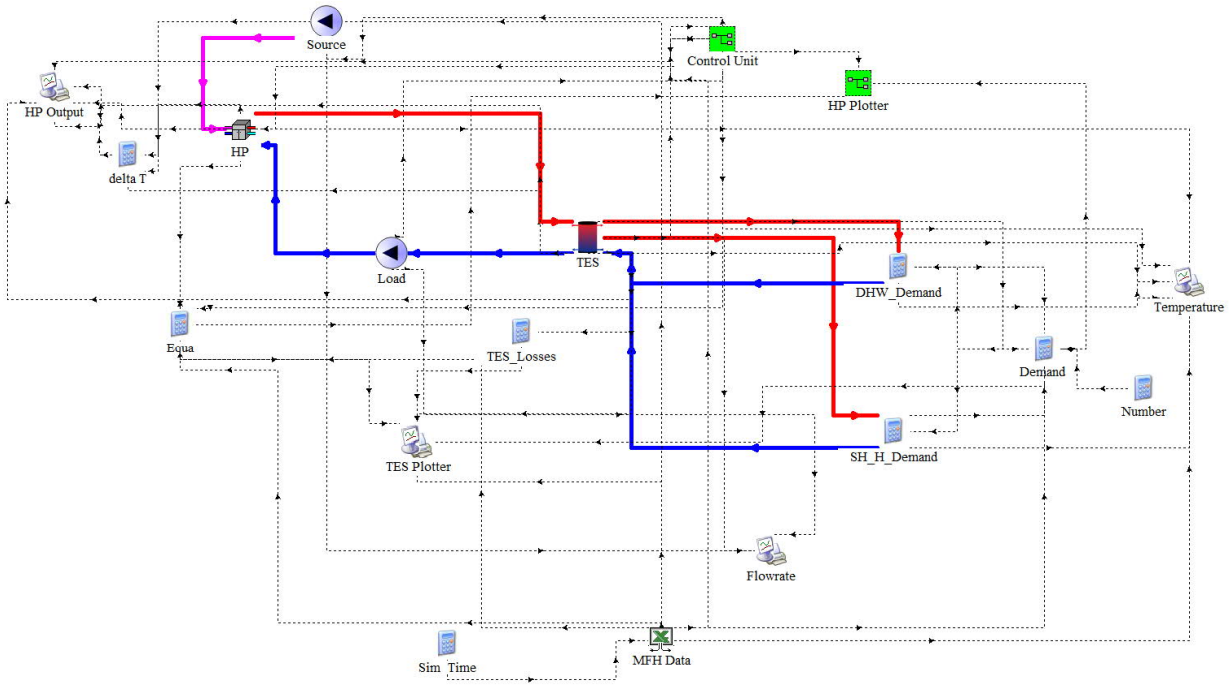

VSHP Model based on 3D interpolation based on performance data

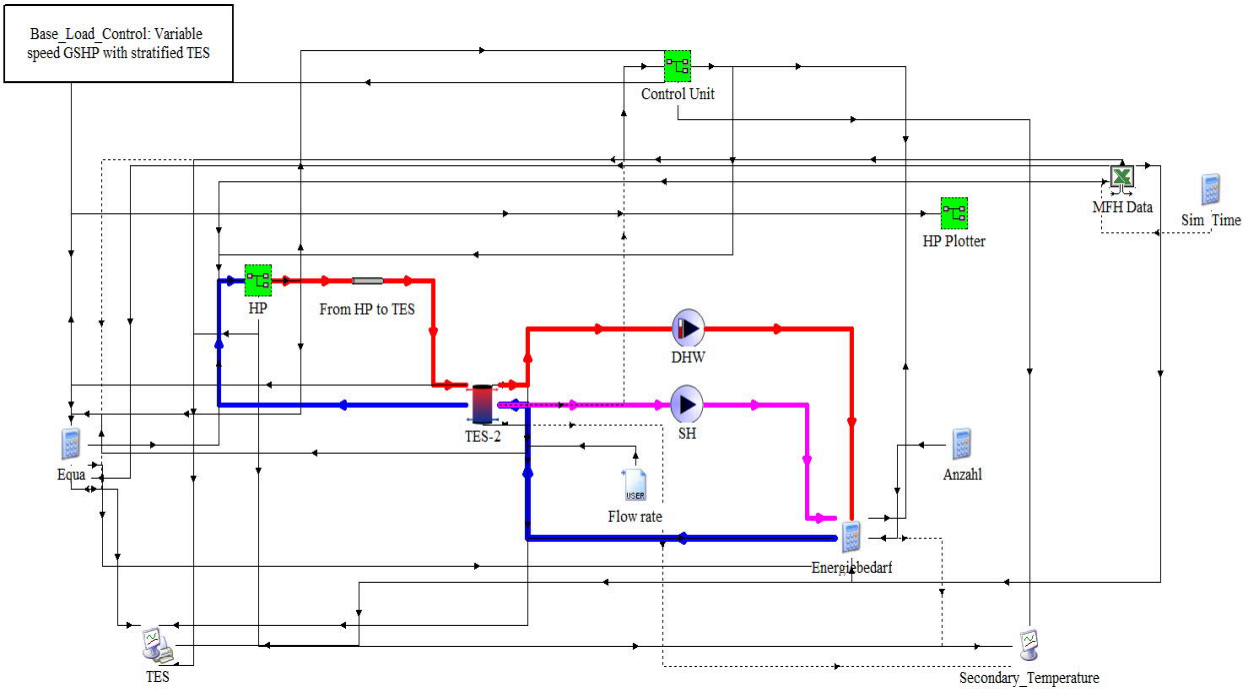

E: Surplus Control Scenario for Heat Pump Models in TRNSYS

(a) Single Speed Heat Pump

```
Strombedarf_kW = Strombedarf/3600   ! Strombedarf=Electricity demand of the heat pump [kW]

Ave_SLP = 30  ! Average heating load of the building [kW]

off_peak_zeit = lt(SLP_Prognose,Ave_SLP)    !  Defining off-peak time periods

Peak_zeit = gt(SLP_Prognose,45)                  ! Defining peak time periods

off_peak_signal = gt(off_peak_zeit ,0.5)

Peak_signal = gt(Peak_zeit,0.5)

Wind_einpeis = gt(Wind_Einspeisung,0)        !Wind_einspeis=Wind Generation

Wind_einspeis_Signal = gt(Wind_einpeis,0.5)

Surplus_Signal = gt(Wind_einspeis_Signal,0.5)*gt(off_peak_zeit,0.5)

Surplus = Wind_Einspeisung*gt(Surplus_Signal,0.5)

T_hp_output_water =
(gt(DHW_Control_Signal,0.5)*T_DHW_setpoint)+(lt(DHW_Control_Signal,0.5)*gt(SH_Control_Signal,0.5)
*T_sh_setpoint)+(lt(DHW_Control_Signal,0.5)*lt(SH_Control_Signal,0.5)*0)

Q_dhW_kW = Warmwasser/3600

Q_sh_kW = Heizung/3600

Q_req_kW = Q_dhW_kW+Q_sh_kW

Q_load = Flowrate_out*4.19*(T_hp_output_water-T_water_in)

Q_load_kW = Q_load/3600

HP_control_signal = lt(Peak_signal,0.5)*gt(Q_load,0)*lt(T_top_node,65)

HP_off_Peak_signal = gt(Surplus_Signal,0.5)*gt(Q_load,0)*lt(T_bottom_node,65)
```

(b) Variable Speed Heat Pump

```
Strombedarf_kW = Strombedarf/3600

off_peak_zeit = lt(SLP_Prognose,Ave_SLP)

Peak_zeit = gt(SLP_Prognose,45)

Ave_SLP = 30

off_peak_signal = gt(off_peak_zeit ,0.5)

Peak_signal = gt(Peak_zeit,0.5)

Wind_einpeis = gt(Wind_Einspeisung,0)

Wind_einspeis_Signal = gt(Wind_einpeis,0.5)

Surplus_Signal = gt(Wind_einspeis_Signal,0.5)*gt(off_peak_zeit,0.5)

Surplus = Wind_Einspeisung*gt(Surplus_Signal,0.5)

T_water_design_out = T_hp_setpoint_water

T_load_hp = T_water_in

m_dot_load = 3000 !kg/hr       !rated load flowrate of the heat pump

Q_load = m_dot_load*4.19*(T_water_design_out-T_water_in) !Generated heat by the heat pump

Q_load_kW = (Q_load/3600)

T_hp_out = T_load_hp+(Q_hp_kW*3600/(4.19*m_dot_load))

Q_hp_kW=Q_cond*gt(Surplus_Signal,0.5)*gt(Q_load,0)*gt(Frequency,30)*lt(T_top_node,60)+(Q_evap_
2+E_dot_2)*lt(Surplus_Signal,0.5)*lt(Peak_signal,0.5)*gt(Q_load,0)*gt(Frequency_2,30)*lt(T_top_node,
60)

E_dot_surplus = E_dot_2*gt(Surplus_Signal,0.5)*gt(Q_load,0)*gt(Frequency_2,30)*lt(T_top_node,60)

E_dot_comp=E_dot_surplus*gt(Frequency,30)+E_dot_2*lt(Surplus_Signal,0.5)*lt(Peak_signal,0.5)*gt(Q_
load,0)*gt(Frequency_2,30)*lt(T_top_node,60)

Q_demand_kW = (DHW_demand+SH_demand)/3600

F=Frequency*gt(Surplus_Signal,0.5)*gt(Q_load,0)*gt(Frequency,30)*lt(T_top_node,60)+Frequency_2*lt(
Surplus_Signal,0.5)*lt(Peak_signal,0.5)*gt(Q_load,0)*gt(Frequency_2,30)*lt(T_top_node,60)
```

HP_control_signal=(HP_surplus_signal*gt(Frequency,30)+lt(Surplus_Signal,0.5)*lt(Peak_signal,0.5)*gt(Q_load,0)*gt(Frequency_2,30)*lt(T_top_node,60))

HP_surplus_signal = gt(Surplus_Signal,0.5)*gt(Q_load,0)*gt(Frequency_2,30)*lt(T_top_node,60)

F2 = Frequency*gt(Frequency,30)*gt(Q_hp_kW ,0)

HP_control_signal_2=(gt(Surplus_Signal,0.5)*gt(Q_load,0)*gt(Frequency_2,30)*lt(T_top_node,60)+lt(Surplus_Signal,0.5)*lt(Peak_signal,0.5)*gt(Q_load,0)*gt(Frequency_2,30)*lt(T_top_node,60))

Q_hp_basecase = Q_evap_2+E_dot_2

F: Wind Integration Factor Vs. Demand Factor of the Ground-source heat pump Model

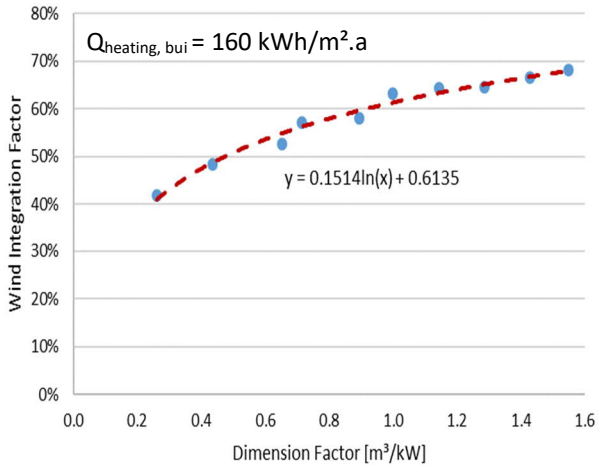

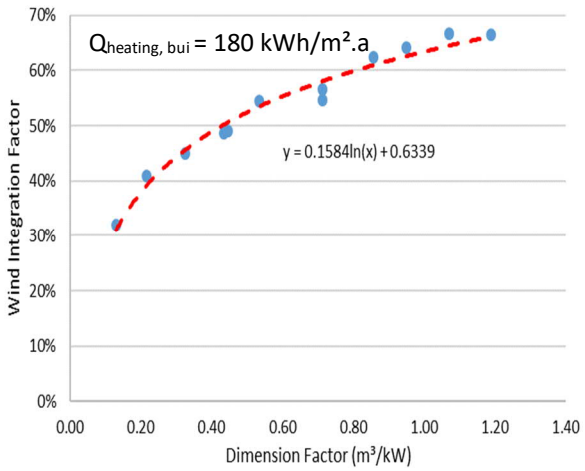

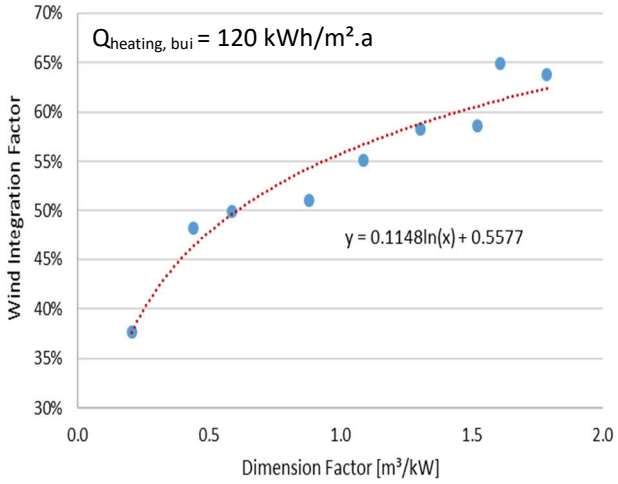

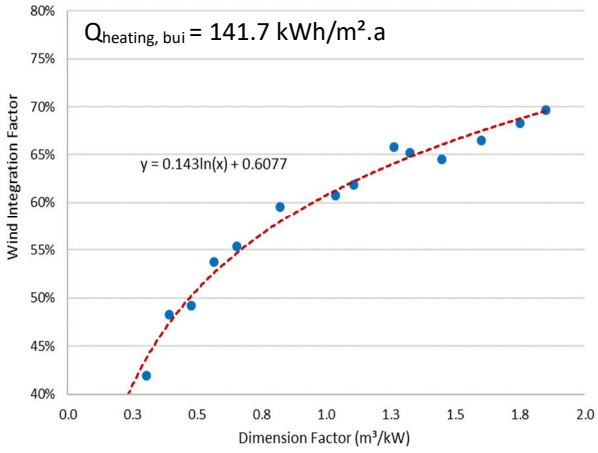

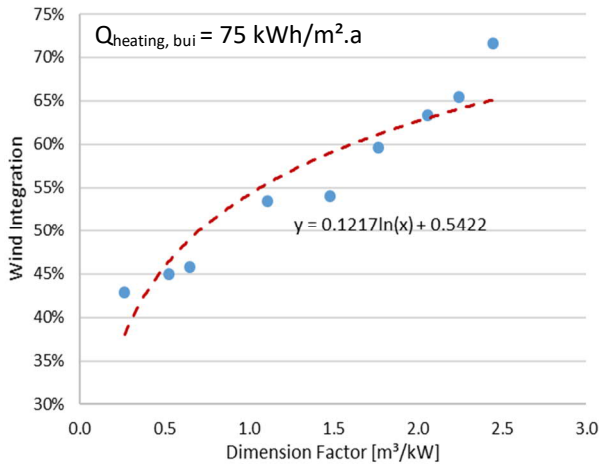

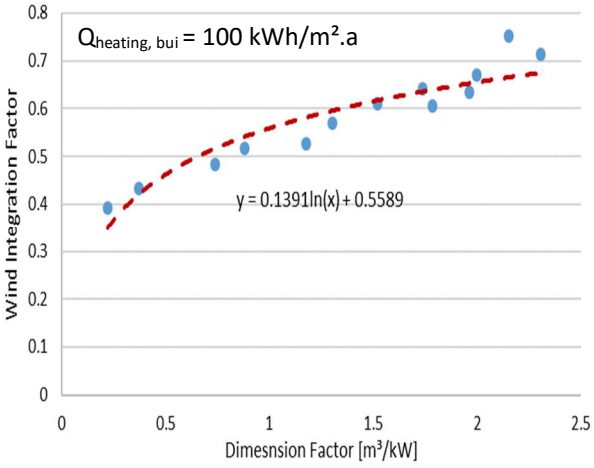

G: The Impact of Enlarging Thermal Storage Volume on SPF of the Heat Pump Unit

Ground Source Heat Pump

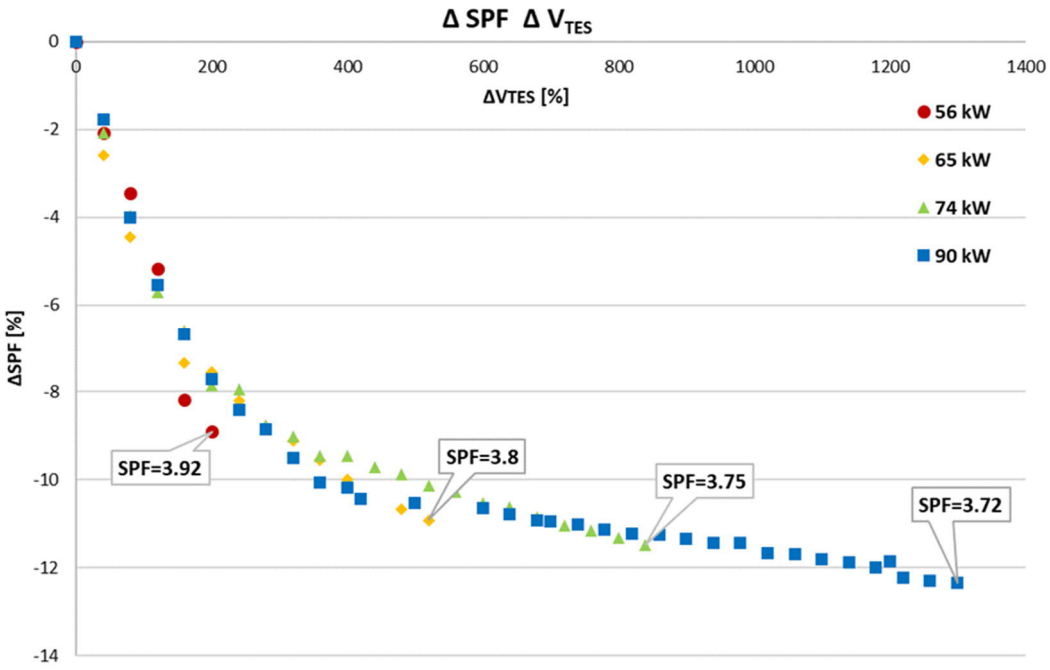

Air Source Heat Pump

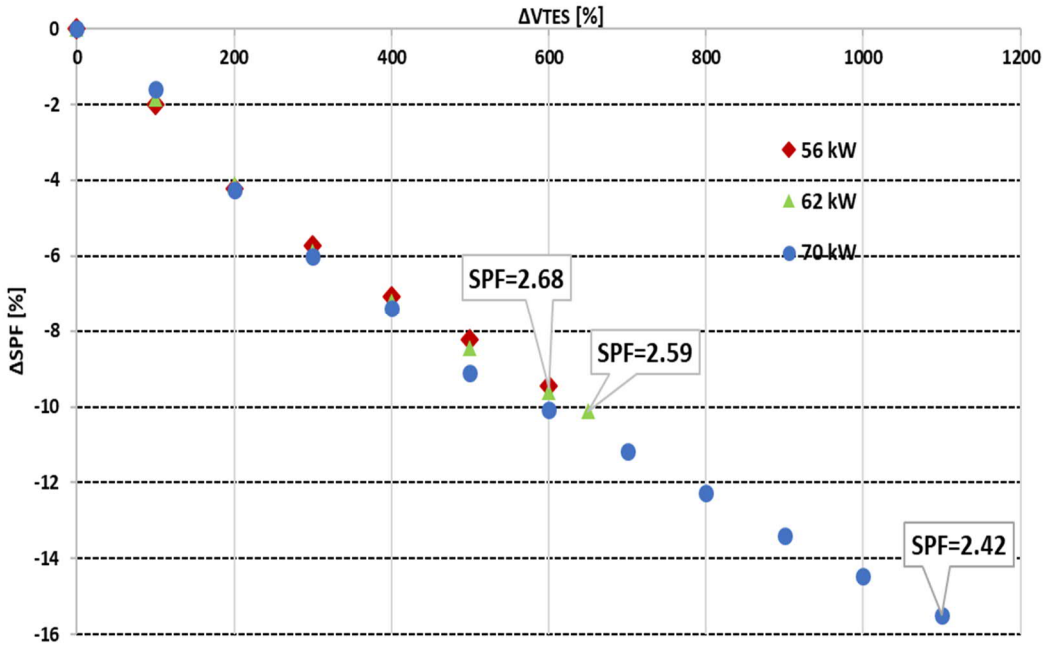

H: Office Building: A Case Study for Single Speed Heat Pumps

For a building office with the overall volume of 4800 m³ and the heating area of 1200 m² is considered. Followings are SH and DHW demands of this building:

SH Demand [kWh/m².a]	DHW Demand [kWh/m².a]	Overall Annual Demand [kWh]
77	12	106800

Since office or commercial buildings includes various categories depending on the demand profiles and the results can not be generalized for the entire office buildings, the effect of increasing specific demand level has been excluded from the investigation; In order to evaluate the impact of over sizing scenario in coordination with standard load profile of the office/commercial buildings (SLP G0) on the wind adaptation performance of the single speed heat pumps. The heating curve of this office building is shown in the below Figure. As it is seen in the below figure the maximum daily heating energy demand for space heating and domestic hot water of the building is about 1500 kWh which takes place at -12˚C as the minimum design ambient temperature of Berlin.

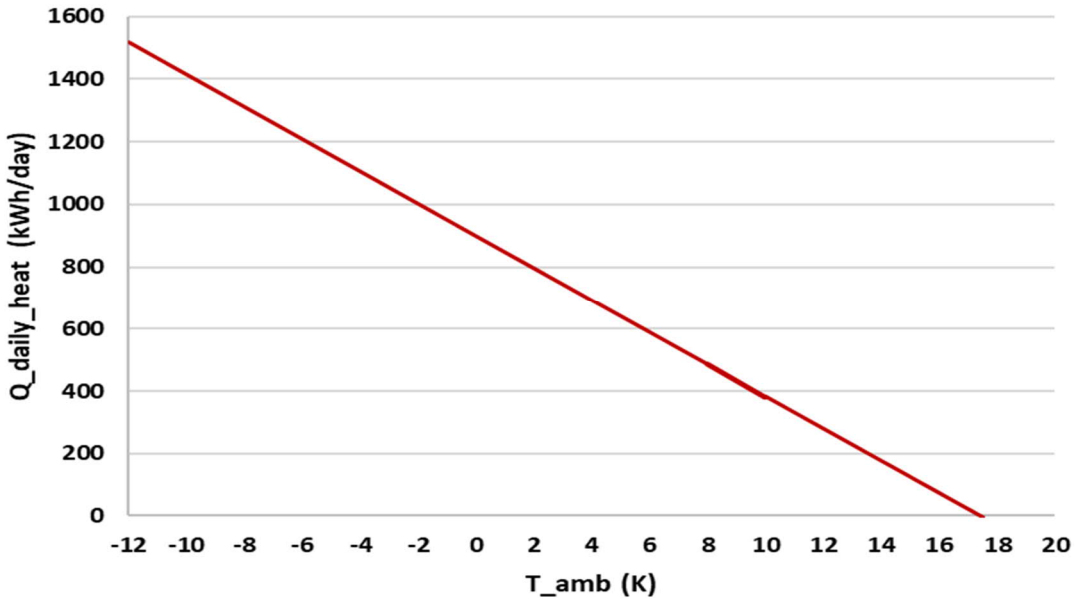

The heating curve of the office building

Following are the simulation results for oversizing GSHP and ASHP systems and their impact on the operation of the system as well as wind integration performance:

Ground Source Heat Pump System

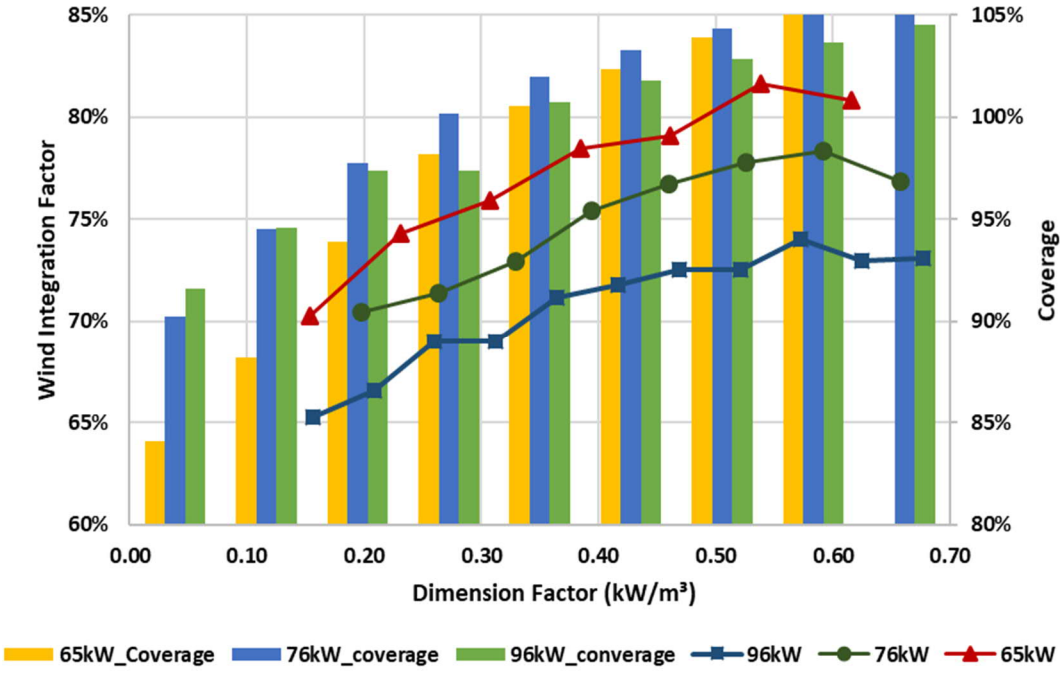

The impact of the oversizing GSHP and thermal storage on the wind integration and Coverage factors $\left(\frac{Q_{TES}}{Q_{Demand}}\right)$ *of the system*

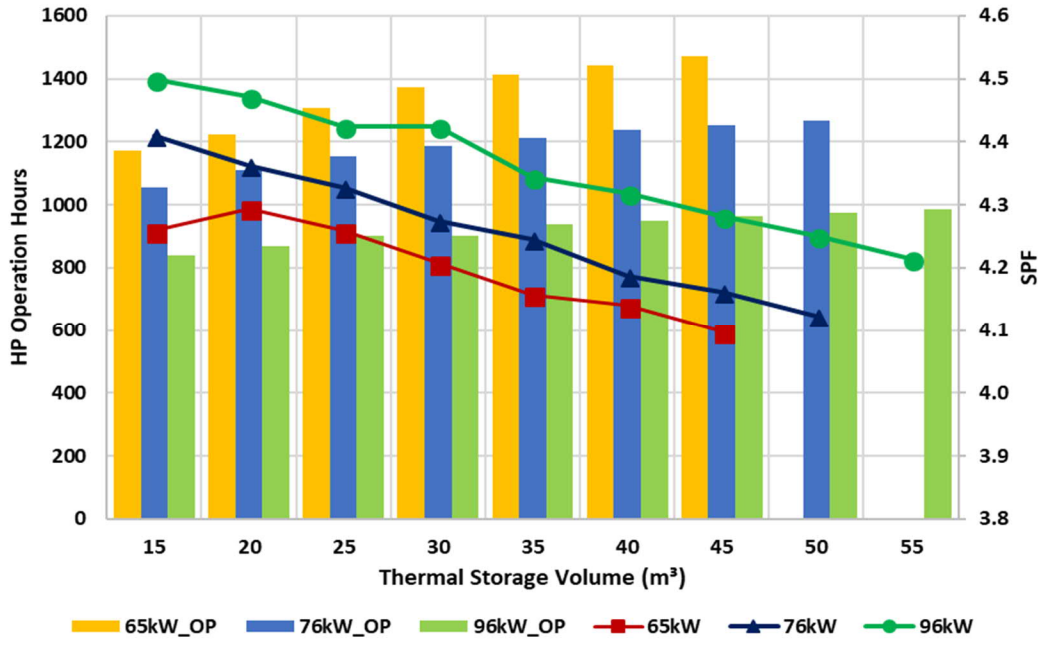

Variation of the Seasonal Performance Factor and Operation hours of the GSHP for Different Storage Volumes

Air Source Heat Pump System

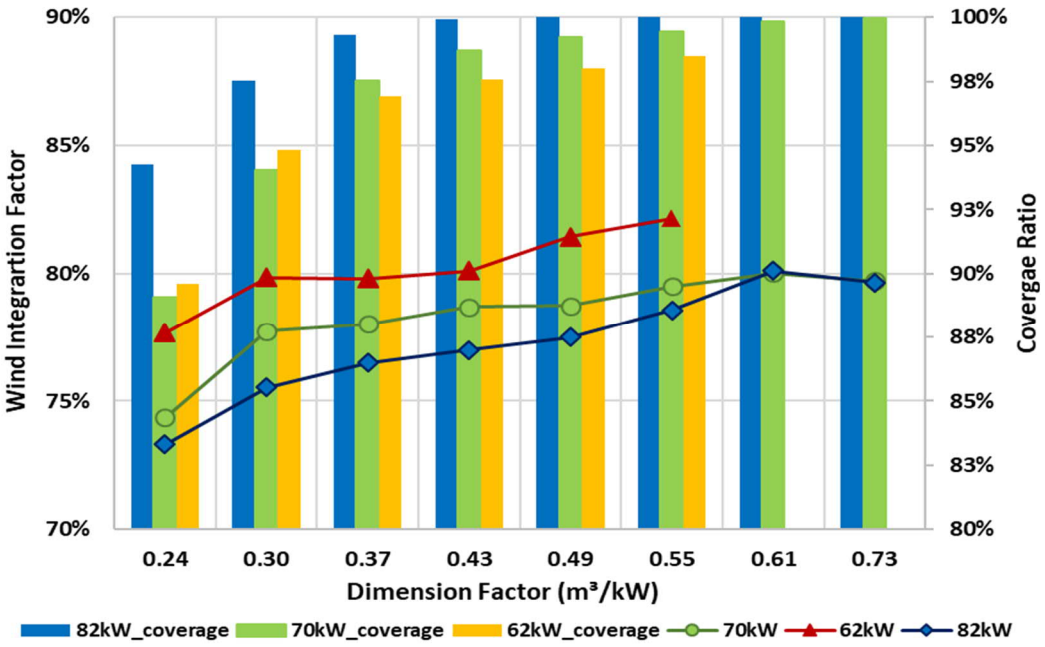

The impact of the coverage ratio on the growth rate of the wind share of the power demand of the heat pump

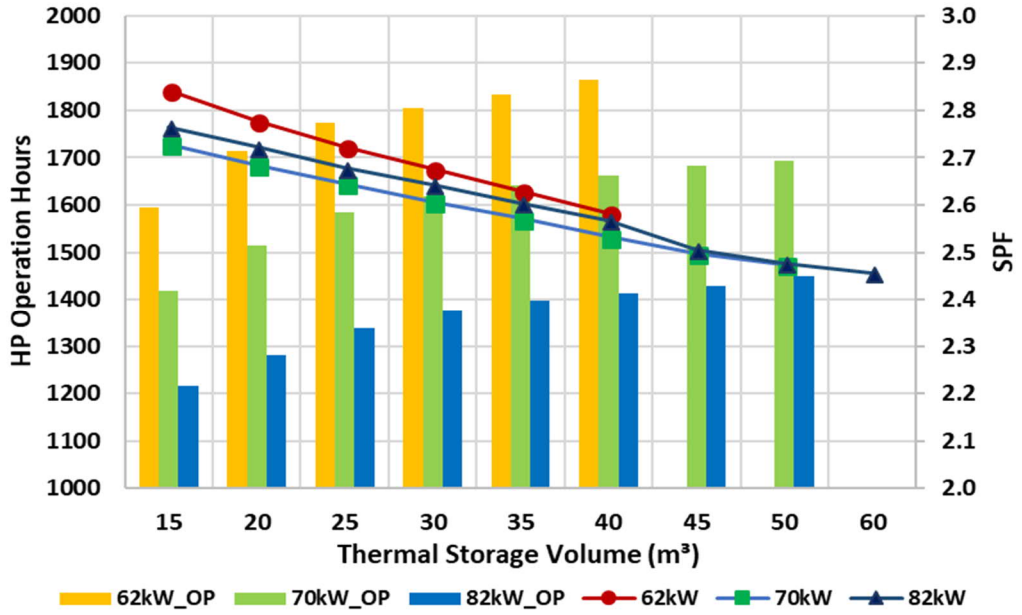

Variation of the Seasonal Performance Factor and Operation hours of the Heat Pump for Different Storage Volumes